HHS Public Access

Author manuscript

*Brain Behav Immun*. Author manuscript; available in PMC 2022 March 04.

Published in final edited form as:

*Brain Behav Immun*. 2020 July ; 87: 610–633. doi:10.1016/j.bbi.2020.02.006.

# Peripheral-to-central immune communication at the area postrema glial-barrier following bleomycin-induced sterile lung injury in adult rats

**David G Litvin**[1,2,3], **Scott J Denstaedt**[2,4], **Lauren F Borkowski**[5], **Nicole L. Nichols**[5], **Thomas E Dick**[2,6], **Corey B Smith**[1], **Frank J Jacono**[2,7,*]

[1]Department of Physiology & Biophysics, Case Western Reserve University School of Medicine, Cleveland, OH 44106, United States

[2]Division of Pulmonary, Critical Care and Sleep Medicine, Department of Medicine, Case Western Reserve University School of Medicine, Cleveland, OH 44106, United States

[3]Department of Fundamental Neuroscience, University of Lausanne, 1005 Lausanne, Switzerland

[4]Division of Pulmonary and Critical Care Medicine, Department of Internal Medicine, University of Michigan Medical School, Ann Arbor, MI 48109, United States

[5]Department of Biomedical Sciences, University of Missouri College of Veterinary Medicine, Columbia, MO 65212, United States

[6]Department of Neurosciences, Case Western Reserve University School of Medicine, Cleveland, OH, 44106, United States

[7]Division of Pulmonary, Critical Care and Sleep Medicine, Louis Stokes VA Medical Center, Cleveland, OH, 44106, United States

## Abstract

The pathways for peripheral-to-central immune communication (P→C I-comm) following sterile lung injury (SLI) are unknown. SLI evokes systemic and central inflammation, which alters central respiratory control and viscerosensory transmission in the nucleus tractus solitarii (nTS). These functional changes coincide with increased interleukin-1 beta (IL-1β) in the area postrema, a sensory circumventricular organ that connects P→C I-comm to brainstem circuits

[*]**Corresponding Author**: Frank J. Jacono M.D., Division of Pulmonary, Critical Care & Sleep Medicine, Case Western Reserve School of Medicine, 11100 Euclid Ave, Wearn 622, Mailstop 5067, Cleveland, OH 44106, Phone: (216) 368-4625, Fax: (216) 844-2187, fjj@case.edu.

Author contributions:

D.G.L.: conception, design, analysis of data, interpretation of data, drafting, revising content of manuscript, and final approval; S.J.D.: analysis of data, revising content of manuscript, and final approval; T.E.D.: analysis of data, interpretation of data, revising content of manuscript, and final approval. C.B.S.: revising content of manuscript, and final approval. N.L.N.: analysis of data, interpretation of data, revising content of manuscript, and final approval. L.F.B.: analysis of data, interpretation of data, revising content of manuscript, and final approval. F.J.J.: conception, interpretation of data, revising content of manuscript, and final approval.

Competing interests:

The authors declare no competing financial interests.

that control homeostasis. We hypothesize that IL-1β and its downstream transcriptional target, cyclooxygenase-2 (COX-2), mediate P→C I-comm in the nTS. In a rodent model of SLI induced by intratracheal bleomycin (Bleo), the sigh frequency and duration of post-sigh apnea increased in Bleo-compared to saline-treated rats one week after injury. This SLI-dependent change in respiratory control occurred concurrently with augmented IL-1β and COX-2 immunoreactivity (IR) in the *funiculus separans* (*FS*), a barrier between the AP and the brainstem. At this barrier, increases in IL-1β and COX-2 IR were confined to processes that stained for glial fibrillary acidic protein (GFAP) and that projected basolaterally to the nTS. Further, *FS* radial-glia did not express TNF-α or IL-6 following SLI. To test our hypothesis, we blocked central COX-1/2 activity by intracerebroventricular (ICV) infusion of Indomethacin (Ind). Continuous ICV Ind treatment prevented Bleo-dependent increases in GFAP+ and IL-1β+ IR, and restored characteristics of sighs that reset the rhythm. These data indicate that changes in sighs following SLI depend partially on activation of a central COX-dependent P→C I-comm via radial-glia of the *FS*.

### Keywords

Peripheral-to-Central Immune Communication; Area Postrema; Circumventricular Organs; Neuroinflammation; *Funiculus Separans* ; Radial-Glia; Sterile Lung Injury; Cyclooxygenase; Sterile Inflammation; Nucleus Tractus Solitarii; Dorsal Motor Nucleus of the Vagus; Central Canal; Bleomycin; Indomethacin; Interleukin-1 Beta

## Introduction

Peripheral organ injury can induce local and systemic release of proinflammatory cytokines through activation of the innate immune system (Frangogiannis et al., 2002; Xu et al., 2006; Liu et al., 2008; Riazi et al., 2008; Butterworth, 2013). Due to absence of microbial activators, this is referred to as sterile injury; the immune response is referred to as sterile inflammation (Chen and Nuñez, 2010; Shen et al., 2013; Rubartelli et al., 2014; Engelhardt et al., 2017).

In the inflammatory response to infections such as septicemia, circulating immune factors communicate with the central nervous system (CNS) (Elmquist et al., 1997; Ericsson et al., 1997; Mastronardi et al., 2007; Wuchert et al., 2008; Jin et al., 2016; Yoshida et al., 2016; Vargas-Caraveo et al., 2017). Peripheral inflammation evokes ‘sickness behavior’ and neuro-inflammation through specific mechanisms via peripheral-to-central immune communication (P→C I-comm). Neuro-inflammation affects homeostatic functions including: i) thermoregulation (Evans et al., 2016), ii) feeding (Platha-Salaman, 2001), iii) blood pressure (Wei et al., 2018), and iv) breathing (Hofstetter et al., 2007; Siljehav et al., 2014). While initially compensatory and beneficial, persistent and excessive neuroinflammation can disrupt homeostatic control (Vandendriessche et al., 2013; Huxtable et al., 2015; Nardocci et al., 2015; Lorea-Hernández et al., 2016; Tohyama et al., 2018).

In contrast to inflammation due to infection, the P→C I-comm for sterile inflammation remains less articulated (Chen and Nuñez, 2010; Shen et al., 2013; Rubartelli et al., 2014; Engelhardt et al., 2017), and may be mechanistically distinct (Lee et al., 2010; Gadani et al., 2015; Fleshner et al., 2017). Yet similar to non-sterile inflammation, sterile inflammation

can become dysregulated and disrupt homeostatic control (Butterworth, 2013; Nongnuch et al., 2014; Li et al., 2015; Tsai et al., 2017; Vaseghi et al., 2017; Litvin et al., 2018). Therefore, understanding the CNS immune response to sterile injury, and how this response acts to modulate homeostatic control is an important line of scientific inquiry independent of the CNS immune response due to infectious injury.

In the current study, we examine P→C I-comm after intratracheal bleomycin (Bleo-IT), which causes sterile lung injury (SLI) and triggers robust peripheral inflammation (Adamson and Bowden, 1974; Jiang et al., 2005, 2007; Hoshino et al., 2009; Chen and Nuñez, 2010). SLI also evokes central immune activation that features microglia hyper-ramification and IL-1β expression throughout the nucleus tractus solitarii (nTS), a collection of dorsomedial (dm)-brainstem nuclei that function as central relays for viscerosensory input (Jacono et al., 2011; Litvin et al., 2018). The nTS is a critical central immune hub because of its ability to: i) rapidly detect various forms of peripheral immune activation (Dantzer et al., 2008; Balan et al., 2011; Pavlov and Tracey, 2012a, 2017; Hsu et al., 2017), and ii) mediate cardiorespiratory (Mollace et al., 2001; Balan et al., 2011; Waki et al., 2013), appetitive (Hsu et al., 2017; Yang et al., 2017), and thermoregulatory (Goehler et al., 2000; Konsman, 2016) changes related to sickness behavior. This ability to mediate physiologic changes depends in part on the immune activation of various cytokine/chemokine receptors expressed within the nTS (Sekiyama et al., 1995; Rummel et al., 2006; Laaris and Weinreich, 2007; Marty et al., 2008; Ruchaya et al., 2012; Waki et al., 2013; Vance et al., 2015).

To understand the source of immune activation in the nTS, we focused on inflammatory changes within the closely juxtaposed area postrema (AP), a dm-brainstem circumventricular organ (CVO) that serves as a P→C I-comm pathway for the nTS (Lee et al., 1998; Goehler et al., 2006; Tsai et al., 2014; Senzacqua et al., 2016; Hsu et al., 2017). We focused on the AP (as opposed to other CVOs) was based on evidence that: i) it receives vagal afferent projections, projects to the nTS, and modulates cardiorespiratory functions (Florez and Borison, 1967; Shapiro and Miselis, 1985; Sun and Spyer, 1991; Srinivasan et al., 1993; Cunningham et al., 1994; Rogers et al., 1995; Chang et al., 2015); ii) it becomes activated during sterile and non-sterile inflammation (Ericsson et al., 1997; Rummel et al., 2004; Lee et al., 2010; Vargas-Caraveo et al., 2015); iii) immune-dependent activation of the AP often directly precedes activation of the nTS (Quan et al., 1997, 1998; Herkenham et al., 1998; Nakano et al., 2015), and iv) activation of the AP is a necessary step in transmitting peripheral immune activation to the nTS (Lee et al., 1998; Tsai et al., 2014).

In response to peripheral inflammation, the AP produces soluble immune factors that diffuse to adjacent nTS nuclei (Vitkovic et al., 2000; Erickson and Banks, 2018; Furube et al., 2018). However, the ventrolateral surface of the AP is surrounded by the *Funiculus Separans (FS)* (McKinley et al., 2003; Price et al., 2008; Maolood and Meister, 2009; Dallaporta et al., 2010; Senzacqua et al., 2016; Fernandez et al., 2017; Guillebaud et al., 2017), which is a diffusion barrier composed of polarized radial-glia and tanycytes. These cells restrict flow of molecules larger than ~1 kDa into the nTS (Faraci et al., 1989; Gross et al., 1990; Willis et al., 2007; Wang et al., 2008; Langlet et al., 2013b; Miyata, 2015). Thus, volume diffusion from the AP is likely not a major source for the immune mediators upregulated in the nTS under systemic inflammatory conditions (Nadjar et al., 2003; Waki et al., 2010,

2013; Jacono et al., 2011; Tsai et al., 2017; Litvin et al., 2018). Alternatively, there is compelling evidence the *FS* may mediate P→C I-comm via mechanisms for producing and trafficking cytokines, as occurs at other glial-barriers (Sofroniew, 2015; Engelhardt et al., 2017; Erickson and Banks, 2018); consequently, *FS* radial-glia may function as interlocutors between immune processes in the AP and nTS (Voss et al., 2007; Dallaporta et al., 2009; Nakano et al., 2015; Vargas-Caraveo et al., 2017). Thus, we hypothesized that following SLI, P→C I-comm occurs through the *FS* via canonical pathways such as cyclooxygenase-1/2 (COX-1/2) dependent prostaglandin E2 ($PGE_2$) synthesis (Matsumura et al., 1998; Ebersberger et al., 1999; Schiltz and Sawchenko, 2002; Akanuma et al., 2011; Tachikawa et al., 2012; Liu et al., 2015; Wei et al., 2018).

Finally, lung injury disrupts normal breathing patterns; increasing respiratory frequency and the predictability of the ventilatory waveform (Jacono et al., 2011; Young et al., 2019). This occurs through central mechanisms that include integration of viscerosensory drive (Vlemincx et al., 2013; Ramirez, 2014; Litvin et al., 2018). Moreover, serum immune factors upregulated in response to lung injury may be involved, given their ability to disrupt central cardiorespiratory circuits that include the nTS (Sekiyama et al., 1995; Rummel et al., 2006; Laaris and Weinreich, 2007; Marty et al., 2008; Ruchaya et al., 2012; Waki et al., 2013; Koch et al., 2015; Vance et al., 2015; Forsberg et al., 2016, 2017). Consequently, ventilatory behaviors such as re-setting sighs that typically act to restore normal ventilatory patterning may be less effective during SLI (Khoo, 2000; Nakamura et al., 2003; Baldwin et al., 2004; Yamauchi et al., 2008; Nguyen et al., 2012; Vlemincx et al., 2012, 2013; Ramirez, 2014). Thus, we hypothesized that SLI would decrease the occurrence rate and effectiveness of resetting sighs and that central application of indomethacin (Ind), a COX-1/2 inhibitor, would reverse this effect.

## 2. Materials & Methods

### 2.1. Animals

Adult Sprague Dawley male rats (200–300g) were purchased from Envigo (Indianapolis, IN, USA), and delivered pathogen free at least 48h before the induction of any procedure. Rats were housed in separate cages under specific-pathogen free conditions where ambient temperature (22–25°C), humidity (40–50%), and light/dark cycles (12h/12h) were controlled. Rats had *ad libitum* access to food and water. All procedures were conducted in accordance with the National Institute of Health guidelines for care and use of laboratory animals and were approved by the Institutional Animal Care and Use Committee at Case Western Reserve University (2016 – 0039).

### 2.2. Treatment groups

Rats received either bleomycin (Bleo) or saline intratrachially (IT), and were plethysmographically recorded and euthanized for immunohistochemical experiments 7d later. In a separate set of studies, a cohort of rats received ICV cannulas, which delivered Indomethacin (Ind) or Vehicle (Veh) by subcutaneous mini-osmotic pump. Two days (2d) following cannula/pump implantation, rats received Bleo-IT or saline-IT; We based the 2d recovery time on previous ICV cannula studies using osmotic pumps, and chose 2d

to minimize constitutive COX-1/2 inhibition by Ind and to allow sufficient time for rats to resume normal feeding and grooming behaviors (Jho et al., 2003; Kirkby et al., 2016; Ineichen et al., 2017; Khansari and Halliwell, 2019). The Ind-ICV dose was based on a survey of previous studies that acutely and/or chronically used central Ind infusion to mitigate neuroinflammation (Catania et al., 1991; Komaki et al., 1992; Tanaka et al., 1993; Bustamante et al., 1997; Netland et al., 1998; Schiltz and Sawchenko, 2002; Serrats et al., 2017).

SLI rats that received Bleo-IT and Veh- or Ind- ICV are referred to as B+V or B+I respectively, and sham-rats that received saline-IT and Veh- or Ind- ICV are referred to as S+V or S+I respectively. The sample size for each study was selected based on: i) our previous studies (Litvin et al., 2018), ii) a power analysis to achieve a power of 0.8 with an alpha value of 0.05; assuming an effect size of 30% and standard deviations that were 15–20% of the mean in a given treatment group (Lenth, 2001). We specify the number of rats for each study with the presentation of group data.

### 2.3. Bleomycin-induced lung injury

Rats received a single IT infusion of either: i) Bleo (3 units, BIOTANG Inc. Lexington, MA) dissolved in 40μl of physiologic saline (0.9%) or ii) 40μl of saline. The Bleo dose was based on previous work in our lab (Jacono et al., 2006, 2011; Litvin et al., 2018), and studies by others showing that Bleo-IT reliably produces dose-dependent injury to the lung parenchyma (Kaminski et al., 2000; Borzone et al., 2001; Cutillo et al., 2002; Babin et al., 2011). To induce SLI, rats were sedated with a ketamine, xylazine and acepromazine cocktail (0.1ml per 50g body weight), and placed supine on a sterilized surgical board. The surgical site was disinfected with betadine and a midline cervical incision (1cm) exposed the trachea. Bleo or Saline was instilled through a 26-gauge needle that was inserted through the tracheal wall. The incision site was sealed using surgical adhesive (Vetbond™, St. Paul, MN, USA). We observed the rats during recovery and once they were moving, we returned them to the animal facility and monitored them daily. Post-surgical pain management involved Bupivacaine for local analgesia (2 mg/kg), and Buprenorphine for systemic analgesia (0.02 mg/kg).

### 2.4. Placing the ICV cannula for Indomethacin treatment

Rats were anesthetized as above and placed prone in a stereotaxic frame (David Kopf instruments, Tujunga, CA) to implant a cannula in the right lateral ventricle. Briefly, the cannula was i) available in the brain infusion kit, (Alzet Osmotic Pumps, Cupertino, CA), ii) positioned ICV using the following stereotaxic coordinates: 0.8mm posterior to Bregma, 1.5mm lateral to the midline and 3.5mm ventral to the surface of the skull; iii) affixed to the skull with dental cement, and iv) connected to a vinyl catheter that was threaded subcutaneously (aligned with the spine) to a mini-osmotic pump. The pump (0.5 μl/h, 200 μl reservoir) contained either vehicle (Veh, 50% DMSO) or Ind (8.3 μg/μl) and was implanted subcutaneously in the mid-scapular space. The incisions for the cannula and pump were closed using surgical adhesive (Vetbond™, St. Paul, MN, USA). Rats were observed during recovery and then returned to the animal facility and monitored daily. Two days following cannula/pump implantation, rats received either Bleo-IT or saline-IT. The exact placement

of the cannula was determined post-mortem by cryo-sectioning and imaging suprapontine brain slices (100 μm) to determine whether the path of the cannula dorsoventrally transected the entirety of the primary motor cortex (M1) between Bregma: 0.2 mm and −0.77 mm. Of the 33 cannula/pump implantations completed for the study, 5 (15%) were placed incorrectly and these rats were excluded from the final analysis

### 2.5. Measurement of breathing patterns

Respiratory waveforms were recorded in awake, freely moving rats using whole-body plethysmography (pleth, (BUXCO Research Systems, Wilmington, NC, USA) (Jacono et al., 2006, 2011). Pressure changes within the chamber were transmitted via pre-amplifier (Max II, BUXCO Research Systems, Wilmington, NC, USA) and recorded at 200 Hz using a data acquisition interface (Power1401, CED, Cambridge, UK) with chart recording software (Spike 2, CED).

We identified post-sigh apneas as pauses in breathing that were preceded by an augmented inspiration, which was defined as having an amplitude that was >1.5 x the resting amplitude. The apnea had a duration >2.5 x the duration of baseline expiration (Mendelson et al., 1988; Montandon et al., 2006; Litvin et al., 2018). We focused on a subset of sighs that reset the respiratory pattern (Cherniack et al., 1981; Vlemincx et al., 2012, 2013; Ramirez, 2014). We identified these sighs by a decrease in the variability of the respiratory frequency (fR) in the breaths immediately after the sigh compared to those immediately before the sigh. We calculated the coefficient of variability for fR (CVfR), which is a normalized measure of variance (standard deviation divided by the mean fR) and is an established measure of variability (Stromberg and Gustafsson, 1996; Yamauchi et al., 2008; Cruz et al., 2014). With resetting sighs, the CVfR from the 10s period before the sigh decreased ≥10% in the 10s period that after the sigh and CVfR was ≤20% after the sigh.

### 2.6. Immunohistochemistry (IHC), imaging and quantification

Rats were anesthetized deeply with isoflurane and euthanized by exsanguination and transcardial perfusion of ice-cold phosphate buffered saline (PBS, 0.9% NaCl + 0.1M phosphate buffer, pH 7.4) followed by ice-cold 4% paraformaldehyde (RT15714, Electron Microscopy Sciences, Hatfield, PA, USA). Brainstems were: i) removed, ii) post-fixed for 2h in 4% paraformaldehyde at 4°C, iii) cryoprotected in 30% sucrose for 48h, iv) frozen with dry ice, v) embedded in Tissue-Tek® OCT compound (Sakura Finetek, Torrance, CA, USA), vi) stored at −80°C and vii) serially sectioned (20-μm coronal sections, Leica CM1850 cryostat, Leica Biosystems Inc., Buffalo Grove, IL, USA). Brainstem sections were mounted onto gelatin-coated slides, and allowed to air-dry for ~45min before being placed into a slide-box and stored at −20° C.

Brainstem sections were immunostained in parallel for a particular antibody. The antibody that we used stained for IL-1β also can stain for pro-IL-1β so constitutive staining apparent in figures of IL-1 staining may be due to staining pro-IL-1β. To stain sections, the slides were thawed, rehydrated with 3x PBS washes, and incubated in sodium citrate buffer (10 mM tri-sodium citrate, 0.05% tween-20, pH 6, heated to 75° C) for antigen retrieval (Litvin et al., 2018). The sections were then permeabilized with PBS containing 0.1% Triton X-100

(PBST). Subsequently, sections were incubated for 1h in blocking buffer (PBST, 5% bovine serum albumin), and 5% normal donkey serum. Then sections were incubated overnight at room temperature with primary antibody diluted in blocking buffer. The next day, sections were incubated for 2h in secondary antibodies (diluted in blocking buffer). Dilutions and manufacturer information for primary and secondary antibodies are summarized in table 1.

For studies using fluorescent secondary antibodies, slides were a) washed, b) cover-slipped c) sealed, and d) stored in the dark at 4°C until the time of imaging (Litvin et al., 2018). For studies using biotinylated secondary antibodies, slides were rinsed and incubated in the VECTASTAIN® Elite ABC (Vector Laboratories, Burlingame, CA) reagent for 2h; and then rinsed and incubated for ~5 min in a fresh solution containing 3,3' diaminobenzidine (0.05%, DAB), nickel chloride (0.05%) and $H_2O_2$ (0.015%) in PBS. Brainstem sections for each particular study were immunostained in parallel (Litvin et al., 2018). To coverslip slides we used ProLong® Diamond Antifade Mountant (ThermoFisher; P36965) and 1.5 coverslips. Following 48hr mountant curing, we used CoverGrip™ (Biotium; #23005) to seal coverslips.

Brightfield and fluorescent images of the dorsomedial brainstem were acquired at x40 (APO, 1.3 NA, oil objective) using a fluorescence microscope (BZ-X710 Keyence Corporation of America, Itasca, IL) or a confocal microscope (TCS-SP8, Leica Biosystems Inc., Buffalo Grove, IL, USA). We used the same microscope to image brainstem sections within datasets (i.e. IL-1β IHC). Quantification of fluorescent images was performed using image analysis software FIJI. Cell number and area per cell were measured on maximally projected, segmented binary images using the "analyze particle" function. Iba-1+ branch endpoints/cell, and total branch length/cell were quantified in a given region of interest using maximally projected binary masks that were "skeletonized" and measured using the "analyze skeleton" function without "pruning" (Arganda-Carreras et al., 2010; Morrison and Filosa, 2013).

### 2.7. Immunostaining control experiments

We employed negative/positive controls to ensure the antibody specificity of IL-1β and COX-2. Namely, we utilized: i) omission of primary antibodies, ii) primary antibody pre-absorption with a 10-fold molar excess of the immunizing peptide antigen, and iii) immunostaining tissue that endogenously/exogenously contained high protein expression (O'Neill and Ford-Hutchinson, 1993; Rocca et al., 2002; Kirkby et al., 2013, 2016).

Negative controls for TNF-α and IL-6 consisted only of primary antibody exclusion. These antibodies were selected based on the literature, which supported their use: i) throughout the CNS/PNS, ii) with pre-absorption (TNF-α: (Wei et al., 2008; Kato et al., 2009; Fuchs et al., 2013); IL-6: (Leibinger et al., 2013; Wei et al., 2013b; Chen et al., 2018)), or iii) for neutralization (TNF-α (Nadeau and Rivest, 2000; Wei et al., 2008; Wang et al., 2019); IL-6 (Faustino et al., 2011; Shrivastava et al., 2017; Sun et al., 2017; Wang et al., 2019)).

In co-localization studies, we took precautions to minimize potential cross-reactivity between antibodies by utilizing a serial protocol (Guo et al., 2007; Wei et al., 2008; Jones et al., 2019). Specifically, we first incubated brain slices with chicken anti-GFAP (overnight)

followed by donkey anti-chicken Alexa Fluor 488 (2h) and following thorough washing with PBS (5 X 10min), we incubated with rabbit anti-IL-1β (overnight) followed by donkey anti-rabbit Alexa Fluor 647 (2h). Furthermore, we used secondary antibodies that were affinity purified and cross-adsorbed. For confocal imaging, serial acquisition was used to image co-labeled sections, whereby a given region was scanned separately for Alexa Fluor 488 labeled epitope (GFAP) and Alexa Fluor 647 labeled epitope (IL-1β).

### 2.8. Data analysis

Statistical analyses were performed using GraphPad Prism 6. Statistical significance was set at a *P*-value less than 0.05. The statistics included: i) unpaired two-tail t-test, ii) Kruskal-Wallis test, a non-parametric analysis of variance with Dunn's multiple comparisons test (post-hoc), or iii) a one-way ANOVA with Tukey multiple comparisons test and are identified with the presentation of the group data. For IHC experiments, measurements from 3–4 brainstem sections per rat were averaged. Data are presented as mean ± SEM.

Brainstem sections immunostained with Iba-1 and DAB were analyzed with the optical fractionator method of stereology to quantify volume density and expressed as cells per unit volume (CPUV, $10^6$ cells/$\mu m^3$) (Long et al., 1998; Beggs and Salter, 2007; Selenica et al., 2013). Brainstem sections immunostained with Iba-1 and a fluorescent secondary antibody were analyzed by acquiring a three-dimensional optical stacks confocally to quantify Iba-1+ cell morphology (Arganda-Carreras et al., 2010; Schindelin et al., 2012; Morrison and Filosa, 2013) (Figure $1A_3$). The strategy for quantifying ramification involved ranking over 100 cells in a section by the number of their branches (Br#), taking the 100 cells with the highest branch number and then averaging Br# and the corresponding numbers for branch endpoints (BEPs) and total branch length (TBL). For these experiments, measurements from 3 – 4 brainstem sections per rat were averaged and compared between groups.

The group data are presented in a consistent format (Bleo-before Saline-IT rats) through the text. The numbers of rats in the groups are the same for the sites analyzed in a particular study. These numbers will be written with the first comparison but not repeated for each comparison.

## 3. Results

### 3.1. Sterile lung injury (SLI) alters microglia morphology in the area postrema (AP) and within adjacent dm-brainstem sites

Microglia in the AP mediate P→C I-comm. Under physiologic conditions, microglia exhibit a *hypo*-ramified phenotype at sites with contact to peripheral circulation; under pathophysiologic conditions, microglia become further hypo-ramified in response to circulating cytokines (Wuchert et al., 2008, 2009; Hermann et al., 2013; Nakano et al., 2015; Takagi et al., 2017). We asked whether SLI evoked changes in the number and morphology of Iba-1 positive microglia/macrophages in the AP (Figure 1A–D).

In the central zone of the AP (czAP), where fenestrated capillaries permit transmission of humoral signals to sensory neurons within the AP parenchyma (Goehler et al., 2006; Willis et al., 2007; Wang et al., 2008; Mannari et al., 2013), we observed Iba-1+ cells

that often localized to perivascular spaces (seen as large cavitations), which suggested their macrophage-related identity (Willis et al., 2007; Maolood and Meister, 2009; Willis, 2011). The volume density of czAP Iba-1+ cells (CPUV) (Long et al., 1998) was similar in Bleo- and saline-treated rats ((Figure $1B_1$) Bleo: 94 ± 5 CPUV, n = 7 vs. saline: 95 ± 3 CPUV, n = 8, $t_{13} = 0.17$, $P = 0.87$, Two-tail t-Test). The morphology of Iba-1+ cells in the czAP developed a *hypo*-ramified phenotype in response to SLI, which consisted of a reduced branch number (Br#, Figure $1B_2$), reduced number of branch endpoints (BEP, Figure $1B_3$), and a reduced total branch length (TBL) ((Figure $1B_4$) Br#: Bleo, 25.1 ± 1.3, n = 7, vs. saline, 30.1 ± 1.4, n = 8, $t_{13} = 2.55$, $P = 0.024$; BEP: Bleo, 12.0 ± 0.5, vs. saline, 13.9 ± 0.6, $t_{13} = 2.43$, $P = 0.03$; TBL: Bleo, 5.0 ± 0.3 $\times 10^2$ μm, vs. saline, 6.3 ± 0.4 $\times 10^2$ μm, $t_{13} = 2.44$, $P = 0.031$, Two-tail t-Test). Thus, microglia morphology becomes *hypo*-ramified in the czAP in both sterile and non-sterile inflammatory conditions (Lee et al., 2010; Vargas-Caraveo et al., 2015; Takagi et al., 2017).

The ventral-most segment of the AP forms the dorsal border (“roof”) of the central canal (dbCC), and thus provides a potential conduit for AP immune activation to reach circulating cerebrospinal fluid (Glattfelder et al., 2007; Miller and Loewy, 2014; Nakano et al., 2015). In contrast to the czAP, volume density of Iba-1+ cells in the dbCC increased in Bleo- compared to saline-treated rats ((Figure $1A_2$ & $1C_1$) Bleo: 11 ± 2 CPUV, n = 7; saline: 6 ± 1, n = 8, $t_{13} = 2.71$, $P = 0.018$, Two-tail t-Test). In further contrast, Iba-1+ cells in the dbCC of Bleo-IT rats exhibited a *hyper*-ramified phenotype with increased: i) Br# Bleo: 12.4 ± 0.9 vs. saline: 9.0 ± 1.0, $t_{13} = 2.49$, $P = 0.027$, ii) BEP Bleo: 7.4 ± 0.5 vs. saline: 5.9 ± 0.4, $t_{13} = 2.18$, $P = 0.049$, and iii) TBL Bleo: 1.2 ± 0.2 $\times 10^2$ μm vs. saline: 0.8 ± 0.1 $\times 10^2$ μm, $t_{13} = 2.35$, $P = 0.035$, Two-tail t-Test (Figures $1C_{2–4}$)

Finally, we examined the microglia morphology in two efferent nuclei: 1) dorsal motor nucleus of the vagus (DMNX), whose neurons make contact with the CC (McLean and Hopkins, 1985; Browning et al., 2005); and 2) the phrenic motor nucleus, located more caudally in the cervical spinal cord (Boulenguez et al., 2007; Mantilla et al., 2007; Anderson et al., 2009). We found no significant difference in the volume density of Iba-1+ cells measured in Bleo-versus saline-IT rats ((Figure $1D_1$) Bleo: 143 ± 8 CPUV vs. saline: 152 ± 11 CPUV, $t_{13} = 0.64$, $P = 0.53$). Similar to the czAP, the absence of a change in the number of Iba-1+ cells was associated with a *hypo*-ramified phenotype ((Figure $1D_2 – 1D_4$) i) Br#: Bleo: 20.74 ± 1.56 vs. saline: 28.97 ± 2.2, $t_{12} = 3.051$, $P = 0.01$; ii) BEP: Bleo: 11.6 ± 0.74 vs. saline: 15.4 ± 0.99, $t_{12} = 3.05$, $P = 0.0$; iii) TBL: Bleo: 0.96 ± 0.1 ×102 μm vs. saline: 1.4 ± 0.1 ×102 μm, $t_{12} = 2.94$, $P = 0.012$, Two-tail t-Test). In contrast, microglia in the phrenic motor column of Bleo-IT rats had no morphological differences compared to saline-IT rats (Supplemental (Sup) Methods, Sup Figure 3).

In summary, our data showed regional differences in the volume density and morphology of Iba-1+ cells in response to SLI. In the czAP and DMNX, the number of Iba-1+ cells was similar in the SLI and Sham groups but their morphology exhibited a *hypo*-ramified phenotype. However in the dbCC, the number of Iba-1+ cells after SLI although small was nearly double than that in Sham rats. Further, the Iba-1+ cells in the dbCC exhibited a *hyper*-ramified morphology following SLI. Together this provides evidence that the AP is a target for the immune response to SLI.

### 3.2. SLI augments Interleukin-1β (IL-1β) immunoreactivity in the dm-brainstem

Previously we showed that Bleo-IT increased IL-1β in the dm-brainstem after 48h in adult rats (Jacono et al., 2011) and after 7d in neonatal rats (Litvin et al., 2018). Because this proinflammatory cytokine is released by "activated" microglia and may mediate the CNS response to peripheral immune challenges, we determined if IL-1β increased at sites that could mediate P→C I-comm following SLI (Ericsson et al., 1997; Schiltz and Sawchenko, 2002; Goehler et al., 2006; Gabriel Knoll et al., 2017). Therefore we evaluated IL-1β+ IR in the: i) the czAP, ii) the dbCC, which is surrounded by iii) the *funiculus separans* and compared IL-1β+ IR in Bleo- (n = 5) and saline- (n = 5) IT rats (Miller and Loewy, 2014; Nakano et al., 2015) ((Figure 2D–F). Quantitative data for each site were as follows: i) czAP: Bleo: 20.9 ± 4.4 AUs vs. saline: 8.5 ± 2.5 AUs, $t_8 = 2.5$, $P = 0.039$; ii) dbCC: Bleo: 34.4 ± 5.3 AUs vs. saline: 15.9 ± 4.6 AUs, n = 5, $t_8 = 2.64$, $P = 0.03$; iii) *FS*: Bleo: 17.5 ± 3.5 AUs vs. saline: 5.4 ± 0.7 AUs, $t_8 = 3.402$, $P = 0.0093$, Two-tail t-Test). Further, IL-1β+ IR increased in adjacent nuclei ((Figure 2G, 2H) i) nTS: Bleo: 28.0 ± 6.4 AUs, vs. saline: 9.6 ± 1.9 AUs, $t_8 = 2.77$, $P = 0.024$, Two-tail t-Test; ii) DMNX: Bleo: 24.1 ± 5.4 AUs, n = 5 vs. saline: 6.3 ± 3.0 AUs, $t_8 = 3.35$, $P = 0.01$, Two-tail t-Test). In both treatment groups, IL-1β+ IR was restricted to radial-glial varicosities in the dbCC and *funiculus separans*. A subset of these varicosities originated from or near the ependymal layer of the CC (Pecchi et al., 2007), and projected basolaterally to the nTS or DMNX (Figure 2B).

In the dbCC, immunostaining for the IL-1β converting enzyme Caspase-1 (CASP-1) was not localized to radial-glia in Bleo- (n = 8) and saline- (n = 8) IT treated rats (Sup Figure 1D–H). Rather, increased CASP-1+ IR was restricted to cuboidal-like cells at the perimeter (ependymal layer) of the CC ($P = 0.048$, Two-tail t-Test) (Sup Figure 1D white arrowheads, 1F). In the czAP or *FS*, CASP-1+ IR did not differ between groups ((Sup Figure 1E, 1F) czAP: $P = 0.7$, *FS:* $P = 0.995$, Two-tail T-test).

Double labeling of brainstem sections from Bleo-IT treated rats (n = 3) with IL-1β and glial fibrillary acidic protein (GFAP) showed co-localization in the dbCC, *funiculus separans*, and medial nTS in Bleo-IT (n = 3) but not saline-IT (n = 3) rats (Sup Figure 1I). Dm-brainstem sections obtained at 24h (n = 2 each in Bleo- & saline-IT groups), 48h (n = 4 each group), and 72h (n = 2, each group) following treatments, had basolaterally projecting radial-glia processes positive for IL-1β at 48 and 72h, but not 24h (Sup Figure 1A–C). Analogously, in the median eminence, a CVO that mediates P→C I-comm to the hypothalamus, Bleo-IT (n = 4) but not saline-IT (n = 3) rats had IL-1β+ IR localized to radial-glia and tanycyte tight junctions at the base of the 3rd ventricle (Sup Figure 1J) (Langlet et al., 2013b). Moreover, this radial-glial IR pattern was completely absent in saline-treated rats (Sup Figure 1J). These data indicate that CVOs in addition to the AP respond to SLI.

Finally, we sought to determine whether other proinflammatory cytokines that: i) are systemically upregulated following lung injury (Tzouvelekis et al., 2005; Meduri et al., 2009), ii) exhibit P→C I-comm (Erickson and Banks, 2018) and, iii) modulate nTS cardiorespiratory circuits (Mollace et al., 2001; Hermann and Rogers, 2009; Takagishi et al., 2011; Rogers and Hermann, 2012), also showed IR specific to *FS* radial glia following SLI. Surprisingly, IL-6 and TNF-α immunostaining were absent in *FS* radial-glia (and their processes) of Bleo-IT and saline-IT treated rats at 48h (n = 3; Sup Figure 2A&2C) and 7d

(Bleo-IT: n = 4, Saline-IT: n = 5; Sup Figure 2B&2D), despite being present throughout the dm-brainstem in both treatment groups. Together these findings indicate that while not all proinflammatory cytokines exhibit localization to *FS* radial-glia following SLI, IL-1β IR is augmented within radial-glia at the barrier between the AP and adjacent dm-brainstem sites.

### 3.3. SLI promotes COX-2 expression in the glial-barrier of the AP and in adjacent sites in the dm-brainstem

Previous studies have demonstrated that structural changes to radial-glial processes can be mediated by cyclooxygenases (Prevot et al., 2003, 2010; de Seranno et al., 2004, 2010), which are downstream transcriptional targets for IL-1β signaling (Catania et al., 1991; Schiltz and Sawchenko, 2002; Mastronardi et al., 2007; Gosselin and Rivest, 2008). Therefore, we determined whether cyclooxygenase-2 (COX-2+) was differentially expressed at AP barrier sites and localized to radial processes. In Bleo- (n=7) compared to saline- (n=7) IT rats, COX-2+ IR staining was greater in the dbCC, *FS,* czAP, and DMNX ((Figure 3B1 - 3B4) 1) czAP: Bleo: 37.6 ± 5.9 vs. saline: 6.1 ± 1.9 AUs, $t_{12} = 5.02$, $P = 0.0003$; 2) dbCC: Bleo: 30.7 ± 4.3 vs. saline: 8.8 ± 3.4 AUs, $t_{12} = 3.96$, $P = 0.0019$; 3); *FS*: Bleo: 24.4 ± 3.6 vs. saline: 5.2 ± 0.9 AUs, $t_{12} = 5.15$, $P = 0.0003$; 4) DMNX: Bleo 18.9 ± 3.9 vs. saline: 3.5 ± 1.8 AUs, $t_{12} = 3.55$, $P = 0.004$, Two-tail t-Test). In Bleo-IT treated rats, heightened COX-2+ IR observed in the DMNX localized to the soma of motor neurons.

COX-2+ IR amplified by a nickel-DAB reaction showed COX-2 localized to radial-glial cells within the dbCC and *FS.* Further in Bleo- and not saline-IT rats, we noted a sparse population of COX-2+ radial-glia with basolateral projections at 24h (n = 2 each group), which became more apparent at 48h (n = 4 each group), and 72h (n = 2 each group) following SLI (Figure 3C–E). Together these findings show that COX-2+ IR spatially and temporally mirrors IL-1β+ IR throughout the radial-glial barrier separating AP and nTS, and suggests that COX-2 activation in the DMNX may also play a role in the CNS response to SLI.

### 3.4. SLI augments GFAP immunoreactivity at the AP glial-barrier and in adjacent dm-brainstem sites

Given that IL-1β co-localized with GFAP+ IR, we asked if GFAP+ IR was different in the glial-barrier in Bleo- (n = 7) compared to saline-IT (n = 7) rats (Figure 4). In both treatment groups, we observed robust GFAP+ IR in the *FS* and dbCC, and IR was greater in Bleo-IT than saline-IT rats ((Figure 4A, 4D&E) *FS*: Bleo: 36.9 ± 2.3 AUs vs. saline: 26.2 ± 2.8 AUs, $t_{12} = 3.02$, $P = 0.0098$; dbCC Bleo: 42.3 ± 3.8 AUs vs. saline: 30.2 ± 3.8 AUs, $t_{12} = 2.23$, $P = 0.044$, Two-tail t-Test). However, in the czAP GFAP+ IR staining was not robust, nor different between groups ((Figure 4F) Bleo: 2.93 ± 0.38 AUs vs. saline: 2.76 ± 0.41 AUs, $t_{12} = 0.29$, $P = 0.77$, Two-tail t-Test). In the DMNX and nTS, GFAP+ IR was greater in Bleo-versus saline-treated rats ((Figure 4G, 4H) DMNX: Bleo: 12.01 ± 1.25 vs. saline: 8.2 ± 1.2, $t_{12} = 2.23$, $P = 0.044$; nTS: Bleo: 57.3 ± 3.1 AUs vs. saline: 45.6 ± 3.8 AUs, $t_{12} = 2.4$, $P = 0.034$; Two-tail t-Test).

With co-labeling for GFAP and NeuN in Bleo (n = 3) and saline (n = 3) treated rats, nTS neurons with proximity to the *FS* appeared to contact the barrier's laterally projecting glial

processes (Figure 4B). Similarly, neurons in the DMNX apposed the glial barrier near the dbCC (Figure 4C).

To further investigate SLI-dependent changes within the *FS* we triple immuno-labeled brainstem sections from Bleo-IT rats (n = 3) for: i) GFAP (green), ii) MAP2, a dendritic microtubule marker (blue), and iii) vGluT2, a presynaptic glutamatergic marker (red) (Figure 4I). In Bleo-treated rats, glial processes localized to the *FS* were near both glutamatergic terminals and dendrites (Figure 4I). Similarly, glial processes emanated from the *FS* that apposed glutamatergic terminals and dendrites in the commissural nTS (Figure 4I). These data indicate that SLI augments GFAP expression at the perimeter of the AP and at adjacent dorsomedial brainstem sites; in particular: i) glutamatergic synapses target the *funiculus separans*, interweaving with dendrites that arise from nTS neurons, and ii) radial-glia originating from the *FS* terminate near to glutamatergic synaptic sites in the nTS. Thus, SLI may potentially alter either of these connections.

### 3.5. Lung injury increases sighs in general but reduces sighs that 'reset' the respiratory rhythm

We identified sighs based on the following three characteristics: 1) an augmented inspiration, 2) increased expiratory airflow and 3) prolonged expiration, which is referred to as post-sigh apnea (Figure 5B, top tracing dashed box). The uninjured groups of rats (S+V, n= 7; S+I, n= 7 rats) had 134 and 145 sighs, respectively; and injured groups (B+V n= 7 & B+I, n= 7 rats) had 301 and 371 (Figure 5C). Sighs occurred episodically throughout the recording; preferentially at the beginning; and then decreased as the rats became acclimatized to the chamber. Overall, the frequencies of sighs were greater in SLI than sham rats ((Figure 5C) B+V: 45.0 ± 4.4 vs. S+V: 29.8 ± 2.3 sighs/h, $P = 0.03$; B+I: 52.0 ± 5.2 vs. S+I: 32.6 ± 0.7 sighs/h, $P = 0.005$; Kruskal-Wallis test with Dunn's post hoc). The frequencies of sighs were not different between sham groups ((Figure 5C) S+V vs. S+I: $P > 0.94$; Kruskal-Wallis test with Dunn's post hoc)) nor between untreated and treated SLI rats ((Figure 5C) B+V vs. B+I, $P = 0.53$; Kruskal-Wallis test with Dunn's post hoc)).

Our subsequent analysis focused on a subset of sighs that act to 'reset' the respiratory rhythm; particularly, in sighs associated with a decrease in fR variability (Vlemincx et al., 2012, 2013). By our definition, a sigh associated with resetting the respiratory rhythm would: 1) decrease in CVfR at least ≥ 0.1 from before to after the sigh and 2) have a post-sigh CVfR ≤ 0.2 (Figure 5B and points contained in the highlighted area in Figure 5G1–5G4). Our criteria excluded a change in fR although fR generally decreased following a sigh in uninjured rats. 'Resetting' sighs (Figure 5B) occurred in each group (S+V, S+I, B+V & B+I; n = 7 rats in each group). In the saline-groups, 26.1% of the sighs in the S-V group and 29.5%, in the S+I group met the criteria for resetting sighs (highlighted in Figure 5G1–5G2 respectively). In contrast, in the lung-injured groups, only 7.3% of the sighs in the B-V group and 10.0% for the B+I group met the criteria for resetting sighs (highlighted in Figure 5G3–5G4 respectively).

We characterized the post-sigh apnea and pre-sigh CVfR for the resetting sighs. In this subgroup of sighs, the post-sigh apneas were less in SLI than sham rats in three of four comparisons between SLI and sham groups ((Figure 5D) B+V: 1.37 ± 0.90 vs. S+V: 1.91

± 0.87 s, $P = 0.05$; B+I: 1.04 ± 0.81 vs. S+I: 1.64 ± 0.61 s, P = 0.05; B+I vs. S+V Kruskal-Wallis test with Dunn's post hoc). The post-sigh apneas were not different between B+V and S-I, nor between sham groups ((Figure 5D) S+V vs. S+I: P > 0.94; Kruskal-Wallis test with Dunn's post hoc)) nor between untreated and treated SLI rats ((Figure 5C) B+V vs. B+I, P = 0.53; Kruskal-Wallis test with Dunn's post hoc)). In Bleo-IT rats that received Veh-ICV, the pre-sigh CVfR for the 10 s epoch preceding the sigh was not significantly different from either of the saline-IT control groups, nor from Bleo-IT rats that received Ind-ICV ((Figure 5E) B+V: 0.35 ± 0.02 vs. S+V: 0.49 ± 0.04, $P = 0.27$; B+V: vs. S+I: 0.48 ± 0.03, $P = 0.06$; B+V vs. B+I: 0.29 ± 0.01, $P = 0.29$; Kruskal-Wallis test with Dunn's post-hoc). However, pre-sigh CVfR for B+I rats was less than those for the control groups ((Figure 5E) B+I vs. S+I: $P < 0.0001$; B+I vs. S+V: $P < 0.0001$).

The post-sigh CVfR for the 10 s epoch after the sigh (and apnea) was greatest in injured untreated rats. The post-sigh CVfR of the Bleo-IT rats that received Veh-ICV was more than those of the control groups and that of the Bleo-IT treated rats that received Ind-ICV ((Figure 5F) B+V: 0.16 ± 0.01 vs. S+V: 0.10 ± 0.01, $P < 0.0001$; B+V: vs. S+I: 0.1 ± 0.01, $P < 0.0001$; B+V vs. B+I: 0.13 ± 0.01, $P = 0.007$; Kruskal-Wallis test with Dunn's post-hoc). In contrast, the post-sigh CVfR of the Bleo-IT rats that received Ind-ICV treatment was significantly greater when compared to those of the control groups ((Figure 5F) B+I vs. S+I: $P = 0.002$; B+I vs. S+V: $P = 0.005$). Thus, Ind-ICV treatment did not fully restore the incidence or magnitude of the effect of resetting sighs in Bleo-IT rats.

Finally we plotted all the pre- against the post- sigh CVfR. First, the distribution of points differed between SLI and sham plots in that the points for the SLI rats were clustered and those for the sham animals had a broad distribution. Second, the values for post-sigh CVfR of the BLEO-IT + Veh-ICV were shifted to the right (Figure 5G3, red arrowhead). This was reversed in those Bleo-IT + Ind-ICV treated rats (Figure 5G4, red arrowhead).

### 3.6. Intracerebroventricular infusion of Ind during the course of SLI prevents GFAP and IL-1β expression in the FS and dbCC

We determined whether COX-1/2 activity was required for changes in GFAP and IL-1β at the glial-barrier using brainstem sections from rats that were euthanized following the plethysmographic recording studies (Figure 5). Consistent with our previous results (Figure 4), the B+V group had increased GFAP+ IR in the dbCC compared to S+V and S+I groups. The increase in GFAP+ IR was prevented by Ind-ICV infusion ((Figure 7A & B) B+V: 16.4 ± 2.8 AUs, n = 10 vs. S+V: 7.1 ± 0.6 AUs, n = 7, $P = 0.008$; B+V vs. S + I: 7.7 ± 1.0 AUs, n = 7, $P = 0.014$; B + V vs. B+I: 6.5 ± 1.0 AUs, n = 14, $P = 0.0005$, One-way ANOVA with Tukey test, $F_{3,35} = 7.61$, treatment effect $P = 0.0005$). Additionally, GFAP+ IR in the dbCC of the B+I group was not different from the S+V and S+I groups, indicating that Ind fully abrogated the augmented GFAP+ IR ((Figure 7A&B) B+I vs. S+V: $P = 0.995$; B+I vs. S+I: $P = 0.969$, One-way ANOVA with Tukey test).

This effect of Ind ICV was evident in the other glial-border elements examined in the study. In the B+V group, GFAP+ IR in the *FS* (Figure 6C) and the DMNX (Figure 6D) increased compared to the other groups S+V, S+I and B+I (*FS*: B+V: 26.4 ± 4.9 AUs vs. S+V: 8.1 ± 1.2 AUs, $P = 0.0042$; B+V vs. S+I: 11.1 ± 2.2 AUs, $P = 0.02$; B+V vs. B+I: 13.3 ± 2.1, $P =$

0.03, One-way ANOVA with Tukey test, $F_{3, 30} = 5.89$, treatment effect $P = 0.0028$) (DMNX: B+V: 11.9 ± 1.7 AUs vs. S+V: 5.6 ± 0.7 AUs, $P = 0.026$; B+V vs. S+I: 5.3 ± 1.0 AUs, $P = 0.019$; B+V vs. B+I: 5.3 ± 1.2, $P = 0.003$, One-way ANOVA with Tukey test, $F_{3, 36} = 5.96$, treatment effect $P = 0.0021$). In both *FS* and DMNX, GFAP+ IR was not different among the B+I, and S+V and S+I groups ((Figure 6C&D) *FS*: B+I vs. S+V: $P = 0.714$; B+I vs. S+I: $P = 0.972$; DMNX: B+I vs. S+V: $P > 0.999$; B+I vs. S+I: $P > 0.999$).

Next we determined whether Ind treatment in SLI rats altered IL-1β expression in the glial-barrier structure of the dm-brainstem (Figure 7). In the B+V group, IL1β+ IR increased in the *FS* and dbCC. This was prevented by continuous Ind-ICV treatment ((Figure 7A&C) *FS*: B+V: 22.8 ± 2.9 AUs, n = 10 vs. S+V: 8.2 ± 1.9 AUs, n = 8, $P < 0.0001$; B+V vs. S+I: 7.1 ± 1.0 AUs, n = 8, $P < 0.0001$; B+V vs. B+I: 8.7 ± 1.0 AUs, n = 13, $P < 0.0001$, One-way ANOVA with Tukey test, $F_{3, 35} = 17.5$, treatment effect $P < 0.0001$) (dbCC: B+V: 15.5 ± 2.7 AUs vs. S+V: 3.3 ± 1.2 AUs, $P = 0.0001$; B+V vs. S+I: 2.3 ± 0.6 AUs, $P < 0.0001$; B+V vs. B+I: 4.9 ± 1.0 AUs, $P < 0.0001$, One-way ANOVA with Tukey test, treatment effect $F_{3, 35} = 13.16$, $P < 0.0001$). In the *FS* and dbCC, IL 1β+ IR was not significantly different between the B+I group and S+V and S+I groups (Figure 7B, 7C) (B+I *FS* vs. S+V *FS*: $P = 0.997$; B+I *FS* vs. S+I *FS*: $P = 0.92$, One-way ANOVA with Tukey test; B+I dbCC vs. S+V dbCC: $P = 0.905$; B+I dbCC vs. S+I dbCC: $P = 0.76$, One-way ANOVA with Tukey test).

Finally, in the B+V group, IL-1β+ IR increased in the czAP and DMNX compared to the S+V and S+I groups. This was also prevented by continuous Ind-ICV treatment ((Figure 7D&E) czAP: B+V: 22.8 ± 8.1 AUs vs. S+V: 0.6 ± 0.3 AUs, $P = 0.006$; B+V vs. S+I: 0.3 ± 0.1 AUs, $P = 0.005$; B+V vs. B+I: 4.8 ± 2.0 AUs, $P = 0.011$, One-way ANOVA with Tukey test, treatment effect, $F_{3, 30} = 6.28$, $P = 0.002$) (DMNX: B+V: 17.4 ± 4.2 AUs vs. S+V: 3.0 ± 0.8 AUs, $P = 0.0008$; B+V vs. S+I: 2.3 ± 1.0, $P = 0.0004$; B+V vs. B+I: 2.8 ± 0.8 AUs, $P < 0.0001$, One-way ANOVA with Tukey test, treatment effect $F_{3, 32} = 11.04$, $P < 0.0001$). Similar to our previous findings, IL-1β+ IR in the B+I group did not differ from S+V and S+I groups ((Figure 7D&E) czAP: B+I vs. S+V: $P = 0.876$; B+I vs. S+I czAP: $P = 859$, One-way ANOVA with Tukey test; DMNX: B+I vs. S+V: $P = 0.999$; B+I vs. S+I: $P = 0.997$, One-way ANOVA with Tukey test). Together these data indicate that central Ind treatment prevents the SLI-dependent increase in IL-1β in the barrier separating AP from other dm-brainstem sites.

## 4. Discussion

### 4.1. Summary of our findings

Using a rodent model of bleomycin-induced SLI (Kaminski et al., 2000; Borzone et al., 2001; Cutillo et al., 2002; Babin et al., 2011), we showed that the dbCC and *funiculus separans*, cellular interfaces separating the AP from neighboring dm-brainstem sites, respond to this peripheral immune challenge by promoting IL-1β accumulation within radial-glial processes. The increase in IL-1β within AP barrier radial-glia occurred concurrently: i) with increases in the astrocyte/tanycyte/ependymal marker GFAP, ii) with increases to COX-2, a downstream transcriptional target for IL-1R signaling, and iii) in the absence of proinflammatory cytokines TNF-α or IL-6, which can also mediate P→C I-comm (Herz and Kipnis, 2016). Thus, analogous to other BBB neuroimmune pathways,

AP radial-glia exhibited specificity for inflammatory stimuli and the immune-mediators they use to transmit inflammation to the CNS (Erickson and Banks, 2018). This specificity may have consequences for cardiorespiratory control. Bleo-IT treated rats had an augmented sigh frequency but a decreased in sighs that reset the rhythm. Continuous central infusion of Ind, a COX-1/2 inhibitor, during the course of the SLI restored a decrease the variability of fR in the post-sigh breathing pattern. Concurrently, Ind-treatment prevented the SLI-dependent increase to GFAP and IL-1β IR within the glial-barrier and also in adjacent dm-brainstem sites. Together these findings demonstrate that the AP and its radial-glia respond to the immune response following SLI, and by virtue of their direct contact with autonomic control sites, likely contribute to changes in cardiorespiratory function.

### 4.2. Microglia/macrophage response within the AP and in adjacent dm-brainstem sites following SLI

In CVO sites that contact fenestrated capillaries, microglia/macrophages exhibit distinct morphologic characteristics relative to microglia/macrophages in adjacent sites (Takagi et al., 2017), and can be activated by some forms of sterile inflammation (Lee et al., 2010). Iba-1+ cells within the AP exhibited discrete morphologic changes following SLI, which corresponded to glial-barrier sites interfacing with fenestrated capillaries (*funiculus separans)* or CSF (dbCC). Microglia/macrophages localized to the dbCC were increased following SLI, and exhibited *hyper*-ramified morphology; this was indicated by an increased length and number of appendages (Streit et al., 1999; Hinwood et al., 2013; Karperien et al., 2013; Hellwig et al., 2016; Litvin et al., 2018). Although it is unclear whether the increase in Iba-1+ cells is due to recruitment or proliferation at the dbCC, SLI caused immune activation of cells lining the CC. This may reflect inflammatory transmission from the AP to the dbCC; or alternatively, inflammatory transmission from the CSF to the dbCC (Furube et al., 2018); or both.

In contrast, microglia/macrophages localized to the czAP did not differ in number and exhibited *hypo*-ramified morphology, decreased length and number of appendages. The *hypo*-ramified morphology was also observed in the DMNX following SLI, and was reminiscent of morphology changes we reported previously (Litvin et al., 2018). Thus, SLI promotes similar microglial morphology changes in the DMNX and the czAP. Indeed, peripheral immune activation by LPS does promote microglia/macrophage changes in CVOs that are “mirrored” in neighboring brain regions, and absent in more distal CNS sites (Furube et al., 2018). Our findings suggest this mirroring can also be present during SLI, but may occur through separate mechanisms from those used by non-sterile inflammation.

### 4.3. IL-1β and COX-2 activation at glial-barrier sites following SLI

In settings of sterile or non-sterile peripheral inflammation, P→C I-comm can occur through an IL-1β-mediated COX-2 dependent $PGE_2$ synthesis at BBB endothelium (Laflamme et al., 1999; Ek et al., 2001; Engström et al., 2012; Wilhelms et al., 2014), which can also occur in CVOs such as the AP (Elmquist et al., 1997; Ericsson et al., 1997; Schiltz and Sawchenko, 2002; Dallaporta et al., 2007). In the current study, a similar pathway could be active within CVOs following the immune response to SLI (Chen and Nuñez, 2010; Shen et al., 2013; Rubartelli et al., 2014). In particular, our findings indicated IL-1β+ IR was present not only

at the site of interface between peripheral circulation and AP parenchyma (czAP), but also at glial-barrier sites contacting the CC, nTS and DMNX. At these barrier sites, IL-1β+ IR was restricted to radial-glia processes and co-localized with GFAP. The identity of these IL-1β+ IR glia is informed in part by the pattern of IL-1β immunostaining in the median eminence, a CVO featuring GFAP+ tanycytes, which similarly separate peripheral circulation from brain parenchyma and CSF (Erickson and Banks, 2018). Importantly, a major function of median eminence tanycytes is the transport of circulating factors into hypothalamic parenchyma and/or CSF (Langlet et al., 2013a; Balland et al., 2014). For example uptake of fluorescently labeled leptin by median eminence tanycytes shows localization within thin elongated processes (Balland et al., 2014), which simulates the pattern of IL-1β IR observed following SLI. This raises the possibility that radial-glia in the AP mediate IL-1β uptake and transport into the CNS rather than *de-novo* synthesis. Indeed, several mechanisms for IL-1β uptake have been reported (Lowenthal and MacDonald, 1986; Qwarnstrom et al., 1988; Blanton et al., 1989; Brissoni et al., 2006; Pan et al., 2011; Sadowska et al., 2015). For example, ERK signaling could mediate radial-glia uptake and release of IL-1β (Qwarnstrom et al., 1988; Brissoni et al., 2006; Skinner et al., 2009). This mechanism is intriguing because of evidence that Ind can block ERK signaling (Pan and Hung, 2002; Nikolopoulou et al., 2014). Thus, Ind-treatment in SLI rats may attenuate the release of endocytosed IL-1β (by radial-glia) into the dorsomedial brainstem following SLI.

Consistent with this interpretation, CASP-1+ IR in the dbCC and *FS* did not exhibit any localization to radial-glia in either treatment group, and was not significantly altered by SLI; the heightened CASP-1+ IR in the dbCC was strictly associated with cuboidal ependymal-like cells interfacing with the CSF that lacked long processes (Pecchi et al., 2007). Contrastingly to barrier sites, we observed heightened CASP-1 IR in the DMNX, suggesting *de-novo* IL-1β synthesis may influence efferent vagal pathways. Importantly, immune-dependent changes to DMNX cardio-pulmonary efferent pathways may not contribute directly to the SLI-dependent changes in respiratory patterning (Kalia and Mesulam, 1980; Kalia, 1981; Pérez Fontán et al., 2000), but could act indirectly through control of airway caliber (Lai et al., 2016) or anti-inflammatory reflexes (Abe et al., 2017; Pavlov and Tracey, 2017).

We also demonstrated that following SLI, COX-2+ IR is concurrently elevated within the same dm-brainstem sites as IL-1β. The processes governing these immune mediators may be functionally linked (Ek et al., 2001). However, a strict serial progression from IL-1β to COX-2 is not necessary. For example, COX-2 expression can: i) occur independently of IL-1β release (Prevot et al., 2003; Rummel et al., 2006; Eskilsson et al., 2014a; Xia et al., 2015), ii) occur in timescales too rapid for cytokine production – especially in the regulation of cerebral blood flow (Takano et al., 2006; Macvicar and Newman, 2015; Masamoto et al., 2015), and iii) act reciprocally to regulate IL-1β release (Hua et al., 2015; Daniels et al., 2016). Consistent with this non-linear view, we observed inhibition of augmented IL-1β immunoreactivity in SLI rats treated with Ind. This suggests alternative central COX-mediated signaling pathways may also play a role in transmitting SLI to the brain.

In Bleo-IT rats, we observed a significant increase in COX-2+ IR within the *FS*, dbCC, czAP, and also in the DMNX. Analogous to our IL-1β findings, COX-2 IR in *FS* and dbCC

of Bleo-treated rats exhibited a progressive accumulation within radial-glia processes. A subset of these processes also projected basolaterally into dm-brainstem sites. COX-2+ IR in the DMNX of Bleo-treated rats was localized to neurons, which was largely absent in saline-treated rats. This raises the possibility of its involvement in processes related to: i) cell-survival or apoptosis, ii) synaptic plasticity, and/or iii) homeostatic functions associated with febrile responses (Kaufmann et al., 1996; Samad et al., 2001; Chen et al., 2002; Marty et al., 2008; Strauss, 2008; Tian et al., 2008; Yang and Chen, 2008; Lacroix et al., 2015). Recent work from our lab demonstrated a SLI-dependent microglia/macrophage-mediated depression of acute hypoxic-hypercapnic ventilatory sensitivity and post-synaptic depression of viscerosensory transmission to the nTS. In the context of our current findings, it is possible that these functional changes are COX-2 mediated, and that similar changes in glutamatergic transmission may be occurring in the DMNX (Litvin et al., 2018).

### 4.4. SLI-dependent increase in GFAP within the glial-barrier

We demonstrated that radial-glia comprising the barrier between AP parenchyma and neighboring dm-brainstem sites exhibited augmented GFAP+ IR following SLI. However, we did not observe significant differences in GFAP+ IR localized to the czAP, which also shows close association with fenestrated capillaries (Langlet et al., 2013b; Mannari et al., 2013; Morita et al., 2016). GFAP+ glia within the czAP contribute to immune-surveillance of the peripheral circulation; however, exposure to a particular morbidity factor (i.e. LPS) did not necessarily cause morphologic changes (Elmquist et al., 1997; Mannari et al., 2013; Nakano et al., 2015; Yoshida et al., 2016). Thus, stimulation of czAP astrocytes/tanycytes by SLI may not necessarily be reflected in GFAP+ IR changes. Additionally, the comparatively low GFAP expression present within the czAP may have encumbered our ability to detect potential IR differences between treatment groups.

Changes in GFAP+ IR were not restricted to the AP-barrier sites, as dm-brainstem sites directly adjacent to the *funiculus separans* also exhibited augmented IR. Moreover, neurons and glutamatergic synapses in close proximity to barriers appeared to share greater contact with GFAP+ processes projecting basolaterally from the barrier. This suggests radial-glia in the *FS* and dbCC may participate directly in gating viscerosensory circuit function in the nTS/DMNX (Mcdougal et al., 2012; Accorsi-Mendonca et al., 2015; Matott et al., 2016). It also suggests the peripheral immune response to Bleo-IT (Xu et al., 2006; Razavi-Azarkhiavi et al., 2014; Skurikhin et al., 2015) may promote functional changes in adjacent dorsomedial brainstem sites (Litvin et al., 2018) by stimulating the glial-barrier. Analogous findings have been reported in other CVOs following peripheral LPS administration (Sofroniew, 2015). These findings are important because they are the first to demonstrate that a form of lung injury, which exhibits a sterile inflammatory response (Adamson and Bowden, 1974; Jiang et al., 2005, 2007; Hoshino et al., 2009; Chen and Nuñez, 2010), can evoke changes to GFAP expression within brainstem sites critical for coordinating febrile response and sickness behavior (Goehler et al., 2006; Wuchert et al., 2008).

### 4.5. Alterations in sighs after SLI are partially mediated through central COX activation

Inflammation in the dorsal vagal complex alters respiratory and autonomic control during systemic inflammation (Gordon, 2000; Hermann et al., 2002; Blatteis, 2007; Jacono et

al., 2011; Pavlov and Tracey, 2012b; Babic and Browning, 2013; Nardocci et al., 2015; Hsu et al., 2017; Litvin et al., 2018). Two obvious changes are that respiratory frequency (fR) and rate of sigh occurrences increased 7d following SLI. However, even though both occurred, in the majority of rats frequency of spontaneous sighs does not correlate to fR (see supplemental data). While this appears inconsistent with COX-1/2 playing a critical role in eliciting sighs, this interpretation assumes that the Ind-ICV reaches the ventrolateral medulla, which contains the Pre-Bötzinger Complex, which is an inspiratory-facilitatory nucleus essential for sighs (Baertsch et al., 2019). Further, sighs are not a single entity; but rather, they have multiple physiologic (relief of atelectasis) and psychological (relief of anxiety) functions; and are associated with arousal. Numerous neuromodulators, including PGE2 elicit sighs (Koch et al., 2015; Forsberg et al., 2016; Li et al., 2016). Thus, distinct neural circuits evoke sighs for various reasons.

We focused on sighs that reset the respiratory rhythm, specifically because resetting sighs require vagal input to evoke the response (Widdicombe, 2003). In our prior studies (Litvin et al., 2018; Getsy et al., 2019), we showed that 7d after SLI the neuroimmune response to the injury reduced the efficacy of synaptic transmission between vagal afferents and 2nd-order nTS neurons. Thus, in understanding mechanisms of variability, neural inflammation in the dm medulla would reduce the 'loop gain' of the vagal feedback, which would attenuate capability of vagal input resetting the rhythm in the SLI rats (Cherniack et al., 1981; Khoo, 2000). In contrast, the persistence of post-sigh apnea, which occurs even in sigh occurring *in vitro* indicate their duration is not as dependent on the strength of vagal input (Ramirez, 2014).

We evaluated respiratory frequency (fR) before and after sighs and identified those that decreased the coefficient of variation of fR (CVfR) ≥10% and resulted in a post-sigh CVfR ≤20%. We used these criteria to define resetting sighs as the respiratory rhythm became more regular after compared to before the sigh. We found that resetting sighs as a percentage of the total number of sighs, decreased dramatically in SLI compared to sham rats. The incidence of resetting sighs doubled in SLI rats treated with Ind ICV, and was halfway between the sham and the untreated SLI groups. Further, while resetting sighs reduced pattern variability much more in sham than SLI rats, treatment with Ind-ICV restored partially the magnitude of reduction CVfR following sighs in SLI rats. In summary, Ind restored characteristics of resetting sighs but did not modest effect on the occurrence of sighs.

## 4.6. Limitations of the study

**4.6.1. Ind-ICV administration—**A key finding of this study was that SLI induced up-regulation of IL-1β within the nTS represented not only an important step in P→C I-comm, but also a mechanism for modulating respiratory pattern. However, the use of Ind-ICV as a pharmacological intervention to block central COX-1/2 signaling raises several important caveats necessary for interpreting our findings. First, 7d after the induction of SLI the respiratory pattern changes that were blunted with continuous Ind-ICV treatment, were associated with two distinct (but likely related) immune-dependent mechanisms. These mechanisms involve: i) the neuromodulatory action of immune mediators in the nTS,

which can acutely alter cardiorespiratory and synaptic activity similar to conventional peptides/transmitters in the CNS (Laaris and Weinreich, 2007; Marty et al., 2008; Takagishi et al., 2011; Huda et al., 2018), and ii) the neuroplastic action of immune mediators in the nTS, which can promote lasting changes to cardiorespiratory and synaptic activity through plasticity-like mechanisms such as postsynaptic receptor insertion/removal (Accorsi-Mendonca et al., 2015; MacFarlane et al., 2016; Hockera et al., 2017; Litvin et al., 2018; Getsy et al., 2019). Thus, ICV-Ind treatment during the course of SLI could affect both the acute and chronic impact of immune activation on the dm-brainstem.

Second, the anti-inflammatory capacity of Ind has been primarily attributed to reversible binding at the COX-1/2 active site; this prevents binding of its endogenous substrate arachidonic acid, blocking Prostaglandin-G2/H2 (PGG2/PGH2) formation (Kurumbail et al., 1996). Its lack pharmacologic specificity raises the possibility that both isoforms may be involved in P→C I-comm following SLI (Griffin et al., 2013; Calvello et al., 2017). Indeed there is evidence that central COX-1 has discrete immune regulatory functions (Choi et al., 2009, 2010, 2013; Aid et al., 2010) and may be selectively induced by IL-1β (Griffin et al., 2013). However COX-2 was elevated in the dm-brainstem following SLI and was a likely target of Ind-ICV treatment. Alternatively, in addition to COX-1, COX-2 is constitutively expressed in the CNS/PNS, and may be functionally distinct from inducible COX-2 (Niwa et al., 2000; Ghilardi et al., 2004; Choi et al., 2009). Thus, inhibition of COX-2 48h before the induction of SLI raises the possibility that Ind-ICV's inhibition of constitutive (rather than inducible) COX-2 was responsible for blunting the neuroimmune response observed at 7d.

Third, Ind can act upon multiple sites in the prostaglandin pathway as follows: i) upstream of COX-1/2, by inhibiting Phospholipase A2 dependent release of arachidonic acid (Kaplan et al., 1978; Singh et al., 2004; Dahan and Hoffman, 2007); ii) downstream of COX-1/2 by inhibiting Prostaglandin Reductase (PTGR2), a terminal step in the inactivation of prostaglandins (Clish et al., 2001; Wu et al., 2008); iii) Ind can mimic endogenous functionality of 15-keto-PGE2 (substrate for PTGR2) as an agonist for Peroxisome proliferator-activated receptors (PPAR) α/γ (Lehmann et al., 1997; Sastre et al., 2003; Wu et al., 2008), which can blunt CNS immune activation (Bernardo and Minghetti, 2006; Villapol, 2018). Thus, Ind's anti-inflammatory capacity is largely dependent upon the modulation of prostaglandin (PG) biosynthesis pathways.

Further, Ind-ICV can act independently of PG-related processes. For example, Ind can inhibit: i) NF-κB signaling (Poligone and Baldwin, 2001; Sung et al., 2004), ii) activation of the NLRP3 inflammasome (Elliott and Sutterwala, 2015; Hua et al., 2015; Daniels et al., 2016; Hoseini et al., 2018), and iii) ERK signaling (Pan and Hung, 2002; Nikolopoulou et al., 2014). Thus, caution is necessary in fully attributing SLI-dependent P→C I-comm specifically to COX-1/2, or more generally to PG-related processes.

Fourth, Ind-ICV could potentially blunt peripheral inflammation through its central action on the (splenic) cholinergic anti-inflammatory pathway (CAP). This pathway includes bulbospinal C1 neurons and their axonal projections to the DMNX (Inoue et al., 2016; Abe et al., 2017; Pavlov and Tracey, 2017; Komegae et al., 2018; Murray et al., 2019). Indeed, there is evidence COX-1/2 and PGE2 can modulate brainstem CAP circuits (Ericsson

et al., 1997; Iyonaga et al., 2019). The SLI-dependent inflammatory changes observed in the DMNX that were inhibited by Ind-ICV, bolster this possibility. Thus, we cannot fully exclude the potential role for Ind-ICV in also blunting SLI-dependent peripheral inflammation by acting centrally on the CAP pathway.

Fifth, it is unclear whether central Ind administration also exerted influence over the peripheral immune response to SLI via efflux across the BBB. Ind exhibits weak BBB permeability that is restricted by its albumin binding (Parepally et al., 2006; Banks, 2019). However, NSAIDs undergo CSF→Blood reverse trancytosis (Stock et al., 2006; Dvir et al., 2007; Mannila et al., 2007). These factors raise the possibility of Ind-ICV efflux into the periphery. To test the effect of Ind efflux across the BBB, Catania et al. administered Ind centrally at a dose that was effective when delivered peripherally. Central Ind failed to affect the peripheral immune response (Catania et al., 1991). The daily dose of Ind delivered ICV that we used was an order of magnitude less than that used by Catania et al. (1991). Thus, efflux of Ind is unlikely to have affected the peripheral response.

Sixth, while most drugs undergo rapid convection (bulk flow) through CSF flow tracts, this is often conflated with the rate of drug diffusion from the CSF into CNS parenchyma, which contrastingly is significantly slower (Blasberg et al., 1975; Mak et al., 1995; Mannila et al., 2005, 2007; Pardridge, 2011, 2012; Di et al., 2013; Metzger et al., 2017). Indeed, drug diffusion into the CNS decreases exponentially with distance from the surface and is further constrained by factors such as molecular weight, drug metabolism, binding at the CNS surface, and glymphatic uptake (Pardridge, 2011; Hladky and Barrand, 2014; Banks, 2019). In practical terms, this means ependymocytes/radial-glia at the interface between the CSF and CNS are maximally exposed to Ind-ICV (Blasberg et al., 1975; Pardridge, 2011), while CNS sites deeper than ~1mm are likely minimally affected (Blasberg et al., 1975; Mannila et al., 2005; Pardridge, 2011; Di et al., 2013). This suggests a majority of the CNS parenchyma was not directly exposed to Ind-ICV, but does not exclude multiple brainstem sites associated with respiratory control that are ≤1 mm from the ventral surface (Feldman et al., 2003; Dick et al., 2018).

Indeed, in addition to evidence for respiratory-control modulation by PG-biosynthesis pathways in the nTS, there is also evidence implicating these immune mediators in direct control of: 1) rhythmogenesis via the pre-Bötzinger complex (preBötC) (Koch et al., 2015; Forsberg et al., 2016), and 2) $CO_2$-sensitivity via the retrotrapezoid nucleus/parafacial respiratory group (RTN/pFRG) (Forsberg et al., 2017). Thus, neuroimmune activation in either the preBötC or RTN/pFRG (rather than the nTS) could be responsible for the changes in respiratory activity observed following SLI. Moreover, both the preBötC and the RTN/pFRG receive direct synaptic input from the nTS, which raises the possibility that central immune activation within the nTS could promote axonal release of PGs at downstream ventromedullary respiratory circuits, and undergo inhibition by Ind-ICV (Wang et al., 2005).

Finally, Ind is largely insoluble in aqueous solution; this necessitated the use of the organic solvent dimethyl sulfoxide (DMSO), which at a concentration of ≤50% (v/v) is compatible with Alzet® osmotic pumps (Williams, 2007). However, DMSO is an antioxidant that has been reported to exhibit both anti-inflammatory (DeForge et al., 1992; Santos et al.,

2003; Elisia et al., 2016) and pro-inflammatory (DeForge et al., 1992; Xing and Remick, 2005; Xiang et al., 2018) properties. Further, there is some evidence DMSO can selectively up-regulate IL-1β transcription (Xing and Remick, 2005), however we did not observe increased IL-1β+ IR in the Ind-ICV control group that received saline-IT. Nonetheless, it is possible that inhibition of SLI-dependent neuroinflammation, which was attributed to Ind-ICV treatment, could have arisen from the use of DMSO as our vehicle.

**4.6.2. Further considerations—**This set of findings represents a brief snapshot of neuroimmune status, focusing primarily on the peak pulmonary immune response to Bleo-IT (at day 7) (Kaminski et al., 2000; Borzone et al., 2001; Cutillo et al., 2002; Babin et al., 2011). It is unclear whether brainstem IL-1β upregulation at 48h post Bleo-IT (Jacono et al., 2011) is also dependent on central COX activation and thus potential positive feedback. Further, there are multiple mechanisms by which administration of Ind into CSF circulation (during SLI) may have inhibited IL-1β expression at both "sides" of the glial-barrier between the AP and adjacent brainstem regions. This could occur through 4th-ventricle CSF diffusion into: i) the AP parenchyma, where it could block *FS* COX-1/2 from the "outside", ii) the dm-brainstem parenchyma that sits lateral to the AP (medial nTS), where it could block *FS* COX-1/2 from the "inside", and iii) the central canal, where it could diffuse into the dorsal brainstem and also act from the "inside". Additional mechanisms include decreased permeability and/or active transport across the BBB, reduced local production of IL-1β, or impaired neural transport of cytokines, (Löscher and Potschka, 2005; Hladky and Barrand, 2014; Novakova et al., 2014; Erickson and Banks, 2018).

Given that the AP is a circumventricular organ that receives neural innervation, it is a confluence of circulating and neural pathways (Shapiro and Miselis, 1985). We have focused on blood borne cytokine induction but viscerosensory projections to the AP/nTS likely contribute to the central immune response characterized in our study. Vagal pathways can trigger central inflammatory cascades in response to peripheral inflammation (Ek et al., 1998, 2001; Balan et al., 2011). For example, vagal afferent fibers form a neural pathway from the trachea and project to the ventrolateral AP. Thus, the AP may serve as a common node mediating multiple pathways to neural inflammation.

There is also sufficient evidence for activation of multiple CVOs following peripheral inflammation (Breder et al., 1994; Elmquist et al., 1997; Quan et al., 1997; Rummel et al., 2004; Erickson and Banks, 2018; Furube et al., 2018). Despite evidence that CVO control of sickness behaviors (i.e. fever, anorexia, hyperalgesia, or tachypnea) exhibits functional overlap/redundancy, sites are specialized for secretion (ME, SCO, or the pineal gland), others are specialized for peripheral humorosensory activity (AP, SFO, or OVLT), and discrete physiologic functions can be attributed to each of the CVOs under pathologic conditions (Wei et al., 2013a; Tsai et al., 2014; Parkash et al., 2015; Konsman, 2016; Hsu et al., 2017). For example, growth differentiation factor (GDF)-15 is a cytokine in the TGF-β superfamily, which is upregulated in the lungs and circulation following pulmonary injury (Verhamme et al., 2017, 2019; Zhang et al., 2019). The central anorexic effects evoked by peripherally circulating GDF-15 are mediated exclusively through an AP/nTS transmission pathway that activates neurons in the lateral parabrachial nucleus (Tsai et al., 2014; Hsu et al., 2017; Yang et al., 2017; Mullican and Rangwala, 2018). Such specificity for a P→C

I-comm pathway is unexpected given evidence the GDF-15 receptor is present not only within the AP/nTS but also at other CNS sites including CVOs (Schober et al., 2001; Uhlen et al., 2005, 2015; Lein et al., 2007; Sunkin et al., 2013; Emmerson et al., 2017; Hsu et al., 2017; Kostuk et al., 2019). Analogously, activation of an AP/nTS dependent P→C I-comm pathway may be necessary for mediating aspects of the altered respiratory pattern evoked by SLI.

Reciprocal connectivity exists between AP and nTS (Cunningham et al., 1994; Cai et al., 1996; Abegg et al., 2017; Kawai, 2018; Ito and Seki, 1998; Kawai, 2018) and between nTS and DMNX (Willis et al., 1996; Babic and Browning, 2013; van der Kooy and Koda, 1983; Babic and Browning, 2013) and from AP to DMNX (Vigier and Portalier, 1979; Ito and Seki, 1998; Abegg et al., 2017). There has also been some evidence indicating that *FS* radial glia ramifications may make contact with nTS neurons (Guillebaud et al., 2017). However, it is unclear whether these contacts serve to further connect the AP and nTS. In published studies DiI and/or other retrograde tracers that readily label astrocytes and tanycytes did not label radial glia in the *FS* following injection in the AP even though fibers of passage between affiliated brainstem sites were labeled following the injection (Shapiro and Miselis, 1985; Chauvet et al., 1995; Ito and Seki, 1998; Malatesta et al., 2000; Sun and Jakobs, 2013; Abegg et al., 2017; Kawai, 2018). Elucidating the connectivity between *FS* and these regions will require a targeted approach such as: i) partial surgical resection of the AP for direct placement of DiI crystals onto the *FS* (without damaging the *FS*), or ii) greater knowledge of specific peptides expressed by radial glia of the *FS* such as *Rax* (Pak et al., 2014; Chen et al., 2017), which could be targeted virally in a CRE-dependent manner.

Finally, the variability of physiologic signals has been used extensively as a biometric for health status; this includes ventilatory pattern variability (Kelsen et al., 1982; Coumel and Leenhardt, 1991; Seely and Christou, 2000; Schmidt et al., 2001; Parati et al., 2013; Haack et al., 2014; Manning et al., 2015; Warren et al., 2018). Furthermore, we and others (Yamauchi et al., 2008; Vlemincx et al., 2012, 2013; Ramirez, 2014) theorize that sighs can reset the breathing pattern and this depends on the sensory signaling of the pulmonary stretch receptors and results in a reduction of the ventilatory pattern variability; resetting of the respiratory rhythm is defined by a reduction in variability following the sigh. This was assessed using coefficient of variability for the respiratory frequency (CVfR), a normalized measure of variance (standard deviation divided by the mean fR), which is an established measure of variability. Our focus on the variability of the pattern after the sigh was based on evidence that the neuroimmune response to SLI reduced synaptic transmission between vagal afferent fibers and 2nd-order neurons in the nTS (Litvin et al., 2018; Getsy et al., 2019). This loss of synaptic efficacy is consistent with the reduction in ‘resetting sighs’; a subset of sighs in which the CVfR had to have decrease ≥0.1 from before to after the sigh, and CVfR after sigh was ≤0.2. Consistent with our hypothesis, the resetting’ sighs were more effective in the B+I than the B+V.

### 4.7. Conclusions

In the current study we demonstrated a pathway to central inflammation activated by a peripheral injury that occurs in the absence of microbial activators. This pathway: i)

activates radial-glia in the dbCC and *FS*, which is a target for the immune response to SLI, ii) is mediated by IL-1β and COX-1/2 within the glial-barrier separating peripheral circulation from autonomic control circuits in the dm-brainstem, and iii) contributes to the increase in post-sigh apneas following SLI. Together this suggests P→C I-comm pathways utilized by sterile immune challenges target AP border radial-glia and may contribute to changes in cardiorespiratory function by virtue of their direct contact with autonomic control sites. These mechanisms are summarized in a conceptual model (Figure 8). Additional studies should examine mechanistic similarities and differences of sterile and non-sterile P→C I-comm pathways.

## Supplementary Material

Refer to Web version on PubMed Central for supplementary material.

## Acknowledgements:

The authors thank the School of Medicine Light Microscopy Imaging Core at Case Western Reserve University for their technical support. The authors also thank Shyue-An Chan and David Nethery for support with experimental design, data analysis and manuscript editing.

Funding:

This work was supported by grants from the National Institutes of Health T32 HL007913 (D.G.L.), by Award IO1BX000873 from the Biomedical Laboratory Research & Development Service of the VA Office of Research and Development (F.J.J.), by the National Institutes of Health U01 EB021960 (T.E.D.), and by NIH 4R00HL119606–02 and the Missouri Spinal Cord Injury/Disease Research Program (N.L.N).

## Abbreviations:

| | |
|---|---|
| **AP** | area postrema |
| **BBB** | Blood Brain Barrier |
| **B+I** | Bleomycin administered intratracheally (Bleo-IT) + Indomethacin administered intracerebroventricularly (Ind-ICV) |
| **B+V** | Bleo-IT + Vehicle-ICV |
| **BEPs** | Branch endpoints |
| **Bleo** | Bleomycin |
| **Br#** | Branch number |
| **CC** | central canal |
| **CNS** | central nervous system |
| **COX-1/2** | cyclooxygenase-1/2 |
| **CPUV** | cells per unit volume ($10^6$ cells/$\mu m^3$) |
| **CV** | coefficient of variation |

| | |
|---|---|
| **CVfR** | coefficient of variation for respiratory frequency (fR) |
| **CVO** | circumventricular organ |
| **czAP** | central zone of the area postrema |
| **dbCC** | dorsal border of the Central Canal |
| **dm** | dorsomedial |
| **DMNX** | dorsal motor nucleus of the vagus |
| **fR** | respiratory frequency |
| ***FS*** | *funiculus separans* |
| **GFAP** | glial fibrillary acidic protein |
| **ICV** | intracerebroventricular |
| **IL-1β** | Interleukin-1 beta |
| **Ind** | indomethacin |
| **IT** | intratracheal |
| **nTS** | nucleus tractus solitarii |
| **P→C I-comm** | Peripheral to central immune communication |
| **PBST** | phosphate buffered saline + triton-x |
| **S+I** | Saline IT+ Ind-ICV |
| **S+V** | Saline IT + Veh-ICV |
| **SLI** | sterile lung injury |
| **TBL** | total branch length |
| **Veh** | vehicle |

## References

Abe C, Inoue T, Inglis MA, Viar KE, Huang L, Ye H, Rosin DL, Stornetta RL, Okusa MD, Guyenet PG (2017) C1 neurons mediate a stress-induced anti-inflammatory reflex in mice. Nat Neurosci 20:700–707. [PubMed: 28288124]

Abegg K, Hermann A, Boyle CN, Bouret SG, Lutz TA, Riediger T (2017) Involvement of Amylin and Leptin in the Development of Projections from the Area Postrema to the Nucleus of the Solitary Tract. Front Endocrinol (Lausanne) 8:4–10. [PubMed: 28163696]

Accorsi-Mendonca D, Almado CEL, Bonagamba LGH, Castania J a., Moraes DJ a., Machado BH (2015) Enhanced Firing in NTS Induced by Short-Term Sustained Hypoxia Is Modulated by Glia-Neuron Interaction. J Neurosci 35:6903–6917 Available at: http://www.jneurosci.org/cgi/doi/10.1523/JNEUROSCI.4598-14.2015. [PubMed: 25926465]

Adamson IY, Bowden DH (1974) The pathogenesis of bleomycin-induced pulmonary fibrosis in mice. Am J Pathol 77:185–197 Available at: http://www.pubmedcentral.nih.gov/articlerender.fcgi?artid=1910906&tool=pmcentrez&rendertype=abstract. [PubMed: 4141224]

Aid S, Silva AC, Candelario-Jalil E, Choi SH, Rosenberg GA, Bosetti F (2010) Cyclooxygenase-1 and-2 differentially modulate lipopolysaccharide-induced blood-brain barrier disruption through matrix metalloproteinase activity. J Cereb Blood Flow Metab 30:370–380 Available at: 10.1038/jcbfm.2009.223. [PubMed: 19844242]

Akanuma SI, Uchida Y, Ohtsuki S, Tachikawa M, Terasaki T, Hosoya KI (2011) Attenuation of prostaglandin E2elimination across the mouse blood-brain barrier in lipopolysaccharide-induced inflammation and additive inhibitory effect of cefmetazole. Fluids Barriers CNS 8:1–11. [PubMed: 21349146]

Anderson CR, Ashwell KW, Collewijn H, Conta A, Harvey A, Heise C, Hodgetts S, Holstege G, Kayalioglu G, Keast JR, McHanwell S, McLachlan EM, Paxinos G, Plant G, Scremin O, Sidhu A, Stelzner D, Watson C (2009) The Spinal Cord: A Christopher and Dana Reeve Foundation Text and Atlas. In: The Spinal Cord.

Arganda-Carreras I, Fernández-González R, Muñoz-Barrutia A, Ortiz-De-Solorzano C (2010) 3D reconstruction of histological sections: Application to mammary gland tissue. Microsc Res Tech 73:1019–1029. [PubMed: 20232465]

Babic T, Browning K (2013) The role of vagal neurocircuits in the regulation of nausea and vomiting. Eur J Pharmacol January 5:38–47 Available at: http://www.ncbi.nlm.nih.gov/pubmed/12181177.

Babin AL, Cannet C, Gérard C, Wyss D, Page CP, Beckmann N (2011) Noninvasive assessment of bleomycin-induced lung injury and the effects of short-term glucocorticosteroid treatment in rats using MRI. J Magn Reson Imaging 33:603–614. [PubMed: 21563244]

Baertsch NA, Severs LJ, Anderson TM, Ramirez JM (2019) A spatially dynamic network underlies the generation of inspiratory behaviors. Proc Natl Acad Sci U S A.

Balan KV, Kc P, Hoxha Z, Mayer CA, Wilson CG, Martin RJ (2011) Vagal afferents modulate cytokine-mediated respiratory control at the neonatal medulla oblongata. Respir Physiol Neurobiol 178:458–464. [PubMed: 21397055]

Baldwin DN, Suki B, Pillow JJ, Roiha HL, Minocchieri S, Frey U (2004) Effect of sighs on breathing memory and dynamics in healthy infants. J Appl Physiol.

Balland E, Dam J, Langlet F, Caron E, Steculorum S, Messina A, Rasika S, Falluel-Morel A, Anouar Y, Dehouck B, Trinquet E, Jockers R, Bouret SG, Prévot V (2014) Hypothalamic tanycytes are an ERK-gated conduit for leptin into the brain. Cell Metab 19:293–301. [PubMed: 24506870]

Banks WA (2019) The blood-brain barrier as an endocrine tissue. Nat Rev Endocrinol 15:444–455. [PubMed: 31127254]

Beggs S, Salter MW (2007) Stereological and somatotopic analysis of the spinal microglial response to peripheral nerve injury. Brain Behav Immun 21:624–633. [PubMed: 17267172]

Bernardo A, Minghetti L (2006) PPAR-gamma agonists as regulators of microglial activation and brain inflammation. Curr Pharm Des 12:93–109. [PubMed: 16454728]

Blanton RA, Kupper TS, McDougall JK, Dower S (1989) Regulation of interleukin 1 and its receptor in human keratinocytes. Proc Natl Acad Sci 86:1273–1277. [PubMed: 2465548]

Blasberg RG, Patlak C, Fenstermacher JD (1975) Intrathecal chemotherapy: brain tissue profiles after ventriculo cisternal perfusion. J Pharmacol Exp Ther.

Blatteis CM (2007) The onset of fever: new insights into its mechanism. Prog Brain Res 162:3–14. [PubMed: 17645911]

Borzone G, Moreno R, Urrea R, Meneses M, Oyarzún M, Lisboa C (2001) Bleomycin-induced chronic lung damage does not resemble human idiopathic pulmonary fibrosis. Am J Respir Crit Care Med 163:1648–1653. [PubMed: 11401889]

Boulenguez P, Gauthier P, Kastner A (2007) Respiratory neuron subpopulations and pathways potentially involved in the reactivation of phrenic motoneurons after C2 hemisection. Brain Res.

Breder CD, Hazuka C, Ghayur T, Klug C, Huginin M, Yasuda K, Teng M, Saper CB (1994) Regional induction of tumor necrosis factor alpha expression in the mouse brain after systemic lipopolysaccharide administration. Proc Natl Acad Sci U S A 91:11393–11397. [PubMed: 7972071]

Brissoni B, Agostini L, Kropf M, Martinon F, Swoboda V, Lippens S, Everett H, Aebi N, Janssens S, Meylan E, Felberbaum-Corti M, Hirling H, Gruenberg J, Tschopp J, Burns K (2006) Intracellular Trafficking of Interleukin-1 Receptor I Requires Tollip. Curr Biol 16:2265–2270. [PubMed: 17113392]

Browning KN, Coleman FH, Travagli RA (2005) Characterization of pancreas-projecting rat dorsal motor nucleus of vagus neurons. Am J Physiol Gastrointest Liver Physiol 288:G950–5 Available at: http://www.ncbi.nlm.nih.gov/pubmed/15637183. [PubMed: 15637183]

Bustamante D, Paeile C, Willer JC, Le Bars D (1997) Effects of intrathecal or intracerebroventricular administration of nonsteroidal anti-inflammatory drugs on a C-fiber reflex in rats. J Pharmacol Exp Ther 281:1381–1391. [PubMed: 9190874]

Butterworth RF (2013) neuroinflammation and encephalopathy. Nat Publ Gr 10:522–528 Available at: 10.1038/nrgastro.2013.99.

Cai Y, Hay M, Bishop VS (1996) Synaptic connections and interactions between area postrema and nucleus tractus solitarius. Brain Res 724:121–124. [PubMed: 8816265]

Calvello R, Lofrumento DD, Perrone MG, Cianciulli A, Salvatore R, Vitale P, De Nuccio F, Giannotti L, Nicolardi G, Panaro MA, Scilimati A (2017) Highly selective cyclooxygenase-1 inhibitors P6 and mofezolac counteract inflammatory state both in vitro and in vivo models of neuroinflammation. Front Neurol 8:1–10. [PubMed: 28138322]

Catania a, Arnold J, Macaluso a, Hiltz ME, Lipton JM (1991) Inhibition of acute inflammation in the periphery by central action of salicylates. Proc Natl Acad Sci U S A 88:8544–8547 Available at: http://www.pubmedcentral.nih.gov/articlerender.fcgi?artid=52545&tool=pmcentrez&rendertype=abstract. [PubMed: 1924313]

Cavarra E, Carraro F, Fineschi S, Naldini A, Bartalesi B, Pucci A, Lungarella G (2004) Early response to bleomycin is characterized by different cytokine and cytokine receptor profiles in lungs. Am J Physiol Lung Cell Mol Physiol 287:L1186–92 Available at: http://www.ncbi.nlm.nih.gov/pubmed/15321784. [PubMed: 15321784]

Chang RB, Strochlic DE, Williams EK, Umans BD, Liberles SD (2015) Vagal sensory neuron subtypes that differentially control breathing. Cell 161:622–633 Available at: 10.1016/j.cell.2015.03.022. [PubMed: 25892222]

Chauvet N, Parmentier ML, Alonso G (1995) Transected axons of adult hypothalamo-neurohypophysial neurons regenerate along tanycytic processes. J Neurosci Res 41:129–144. [PubMed: 7674374]

Chen C, Magee JC, Bazan NG (2002) Cyclooxygenase-2 regulates prostaglandin E2 signaling in hippocampal long-term synaptic plasticity. J Neurophysiol 87:2851–2857 Available at: http://www.ncbi.nlm.nih.gov/pubmed/12037188. [PubMed: 12037188]

Chen GY, Nuñez G (2010) Sterile inflammation: Sensing and reacting to damage. Nat Rev Immunol 10:826–837. [PubMed: 21088683]

Chen R, Wu X, Jiang L, Zhang Y (2017) Single-Cell RNA-Seq Reveals Hypothalamic Cell Diversity. Cell Rep 18:3227–3241. [PubMed: 28355573]

Chen SX, Wang SK, Yao PW, Liao GJ, Na XD, Li YY, Zeng WA, Liu XG, Zang Y (2018) Early CALP2 expression and microglial activation are potential inducers of spinal IL-6 up-regulation and bilateral pain following motor nerve injury. J Neurochem 145:154–169. [PubMed: 29423951]

Cherniack NS, Von EC, Glogowski M, Homma I (1981) Characteristics and rate of occurrence of spontaneous and provoked augmented breaths. Acta Physiol Scand.

Choi S-H, Aid S, Bosetti F (2009) The distinct roles of cyclooxygenase-1 and −2 in neuroinflammation: implications for translational research. Trends Pharmacol Sci 30:174–181. [PubMed: 19269697]

Choi S-H, Aid S, Caracciolo L, Minami SS, Niikura T, Matsuoka Y, Turner RS, Mattson MP, Bosetti F (2013) Cyclooxygenase-1 inhibition reduces amyloid pathology and improves memory deficits in a mouse model of Alzheimer's disease. J Neurochem 124:59–68. [PubMed: 23083210]

Choi S-H, Aid S, Choi U, Bosetti F (2010) Cyclooxygenases-1 and −2 differentially modulate leukocyte recruitment into the inflamed brain. Pharmacogenomics J 10:448–457. [PubMed: 20038958]

Clish CB, Sun YP, Serhan CN (2001) Identification of dual cyclooxygenase-eicosanoid oxidoreductase inhibitors: NSAIDs that inhibit PG-LX reductase/LTB4 dehydrogenase. Biochem Biophys Res Commun.

Coleridge HM, Coleridge JC (1994) Pulmonary reflexes: neural mechanisms of pulmonary defense. Annu Rev Physiol 56:69–91. [PubMed: 8010756]

Coleridge HM, Coleridge JCG, Ginzel KH, Baker DG, Banzett RB, Morrison MA (1976) Stimulation of “irritant” receptors and afferent C-fibres in the lungs by prostaglandins. Nature 264:451–453. [PubMed: 1004577]

Coumel P, Leenhardt A (1991) Mental activity, adrenergic modulation, and cardiac arrhythmias in patients with heart disease. Circulation 83:II58–70.

Cross L, Matthay M (2011) Biomarkers in acute lung injury: insights into the pathogenesis of acute lung injury. Crit Care Clin 27:355–377 Available at: http://www.sciencedirect.com/science/article/pii/S0749070410001211. [PubMed: 21440206]

Cruz MR, Camilo LM, Paula LFSC, Japiass ÚAM, Beda A, Carvalho AR, Bozza FA, Medeiros DM (2014) Effects of different levels of pressure support on Intra-Individual Breath-to-Breath variability. Respir Care.

Cunningham ET, Miselis RR, Sawchenko PE (1994) The relationship of efferent projections from the area postrema to vagal motor and brain stem catecholamine-containing cell groups: An axonal transport and immunohistochemical study in the rat. Neuroscience 58:635–648. [PubMed: 7513390]

Cutillo AG, Chan PH, Ailion DC, Watanabe S, Rao NV., Hansen CB, Albertine KH, Laicher G, Durney CH (2002) Characterization of bleomycin lung injury by nuclear magnetic resonance: Correlation between NMR relaxation times and lung water and collagen content. Magn Reson Med 47:246–256. [PubMed: 11810667]

Dahan A, Hoffman A (2007) Mode of administration-dependent brain uptake of indomethacin: Sustained systemic input increases brain influx. Drug Metab Dispos.

Dallaporta M, Bonnet MS, Horner K, Trouslard J, Jean A, Troadec JD (2010) Glial cells of the nucleus tractus solitarius as partners of the dorsal hindbrain regulation of energy balance: A proposal for a working hypothesis. Brain Res 1350:35–42. [PubMed: 20451504]

Dallaporta M, Pecchi E, Jacques C, Berenbaum F, Jean A, Thirion S, Troadec JD (2007) c-Fos immunoreactivity induced by intraperitoneal LPS administration is reduced in the brain of mice lacking the microsomal prostaglandin E synthase-1 (mPGES-1). Brain Behav Immun 21:1109–1121. [PubMed: 17604949]

Dallaporta M, Pecchi E, Pio J, Jean a, Horner KC, Troadec JD (2009) Expression of leptin receptor by glial cells of the nucleus tractus solitarius: possible involvement in energy homeostasis. J Neuroendocrinol 21:57–67 Available at: http://www.ncbi.nlm.nih.gov/pubmed/19094094 [Accessed September 30, 2014]. [PubMed: 19094094]

Daniels MJD et al. (2016) Fenamate NSAIDs inhibit the NLRP3 inflammasome and protect against Alzheimer’s disease in rodent models. Nat Commun 7:1–10 Available at: 10.1038/ncomms12504.

Dantzer R, O’Connor JC, Freund GG, Johnson RW, Kelley KW (2008) From inflammation to sickness and depression: When the immune system subjugates the brain. Nat Rev Neurosci 9:46–56. [PubMed: 18073775]

de Seranno S, d’Anglemont de Tassigny X, Estrella C, Loyens A, Kasparov S, Leroy D, Ojeda SR, Beauvillain J-C, Prevot V (2010) Role of estradiol in the dynamic control of tanycyte plasticity mediated by vascular endothelial cells in the median eminence. Endocrinology 151:1760–1772. [PubMed: 20133455]

de Seranno S, Estrella C, Loyens A, Anda Cornea 2, Ojeda SR, Beauvillai J-C, Prevot V (2004) Vascular Endothelial Cells Promote Acute Plasticity in Ependymoglial Cells of the Neuroendocrine Brain. J Neurosci 24:10353–10363 Available at: http://www.jneurosci.org/cgi/doi/10.1523/JNEUROSCI.3228-04.2004. [PubMed: 15548649]

DeForge LE, Fantone JC, Kenney JS, Remick DG (1992) Oxygen radical scavengers selectively inhibit interleukin 8 production in human whole blood. J Clin Invest 90:2123–2129. [PubMed: 1331181]

Di L, Rong H, Feng B (2013) Demystifying brain penetration in central nervous system drug discovery. J Med Chem 56:2–12. [PubMed: 23075026]

Dick TE, Dutschmann M, Feldman JL, Fong AY, Hulsmann S, Morris KM, Ramirez JM, Smith JC (2018) Facts and challenges in respiratory neurobiology. Respir Physiol Neurobiol 258:104–107. [PubMed: 25644207]

Dolinay T et al. (2012) Inflammasome-regulated cytokines are critical mediators of acute lung injury. Am J Respir Crit Care Med 185:1225–1234. [PubMed: 22461369]

Dvir E, Elman A, Simmons D, Shapiro I, Duvdevani R, Dahan A, Hoffman A, Friedman JE (2007) DP-155, a lecithin derivative of indomethacin, is a novel nonsteroidal antiinflammatory drug for analgesia and Alzheimer's disease therapy. CNS Drug Rev 13:260–277. [PubMed: 17627676]

Ebersberger A, Averbeck B, Messlinger K, Reeh PW (1999) Release of substance P, calcitonin gene-related peptide and prostaglandin E2 from rat dura mater encephali following electrical and chemical stimulation in vitro. Neuroscience 89:901–907. [PubMed: 10199623]

Ek M, Engblom D, Saha S, Blomqvist a, Jakobsson PJ, Ericsson-Dahlstrand a (2001) Inflammatory response: pathway across the blood-brain barrier. Nature 410:430–431.

Ek M, Kurosawa M, Lundeberg T, Ericsson a (1998) Activation of vagal afferents after intravenous injection of interleukin-1beta: role of endogenous prostaglandins. J Neurosci 18:9471–9479. [PubMed: 9801384]

Elisia I, Nakamura H, Lam V, Hofs E, Cederberg R, Cait J, Hughes MR, Lee L, Jia W, Adomat HH, Guns ES, McNagny KM, Samudio I, Krystal G (2016) DMSO represses inflammatory cytokine production from human blood cells and reduces autoimmune arthritis. PLoS One.

Elliott EI, Sutterwala FS (2015) Initiation and perpetuation of NLRP3 inflammasome activation and assembly. Immunol Rev 265:35–52. [PubMed: 25879282]

Elmquist J, Breder C, Sherin J, Scammell T, Hickey W, Dewitt D, Saper C (1997) Intravenous lipopolysaccharide induces cyclooxygenase 2-like immunoreactivity in rat brain perivascular microglia and meningeal macrophages. J Comp Neurol 381:119–128 Available at: http://doi.wiley.com/10.1002/(SICI)1096-9861(19970505)381:2%3C119::AID-CNE1%3E3.3.CO%3B2-M%5Cnpapers2://publication/uuid/B68968F0-2141-4990-A035-D280AF2DFACD. [PubMed: 9130663]

Emmerson PJ et al. (2017) The metabolic effects of GDF15 are mediated by the orphan receptor GFRAL. Nat Med 23:1215–1219. [PubMed: 28846098]

Engelhardt B, Vajkoczy P, Weller RO (2017) The movers and shapers in immune privilege of the CNS. Nat Publ Gr 18:123–131 Available at: 10.1038/ni.3666.

Engström L, Ruud J, Eskilsson A, Larsson A, Mackerlova L, Kugelberg U, Qian H, Vasilache AM, Larsson P, Engblom D, Sigvardsson M, Jönsson JI, Blomqvist A (2012) Lipopolysaccharide-induced fever depends on prostaglandin E2 production specifically in brain endothelial cells. Endocrinology 153:4849–4861. [PubMed: 22872578]

Erickson MA, Banks WA (2018) Neuroimmune Axes of the Blood–Brain Barriers and Blood–Brain Interfaces: Bases for Physiological Regulation, Disease States, and Pharmacological Interventions. Pharmacol Rev 70:278–314 Available at: http://pharmrev.aspetjournals.org/lookup/doi/10.1124/pr.117.014647. [PubMed: 29496890]

Ericsson A, Arias C, Sawchenko PE (1997) Evidence for an intramedullary prostaglandin-dependent mechanism in the activation of stress-related neuroendocrine circuitry by intravenous interleukin-1. J Neurosci 17:7166–7179 Available at: http://www.ncbi.nlm.nih.gov/pubmed/9278551. [PubMed: 9278551]

Eskilsson A, Mirrasekhian E, Dufour S, Schwaninger XM, Engblom D, Blomqvist A (2014a) Immune-Induced Fever Is Mediated by IL-6 Receptors on Brain Endothelial Cells Coupled to STAT3-Dependent Induction of Brain Endothelial Prostaglandin Synthesis. 34:15957–15961.

Eskilsson A, Tachikawa M, Hosoya KI, Blomqvist A (2014b) Distribution of microsomal prostaglandin E synthase-1 in the mouse brain. J Comp Neurol 522:3229–3244. [PubMed: 24668417]

Evans SS, Repasky EA, Fisher DT (2016) Fever and the thermal regulation of immunity: the immune system feels the heat. 15:335–349.

Faraci FM, Choi J, Baumbach GL, Mayhan WG, Heistad DD (1989) Microcirculation of the area postrema. Permeability and vascular responses. Circ Res 65:417–425 Available at:

http://circres.ahajournals.org/cgi/doi/10.1161/01.RES.65.2.417 [Accessed September 30, 2014]. [PubMed: 2752549]

Faustino J V, Wang X, Johnson CE, Klibanov A, Derugin N, Wendland MF, Vexler ZS (2011) Microglial cells contribute to endogenous brain defenses after acute neonatal focal stroke. J Neurosci 31:12992–13001. [PubMed: 21900578]

Feldman JL, Mitchell GS, Nattie EE (2003) Breathing: rhythmicity, plasticity, chemosensitivity. Annu Rev Neurosci 26:239–266. [PubMed: 12598679]

Fernandez G, Cabral A, Cornejo P, Francesco PN De, Garcia-romero G, Uriarte M, Zigman JM, Portiansky E, Reynaldo M, Perello M (2017) Circulating Ghrelin Acts on GABA Neurons of the Area Postrema and Mediates Gastric Emptying in Male Mice ´. Endocrinology 158:1436–1449. [PubMed: 28204197]

Fleshner M, Frank M, Maier SF (2017) Danger Signals and Inflammasomes: Stress-Evoked Sterile Inflammation in Mood Disorders. Neuropsychopharmacology 42:36–45 Available at: 10.1038/npp.2016.125. [PubMed: 27412959]

Florez J, Borison H (1967) Tidal volume in CO2 regulation: peripheral denervations and ablation of area postrema. Am J Physiol 212:985–991. [PubMed: 6023883]

Forsberg D, Horn Z, Tserga E, Smedler E, Silberberg G, Shvarev Y, Kaila K, Uhlén P, Herlenius E (2016) CO2-evoked release of PGE2 modulates sighs and inspiration as demonstrated in brainstem organotypic culture. Elife 5:1–41.

Forsberg D, Ringstedt T, Herlenius E (2017) Astrocytes release prostaglandin E2 to modify respiratory network activity. Elife 6:1–15.

Frangogiannis NG, Smith CW, Entman ML (2002) The inflammatory response in myocardial infarction. Cardiovasular Res 53:31–47.

Fuchs F, Damm J, Gerstberger R, Roth J, Rummel C (2013) Activation of the inflammatory transcription factor nuclear factor interleukin-6 during inflammatory and psychological stress in the brain. J Neuroinflammation 10.

Furube E, Kawai S, Inagaki H, Takagi S, Miyata S (2018) Brain Region-dependent Heterogeneity and Dose-dependent Difference in Transient Microglia Population Increase during Lipopolysaccharide-induced Inflammation. Sci Rep 8:1–15 Available at: 10.1038/s41598-018-20643-3. [PubMed: 29311619]

Gabriel Knoll J, Krasnow SM, Marks DL (2017) Interleukin-1β signaling in fenestrated capillaries is sufficient to trigger sickness responses in mice. J Neuroinflammation 14:1–21. [PubMed: 28086917]

Gadani SP, Walsh JT, Lukens JR, Kipnis J (2015) Dealing with Danger in the CNS: The Response of the Immune System to Injury. Neuron 87:47–62 Available at: 10.1016/j.neuron.2015.05.019. [PubMed: 26139369]

Getsy PM, Mayer CA, MacFarlane PM, Jacono FJ, Wilson CG (2019) Acute lung injury in neonatal rats causes postsynaptic depression in nucleus tractus solitarii second-order neurons. Respir Physiol Neurobiol 269:103250 Available at: 10.1016/j.resp.2019.103250.

Ghilardi JR, Svensson C, Rogers SD, Yaksh TL, Mantyh PW (2004) Constitutive Spinal Cyclooxygenase-2 Participates in the Initiation of Tissue Injury-Induced Hyperalgesia. J Neurosci 24:2727–2732 Available at: http://www.jneurosci.org/cgi/doi/10.1523/JNEUROSCI.5054-03.2004. [PubMed: 15028765]

Glattfelder K, Ng L, Morris J (2007) Area Postrema (AP). Allen Brain Atlas Mouse Brain:1–17.

Goehler LE, Erisir A, Gaykema RPA (2006) Neural-immune interface in the rat area postrema. Neuroscience 140:1415–1434. [PubMed: 16650942]

Goehler LE, Gaykema RPA, Hansen MK, Anderson K, Maier SF, Watkins LR (2000) Vagal immune-to-brain communication: A visceral chemosensory pathway. In: Autonomic Neuroscience: Basic and Clinical, pp 49–59.

Gordon FJ (2000) Effect of nucleus tractus solitarius lesions on fever produced by interleukin-1β. In: Autonomic Neuroscience: Basic and Clinical, pp 102–110. [PubMed: 11189016]

Gosselin D, Rivest S (2008) MyD88 signaling in brain endothelial cells is essential for the neuronal activity and glucocorticoid release during systemic inflammation. Mol Psychiatry 13:480–497. [PubMed: 18180766]

Griffin ÉW, Skelly DT, Murray CL, Cunningham C (2013) Cyclooxygenase-1-dependent prostaglandins mediate susceptibility to systemic inflammation-induced acute cognitive dysfunction. J Neurosci 33:15248–15258. [PubMed: 24048854]

Gross PM, Wall KM, Pang JJ, Shaver SW, Wainman DS (1990) Microvascular specializations promoting rapid interstitial solute dispersion in nucleus tractus solitarius. Am J Physiol 259:R1131–R1138. [PubMed: 2260724]

Guillebaud F, Girardet C, Abysique A, Gaigé S, Barbouche R, Verneui J, Jean A, Leprince J, Tonon MC, Dallaporta M, Lebrun B, Troadec JD (2017) Glial endozepines inhibit feeding-related autonomic functions by acting at the brainstem level. Front Neurosci 11:1–15. [PubMed: 28154520]

Guo W, Wang H, Watanabe M, Shimizu K, Zou S, Lagraize SC, Wei F, Dubner R, Ren K (2007) Glial – Cytokine – Neuronal Interactions Underlying the Mechanisms of Persistent Pain. J Neurosci 27:6006–6018. [PubMed: 17537972]

Haack KK V, Marcus NJ, Del Rio R, Zucker IH, Schultz HD (2014) Simvastatin treatment attenuates increased respiratory variability and apnea/hypopnea index in rats with chronic heart failure. Hypertens (Dallas, Tex 1979) 63:1041–1049.

Hellwig S, Brioschi S, Dieni S, Frings L, Masuch A, Blank T, Biber K (2016) Altered microglia morphology and higher resilience to stress-induced depression-like behavior in CX3CR1-deficient mice. Brain Behav Immun 55:126–137 Available at: 10.1016/j.bbi.2015.11.008. [PubMed: 26576722]

Herkenham M, Lee HY, Baker RA (1998) Temporal and spatial patterns of c-fos mRNA induced by intravenous interleukin-1: A cascade of non-neuronal cellular activation at the blood-brain barrier. J Comp Neurol 400:175–196. [PubMed: 9766398]

Hermann GE, Rogers RC (2009) TNF activates astrocytes and catecholaminergic neurons in the solitary nucleus: implications for autonomic control. Brain Res June 1:72–82.

Hermann GE, Tovar CA, Rogers RC (2002) LPS-induced suppression of gastric motility relieved by TNFR:Fc construct in dorsal vagal complex. Am J Physiol Gastrointest Liver Physiol 283:G634–9 Available at: http://www.ncbi.nlm.nih.gov/pubmed/12181177. [PubMed: 12181177]

Hermann GE, Van Meter MJ, R C. Rogers (2013) CXCR4 receptors in the dorsal medulla: implications for autonomic dysfunction Gerlinda. 31:1713–1723.

Herz J, Kipnis J (2016) Bugs and Brain : How Infection Makes You Feel Blue. Immunity 44:718–720 Available at: 10.1016/j.immuni.2016.03.010. [PubMed: 27096312]

Hinwood M, Tynan RJ, Charnley JL, Beynon SB, Day TA, Walker FR (2013) Chronic stress induced remodeling of the prefrontal cortex: Structural re-organization of microglia and the inhibitory effect of minocycline. Cereb Cortex 23:1784–1797. [PubMed: 22710611]

Hladky SB, Barrand MA (2014) Mechanisms of fluid movement into, through and out of the brain: Evaluation of the evidence. Fluids Barriers CNS 11:1–32. [PubMed: 24467887]

Hockera AD, Stokes JA, Powell FL, Huxtable AG (2017) The impact of inflammation on respiratory plasticity. Exp Neurol 287:243–253. [PubMed: 27476100]

Hofstetter AO, Saha S, Siljehav V, Jakobsson P-J, Herlenius E (2007) The induced prostaglandin E2 pathway is a key regulator of the respiratory response to infection and hypoxia in neonates. Proc Natl Acad Sci U S A 104:9894–9899. [PubMed: 17535900]

Hoseini Z, Sepahvand F, Rashidi B, Sahebkar A, Masoudifar A, Mirzaei H (2018) NLRP3 inflammasome: Its regulation and involvement in atherosclerosis. J Cell Physiol 233:2116–2132. [PubMed: 28345767]

Hoshino T, Okamoto M, Sakazaki Y, Kato S, Young HA, Aizawa H (2009) Role of proinflammatory cytokines IL-18 and IL-1β in bleomycin-induced lung injury in humans and mice. Am J Respir Cell Mol Biol 41:661–670. [PubMed: 19265174]

Hsu JY et al. (2017) Non-homeostatic body weight regulation through a brainstem-restricted receptor for GDF15. Nature 550:255–259 Available at: 10.1038/nature24042. [PubMed: 28953886]

Hua KF, Chou JC, Ka SM, Tasi YL, Chen A, Wu SH, Chiu HW, Wong WT, Wang YF, Tsai CL, Ho CL, Lin CH (2015) Cyclooxygenase-2 regulates NLRP3 inflammasome-derived IL-1β production. J Cell Physiol 230:863–874. [PubMed: 25294243]

Huda R, Chang Z, Do J, McCrimmon DR, Martina M (2018) Activation of astrocytic PAR1 receptors in the rat nucleus of the solitary tract regulates breathing through modulation of presynaptic TRPV1. J Physiol 596:497–513. [PubMed: 29235097]

Huxtable AG, Smith SMC, Peterson TJ, Watters JJ, Mitchell GS (2015) Intermittent Hypoxia-Induced Spinal Inflammation Impairs Respiratory Motor Plasticity by a Spinal p38 MAP Kinase-Dependent Mechanism. J Neurosci 35:6871–6880 Available at: http://www.jneurosci.org/cgi/doi/10.1523/JNEUROSCI.4539-14.2015. [PubMed: 25926462]

Ineichen B V, Schnell L, Gullo M, Kaiser J, Schneider MP, Mosberger AC, Good N, Linnebank M, Schwab ME (2017) Direct, long-Term intrathecal application of therapeutics to the rodent CNS. Nat Protoc 12:104–121. [PubMed: 27977023]

Inoue T, Abe C, Sung SSJ, Moscalu S, Jankowski J, Huang L, Ye H, Rosin DL, Guyenet PG, Okusa MD (2016) Vagus nerve stimulation mediates protection from kidney ischemia-reperfusion injury through α7nAChR+splenocytes. J Clin Invest 126:1939–1952. [PubMed: 27088805]

Ito H, Seki M (1998) Ascending projections from the area postrema and the nucleus of the solitary tract of Suncus murinus: anterograde tracing study using Phaseolus vulgaris leucoagglutinin. Okajimas Folia Anat Jpn 75:9–31 Available at: http://www.ncbi.nlm.nih.gov/entrez/query.fcgi?cmd=Retrieve&db=PubMed&dopt=Citation&list_uids=9715082. [PubMed: 9715082]

Iyonaga T, Shinohara K, Mastuura T, Hirooka Y, Tsutsui H (2019) Brain perivascular macrophages contribute to the development of hypertension in stroke-prone spontaneously hypertensive rats via sympathetic activation. Hypertens Res Available at: 10.1038/s41440-019-0333-4.

Jacono FJ, Mayer CA, Hsieh Y-H, Wilson CG, Dick TE (2011) Lung and brainstem cytokine levels are associated with breathing pattern changes in a rodent model of acute lung injury. Respir Physiol Neurobiol 178:429–438. [PubMed: 21569869]

Jacono FJ, Peng Y, Nethery D, Faress JA, Lee Z, Kern JA, Prabhakar NR (2006) Acute lung injury augments hypoxic ventilatory response in the absence of systemic hypoxemia Acute lung injury augments hypoxic ventilatory response in the absence of systemic hypoxemia. J Appl Physiol 101:1795–1802. [PubMed: 16888052]

Jho DH, Engelhard HH, Juarez A, Espat NJ (2003) Simplified Surgical Placement and Stabilization Methods for Intracerebroventricular Cannulas in Rat Lateral Ventricles. Lab Anim (NY) 32:43–48.

Jiang D, Liang J, Fan J, Yu S, Chen S, Luo Y, Prestwich GD, Mascarenhas MM, Garg HG, Quinn DA, Homer RJ, Goldstein DR, Bucala R, Lee PJ, Medzhitov R, Noble PW (2005) Regulation of lung injury and repair by Toll-like receptors and hyaluronan. Nat Med 11:1173–1179. [PubMed: 16244651]

Jiang D, Liang J, Noble PW (2007) Hyaluronan in Tissue Injury and Repair. Annu Rev Cell Dev Biol 23:435–461 Available at: http://www.annualreviews.org/doi/10.1146/annurev.cellbio.23.090506.123337. [PubMed: 17506690]

Jin S, Kim JG, Park JW, Koch M, Horvath TL, Lee BJ (2016) Hypothalamic TLR2 triggers sickness behavior via a microglia-neuronal axis. Sci Rep 6:1–13 Available at: 10.1038/srep29424. [PubMed: 28442746]

Jones ME, Lebonville CL, Paniccia JE, Balentine ME, Reissner KJ, Lysle DT (2019) Hippocampal interleukin-1 mediates stress-enhanced fear learning: A potential role for astrocyte-derived interleukin-1β. Brain Behav Immun:355–363.

Jung WJ, Lee SY, Choi SI, Kim B-K, Lee EJ, In KH, Lee M-G (2018) Toll-like receptor expression in pulmonary sensory neurons in the bleomycin-induced fibrosis model. PLoS One 13:1–13.

Kalia M (1981) Brain stem localization of vagal preganglionic neurons. J Auton Nerv Syst 3:451–481. [PubMed: 7276442]

Kalia M, Mesulam M-M (1980) Brain stem projections of sensory and motor components of the vagus complex in the cat: I. The cervical vagus and nodose ganglion. J Comp Neurol.

Kaminski N, Allard JD, Pittet JF, Zuo F, Griffiths MJD, Morris D, Huang X, Sheppard D, Heller RA (2000) Global analysis of gene expression in pulmonary fibrosis reveals distinct programs regulating lung inflammation and fibrosis. Proc Natl Acad Sci 97:1778–1783 Available at: http://www.pnas.org/cgi/doi/10.1073/pnas.97.4.1778. [PubMed: 10677534]

Kaplan L, Weiss J, Elsbach P (1978) Low concentrations of indomethacin inhibit phospholipase A 2 of rabbit polymorphonuclear leukocytes. Proc Natl Acad Sci U S A 75:2955–2958. [PubMed: 275865]

Karperien A, Ahammer H, Jelinek HF (2013) Quantitating the subtleties of microglial morphology with fractal analysis. Front Cell Neurosci 7:3 Available at: http://www.ncbi.nlm.nih.gov/pubmed/23386810%5Cnhttp://www.pubmedcentral.nih.gov/articlerender.fcgi?artid=PMC3558688. [PubMed: 23386810]

Kato K, Kikuchi S, Shubayev VI, Myers RR (2009) Distribution and tumor necrosis factor-alpha isoform binding specificity of locally administered etanercept into injured and uninjured rat sciatic nerve. Neuroscience 160:492–500 Available at: 10.1016/j.neuroscience.2009.02.038. [PubMed: 19250961]

Kaufmann WE, Worley PF, Pegg J, Bremer M, Isakson P (1996) COX-2, a synaptically induced enzyme, is expressed by excitatory neurons at postsynaptic sites in rat cerebral cortex. Proc Natl Acad Sci U S A 93:2317–2321 Available at: http://www.pubmedcentral.nih.gov/articlerender.fcgi?artid=39793&tool=pmcentrez&rendertype=abstract. [PubMed: 8637870]

Kawai Y (2018) Differential Ascending Projections From the Male Rat Caudal Nucleus of the Tractus Solitarius: An Interface Between Local Microcircuits and Global Macrocircuits. Front Neuroanat 12:63 Available at: https://www.frontiersin.org/article/10.3389/fnana.2018.00063. [PubMed: 30087599]

Kelsen SG, Shustack A, Hough W (1982) The effect of vagal blockade on the variability of ventilation in the awake dog. Respir Physiol 49:339–353. [PubMed: 6815753]

Khansari PS, Halliwell RF (2019) Mechanisms underlying neuroprotection by the NSAID mefenamic acid in an experimental model of stroke. Front Neurosci 13:1–10. [PubMed: 30740042]

Khoo MCK (2000) Determinants of ventilatory instability and variability. Respir Physiol 122:167–182. [PubMed: 10967342]

Kirkby NS, Chan MV., Zaiss AK, Garcia-Vaz E, Jiao J, Berglund LM, Verdu EF, Ahmetaj-Shala B, Wallace JL, Herschman HR, Gomez MF, Mitchell JA (2016) Systematic study of constitutive cyclooxygenase-2 expression: Role of NF-κB and NFAT transcriptional pathways. Proc Natl Acad Sci U S A 113:434–439. [PubMed: 26712011]

Kirkby NS, Zaiss AK, Urquhart P, Jiao J, Austin PJ, Al-Yamani M, Lundberg MH, MacKenzie LS, Warner TD, Nicolaou A, Herschman HR, Mitchell JA (2013) LC-MS/MS Confirms That COX-1 Drives Vascular Prostacyclin Whilst Gene Expression Pattern Reveals Non-Vascular Sites of COX-2 Expression. PLoS One 8:1–9.

Koch H, Caughie C, Elsen FP, Doi A, Garcia AJ, Zanella S, Ramirez J-M (2015) Prostaglandin E2 differentially modulates the central control of eupnoea, sighs and gasping in mice. J Physiol 593:305–319 Available at: 10.1113/jphysiol.2014.279794. [PubMed: 25556802]

Komaki G, Arimura A, Koves K (1992) Effect of intravenous injection of IL-1 beta on PGE2 levels in several brain areas as determined by microdialysis. Am J Physiol 262:E246–51 Available at: http://www.ncbi.nlm.nih.gov/entrez/query.fcgi?cmd=Retrieve&db=PubMed&dopt=Citation&list_uids=1539653. [PubMed: 1539653]

Komegae EN, Farmer DGS, Brooks VL, McKinley MJ, McAllen RM, Martelli D (2018) Vagal afferent activation suppresses systemic inflammation via the splanchnic anti-inflammatory pathway. Brain Behav Immun 73:441–449. [PubMed: 29883598]

Konsman JP (2016) Immune-to-brain signaling and substrates of altered behavior during inflammation. Neuroimmunol Neuroinflammation 3:207.

Kostuk EW, Cai J, Iacovitti L (2019) Subregional differences in astrocytes underlie selective neurodegeneration or protection in Parkinson's disease models in culture. Glia 67:1542–1557. [PubMed: 31025779]

Kubin L, Kimura H, Davies R. (1991) The medullary projections of afferent bronchopulmonary C fibres in the cat as shown by antidromic mapping. J Physiol:207–228.

Kurumbail RG, Stevens AM, Gierse JK, McDonald JJ, Stegeman RA, Pak JY, Gildehaus D, Miyashiro JM, Penning TD, Seibert K, Isakson PC, Stallings WC (1996) Structural basis for selective inhibition of cyciooxygenase-2 by anti-inflammatory agents. Nature.

Laaris N, Weinreich D (2007) PGE2 Depresses solitary Tract-Mediated Synaptic Transmission In The nTS. Neuroscience 146:792–801. [PubMed: 17367942]

Lacroix A, Toussay X, Anenberg E, Lecrux C, Ferreiros N, Karagiannis A, Plaisier F, Chausson P, Jarlier F, Burgess SA, Hillman EMC, Tegeder I, Murphy TH, Hamel E, Cauli B (2015) COX-2-Derived Prostaglandin E2 Produced by Pyramidal Neurons Contributes to Neurovascular Coupling in the Rodent Cerebral Cortex. J Neurosci 35:11791–11810 Available at: http://www.jneurosci.org/cgi/doi/10.1523/JNEUROSCI.0651-15.2015. [PubMed: 26311764]

Laflamme N, Lacroix S, Rivest S (1999) An essential role of interleukin-1beta in mediating NF-kappaB activity and COX-2 transcription in cells of the blood-brain barrier in response to a systemic and localized inflammation but not during endotoxemia. J Neurosci 19:10923–10930 Available at: file:///Unknown/AnEssentialRoleofInterleukin-1β inMediatingNF-BActivityandCOX-2TranscriptioninCellsof-0.pdf. [PubMed: 10594073]

Lai YT, Su CK, Jiang ST, Chang YJ, Lai ACY, Huang YS (2016) Deficiency of CPEB2-confined choline acetyltransferase expression in the dorsal motor nucleus of vagus causes hyperactivated parasympathetic signaling-associated bronchoconstriction. J Neurosci 36:12661–12676. [PubMed: 27810937]

Langlet F, Levin BE, Luquet S, Mazzone M, Messina A, Dunn-Meynell AA, Balland E, Lacombe A, Mazur D, Carmeliet P, Bouret SG, Prevot V, Dehouck B, S G.Bouret, Vincent Prevot, Dehouck B (2013a) Tanycytic VEGF-A Boosts Blood-Hypothalamus Barrier Plasticity and Access of Metabolic Signals to the Arcuate Nucleus in Response to Fasting. Cell Metab 17:607–617. [PubMed: 23562080]

Langlet F, Mullier A, Bouret SG, Prevot V, Dehouck and B (2013b) Tanycyte-Like Cells Form a Blood–Cerebrospinal Fluid Barrier in the Circumventricular Organs of the Mouse Brain. J Comp Neurol 521:3389–3405. [PubMed: 23649873]

Lee HY, Whiteside MB, Herkenham M (1998) Area postrema removal abolishes stimulatory effects of intravenous interleukin-1beta on hypothalamic-pituitary-adrenal axis activity and c-fos mRNA in the hypothalamic paraventricular nucleus. Brain Res Bull 46:495–503. [PubMed: 9744286]

Lee S, Zhao YQ, Ribeiro-da-Silva A, Zhang J (2010) Distinctive response of CNS glial cells in oro-facial pain associated with injury, infection and inflammation. Mol Pain 6:79 Available at: http://www.molecularpain.com/content/6/1/79. [PubMed: 21067602]

Lehmann JM, Lenhard JM, Oliver BB, Ringold GM, Kliewer SA (1997) Peroxisome proliferator-activated receptors α and γ are activated by indomethacin and other non-steroidal anti-inflammatory drugs. J Biol Chem 272:3406–3410. [PubMed: 9013583]

Leibinger M, Müller A, Gobrecht P, Diekmann H, Andreadaki A, Fischer D (2013) Interleukin-6 contributes to CNS axon regeneration upon inflammatory stimulation. Cell Death Dis 4:1–13.

Lein ES et al. (2007) Genome-wide atlas of gene expression in the adult mouse brain. Nature 445:168–176. [PubMed: 17151600]

Lenth RV (2001) Some practical guidelines for effective sample size determination. Am Stat 55:187–193.

Li J, Zhang M-M, Tu K, Wang J, Feng B, Zhang Z-N, Lei J, Li Y-Q, Du J-Q, Chen T (2015) The excitatory synaptic transmission of the nucleus of solitary tract was potentiated by chronic myocardial infarction in rats. PLoS One 10:e0118827.

Li P, Janczewski WA, Yackle K, Kam K, Pagliardini S, Krasnow MA, Feldman JL (2016) The peptidergic control circuit for sighing. Nature 530:293–297. [PubMed: 26855425]

Litvin DG, Dick TE, Smith CB, Jacono FJ (2018) Lung-injury depresses glutamatergic synaptic transmission in the nucleus tractus solitarii via discrete age-dependent mechanisms in neonatal rats. Brain Behav Immun Available at: https://www.sciencedirect.com/science/article/pii/S0889159118300849.

Liu M, Liang Y, Chigurupati S, Lathia JD, Sun Z, Crow M, Ross CA, Mattson MP, Rabb H (2008) Acute kidney injury leads to brain inflamation and functional changes. J am Soc Nephrol 19:1360–1370. [PubMed: 18385426]

Liu X, Yamashita T, Chen Q, Belevych N, Mckim DB, Tarr AJ, Coppola V, Nath N, Nemeth DP, Syed ZW, Sheridan JF, Godbout JP, Zuo J, Quan N (2015) Interleukin 1 Type 1 Receptor Restore: A Genetic Mouse Model for Studying Interleukin 1 Receptor-Mediated Effects in

Specific Cell Types. J Neurosci 35:2860–2870 Available at: http://www.jneurosci.org/cgi/doi/10.1523/JNEUROSCI.3199-14.2015. [PubMed: 25698726]

Long JM, Kalehua AN, Muth NJ, Calhoun ME, Jucker M, Hengemihle JM, Ingram DK, Mouton PR, Kalehua AN, Muth NJ, Calhoun ME, Jucker M, Hengemihle JM, Ingram DK, Mouton PR (1998) Stereological Analysis of Astrocyte and Microglia in Aging Mouse Hippocampus Stereology CA1 Dentate Gyrus Hilus Glia Mouse. 19:497–503 Available at: https://ac.els-cdn.com/S0197458098000888/1-s2.0-S0197458098000888-main.pdf?_tid=93b3348c-f172-11e7-b5c3-00000aab0f6c&acdnat=1515086186_3220213e860abedc0ed47cd19d71d25b.

Lorea-Hernández JJ, Morales T, Rivera-Angulo AJ, Alcantara-Gonzalez D, Peña-Ortega F (2016) Microglia modulate respiratory rhythm generation and autoresuscitation. Glia 64:603–619. [PubMed: 26678570]

Löscher W, Potschka H (2005) Blood-brain barrier active efflux transporters: ATP-binding cassette gene family. NeuroRx 2:86–98. [PubMed: 15717060]

Lowenthal JW, MacDonald HR (1986) Binding and internalization of interleukin 1 by T cells. J Exp Med 164:1060–1074. [PubMed: 2944981]

MacFarlane PMM, Mayer CAA, Litvin DG (2016) Microglia modulate brainstem serotonergic expression following neonatal sustained hypoxia exposure: implications for sudden infant death syndrome. J Physiol 594:3079–3094 Available at: http://doi.wiley.com/10.1113/JP271845. [PubMed: 26659585]

Macvicar BA, Newman EA (2015) Astrocyte Regulation of Blood Flow in the Brain. Cold Spring Harb Perspect Biol:1–14.

Mak M, Fung L, Strasser JF, Saltzman WM (1995) Distribution of drugs following controlled delivery to the brain interstitium. J Neurooncol.

Malatesta P, Hartfuss E, Götz M (2000) Isolation of radial glial cells by fluorescent-activated cell sorting reveals a neuronal lineage. Development 5263:5253–5263.

Mannari T, Morita S, Furube E, Tominaga M, Miyata S (2013) Astrocytic TRPV1 ion channels detect blood-borne signals in the sensory circumventricular organs of adult mouse brains. Glia 61:957–971. [PubMed: 23468425]

Mannila A, Kumpulainen E, Lehtonen M, Heikkinen M, Laisalmi M, Salo T, Rautio J, Savolainen J, Kokki H (2007) Plasma and cerebrospinal fluid concentrations of indomethacin in children after intravenous administration. J Clin Pharmacol.

Mannila A, Rautio J, Lehtonen M, Järvinen T, Savolainen J (2005) Inefficient central nervous system delivery limits the use of ibuprofen in neurodegenerative diseases. Eur J Pharm Sci.

Manning LS, Rothwell PM, Potter JF, Robinson TG (2015) Prognostic Significance of Short-Term Blood Pressure Variability in Acute Stroke: Systematic Review. Stroke 46:2482–2490. [PubMed: 26243226]

Mantilla CB, Rowley KL, Zhan WZ, Fahim MA, Sieck GC (2007) Synaptic vesicle pools at diaphragm neuromuscular junctions vary with motoneuron soma, not axon terminal, inactivity. Neuroscience.

Maolood N, Meister B (2009) Protein components of the blood-brain barrier (BBB) in the brainstem area postrema-nucleus tractus solitarius region. J Chem Neuroanat 37:182–195. [PubMed: 19146948]

Marty V, El Hachmane M, Amédée T (2008) Dual modulation of synaptic transmission in the nucleus tractus solitarius by prostaglandin E2 synthesized downstream of IL-1beta. Eur J Neurosci 27:3132–3150 Available at: http://www.ncbi.nlm.nih.gov/pubmed/18598258 [Accessed September 30, 2014]. [PubMed: 18598258]

Masamoto K, Unekawa M, Watanabe T, Toriumi H (2015) Unveiling astrocytic control of cerebral blood flow with optogenetics. Nat Publ Gr Jun 16:1–11 Available at: 10.1038/srep11455.

Mastronardi C, Whelan F, Yildiz O a, Hannestad J, Elashoff D, McCann SM, Licinio J, Wong M-L (2007) Caspase 1 deficiency reduces inflammation-induced brain transcription. Proc Natl Acad Sci U S A 104:7205–7210. [PubMed: 17409187]

Matott MP, Ruyle BC, Hasser EM, Kline DD (2016) Excitatory amino acid transporters tonically restrain nTS synaptic and neuronal activity to modulate cardiorespiratory function. J Neurophysiol 115:1691–1702 Available at: http://

jn.physiology.org/lookup/doi/10.1152/jn.01054.2015%5Cnhttp://www.ncbi.nlm.nih.gov/pubmed/26719090%5Cnhttp://www.pubmedcentral.nih.gov/articlerender.fcgi?artid=PMC4808102. [PubMed: 26719090]

Matsumura K, Cao C, Ozaki M, Morii H, Nakadate K, Watanabe Y (1998) Brain endothelial cells express cyclooxygenase-2 during lipopolysaccharide-induced fever: light and electron microscopic immunocytochemical studies. J Neurosci 18:6279–6289 Available at: file:///Unknown/BrainEndothelialCellsExpressCyclooxygenase-2duringLipopolysaccharide-InducedFever-Lightand-0.pdf. [PubMed: 9698320]

Matthay MA, Howard JP (2012) Progress in modelling acute lung injury in a pre-clinical mouse model. Eur Respir J 39:1062–1063. [PubMed: 22547731]

Matute-Bello G, Frevert CW, Martin TR (2008) Animal models of acute lung injury. Am J Physiol:379–399.

Mcdougal DH, Hermann GE, Rogers RC (2012) Vagal afferent stimulation activates astrocytes in the nucleus of the solitary tract via AMPA receptors: Evidence of an atypical neural-glial interaction in the brainstem. 31:14037–14045.

McKinley MJ, McAllen RM, Davern P, Giles ME, Penschow J, Sunn N, Uschakov A, Oldfield BJ (2003) The sensory circumventricular organs of the mammalian brain. Adv Anat Embryol Cell Biol 172:III—XII, 1−−122, back cover Available at: http://www.ncbi.nlm.nih.gov/pubmed/12901335. [PubMed: 12901335]

McLean JH, Hopkins DA (1985) Ultrastructure of the dorsal motor nucleus of the vagus nerve in monkey with a comparison of synaptology in monkey and cat. J Comp Neurol 231:162–174. [PubMed: 3968233]

Meduri GU, Annane D, Chrousos GP, Marik PE, Sinclair SE (2009) Activation and regulation of systemic inflammation in ARDS: Rationale for prolonged glucocorticoid therapy. Chest 136:1631–1643 Available at: 10.1378/chest.08-2408. [PubMed: 19801579]

Meduri GU, Kohler G, Headley S, Tolley E, Stentz F, Postlethwaite A (1995) Inflammatory cytokines in the BAL of patients with ARDS: Persistent elevation over time predicts poor outcome. Chest.

Mendelson WB, Martin JV, Perlis M, Giesen H, Wagner R, Rapoport SI (1988) Periodic cessation of respiratory effort during sleep in adult rats. Physiol Behav 43:229–234. [PubMed: 3212061]

Metzger F, Mischek D, Stoffers F (2017) The connected steady state model and the interdependence of the CSF proteome and CSF flow characteristics. Front Neurosci 11.

Miller RL, Loewy AD (2014) ENaC γ-expressing astrocytes in the circumventricular organs, white matter, and ventral medullary surface: sites for Na+ regulation by glial cells. :72–80.

Miyata S (2015) New aspects in fenestrated capillary and tissue dynamics in the sensory circumventricular organs of adult brains. Front Neurosci 9.

Mollace V, Muscoli C, Palma E, Iannone M, Granato T, Nistico R, Rotiroti D (2001) Central cardiovascular responses induced by interleukin 1β and tumor necrosis factor α infused into nucleus tractus solitarii, nucleus parabrachialis medialis and third cerebral ventricle of normotensive rats. Neurosci Lett 314:53–56. [PubMed: 11698145]

Montandon G, Bairam A, Kinkead R (2006) Long-term consequences of neonatal caffeine on ventilation, occurrence of apneas, and hypercapnic chemoreflex in male and female rats. Pediatr Res 59:519–524. [PubMed: 16549522]

Morita S, Furube E, Mannari T, Okuda H, Tatsumi K, Wanaka A, Miyata S (2016) Heterogeneous vascular permeability and alternative diffusion barrier in sensory circumventricular organs of adult mouse brain. Cell Tissue Res 363:497–511. [PubMed: 26048259]

Morrison HW, Filosa JA (2013) A quantitative spatiotemporal analysis of microglia morphology during ischemic stroke and reperfusion. J Neuroinflammation 10:782 Available at: http://jneuroinflammation.biomedcentral.com/articles/10.1186/1742-2094-10-4.

Mullican SE, Rangwala SM (2018) Uniting GDF15 and GFRAL: Therapeutic Opportunities in Obesity and Beyond. Trends Endocrinol Metab.

Murray K, Barboza M, Rude KM, Brust-Mascher I, Reardon C (2019) Functional circuitry of neuro-immune communication in the mesenteric lymph node and spleen. Brain Behav Immun 82:214–223 Available at: 10.1016/j.bbi.2019.08.188. [PubMed: 31445965]

Nadeau S, Rivest S (2000) Role of microglial-derived tumor necrosis factor in mediating CD14 transcription and nuclear factor κ B activity in the brain during endotoxemia. J Neurosci 20:3456–3468. [PubMed: 10777809]

Nadjar A, Combe C, Layé S, Tridon V, Dantzer R, Amédée T, Parnet P (2003) Nuclear factor κB nuclear translocation as a crucial marker of brain response to interleukin-1. A study in rat and interleukin-1 type I deficient mouse. J Neurochem 87:1024–1036. [PubMed: 14622131]

Nakamura A, Fukuda Y, Kuwaki T (2003) Sleep apnea and effect of chemostimulation on breathing instability in mice. J Appl Physiol.

Nakano Y, Furube E, Morita S, Wanaka A, Nakashima T, Miyata S (2015) Astrocytic TLR4 expression and LPS-induced nuclear translocation of STAT3 in the sensory circumventricular organs of adult mouse brain. J Neuroimmunol 278:144–158 Available at: 10.1016/j.jneuroim.2014.12.013. [PubMed: 25595264]

Nardocci G, Martin A, Abarzúa S, Rodríguez J, Simon F, Reyes EP, Acuña-Castillo C, Navarro C, Cortes PP, Fernández R (2015) Sepsis progression to multiple organ dysfunction in carotid chemo/baro-denervated rats treated with lipopolysaccharide. J Neuroimmunol 278:44–52 Available at: 10.1016/j.jneuroim.2014.12.002. [PubMed: 25595251]

Netland EE, Newton JL, Majocha RE, Tate BA (1998) Indomethacin Reverses the Microglial Response to Amyloid Beta-Protein. Neurobiol Aging 19:201–204. [PubMed: 9661994]

Nguyen CD, Dakin C, Yuill M, Crozier S, Wilson S (2012) The Effect of Sigh on Cardiorespiratory Synchronization in Healthy Sleeping Infants. Sleep.

Nikolopoulou E, Papacleovoulou G, Jean-Alphonse F, Grimaldi G, Parker MG, Hanyaloglu AC, Christian M (2014) Arachidonic acid-dependent gene regulation during preadipocyte differentiation controls adipocyte potential. J Lipid Res 55:2479–2490 Available at: http://www.jlr.org/lookup/doi/10.1194/jlr.M049551. [PubMed: 25325755]

Niwa K, Araki E, Morham SG, Ross ME, Iadecola C (2000) Cyclooxygenase-2 contributes to functional hyperemia in whisker-barrel cortex. J Neurosci 20:763–770. [PubMed: 10632605]

Nongnuch A, Panorchan K, Davenport A (2014) Brain-kidney crosstalk. Crit Care 18:1–11.

Novakova I, Subileau EA, Toegel S, Gruber D, Lachmann B, Urban E, Chesne C, Noe CR, Neuhaus W (2014) Transport rankings of non-steroidal antiinflammatory drugs across blood-brain barrier in vitro models. PLoS One 9:1–14.

O'Neill GP, Ford-Hutchinson AW (1993) Expression of mRNA for cyclooxygenase-1 and cyclooxygenase-2 in human tissues. FEBS Lett.

Pak T, Yoo S, Miranda-Angulo AM, Wang H, Blackshaw S (2014) Rax-CreERT2 knock-in mice: A tool for selective and conditional gene deletion in progenitor cells and radial glia of the retina and hypothalamus. PLoS One 9:1–13.

Pan MR, Hung WC (2002) Nonsteroidal anti-inflammatory drugs inhibit matrix metalloproteinase-2 via suppression of the ERK/Sp1-mediated transcription. J Biol Chem 277:32775–32780. [PubMed: 12087091]

Pan W, Stone KP, Hsuchou H, Manda VK, Zhang Y, Kastin AJ (2011) Cytokine Signaling Modulates Blood-Brain Barrier Function. Curr Pharm Des November:3729–3740. [PubMed: 21834767]

Parati G, Ochoa JE, Lombardi C, Bilo G (2013) Assessment and management of blood-pressure variability. Nat Rev Cardiol 10:143–155. [PubMed: 23399972]

Pardridge WM (2011) Drug transport in brain via the cerebrospinal fluid. Fluids Barriers CNS 8:7 Available at: http://www.fluidsbarrierscns.com/content/8/1/7. [PubMed: 21349155]

Pardridge WM (2012) Drug transport across the blood-brain barrier. J Cereb Blood Flow Metab 32:1959–1972 Available at: 10.1038/jcbfm.2012.126. [PubMed: 22929442]

Parepally JMR, Mandula H, Smith QR (2006) Brain uptake of nonsteroidal anti-inflammatory drugs: Ibuprofen, flurbiprofen, and indomethacin. Pharm Res 23:873–881. [PubMed: 16715377]

Parkash J, Messina A, Langlet F, Cimino I, Loyens A, Mazur D, Gallet S, Balland E, Malone SA, Pralong F, Cagnoni G, Schellino R, De Marchis S, Mazzone M, Pasterkamp RJ, Tamagnone L, Prevot V, Giacobini P (2015) Semaphorin7A regulates neuroglial plasticity in the adult hypothalamic median eminence. Nat Commun 6.

Pavlov V a Tracey KJ (2012a) The vagus nerve and the inflammatory reflex--linking immunity and metabolism. Nat Rev Endocrinol 8:743–754 Available at: http://www.pubmedcentral.nih.gov/articlerender.fcgi?artid=4082307&tool=pmcentrez&rendertype=abstract. [PubMed: 23169440]

Pavlov V, Tracey K (2012b) The vagus nerve and the inflammatory reflex - linking immunity and metabolism. Nat Rev Endocrinol December 8:743–754.

Pavlov VA, Tracey KJ (2017) Neural regulation of immunity: Molecular mechanisms and clinical translation. Nat Neurosci 20:156–166. [PubMed: 28092663]

Pecchi E, Dallaporta M, Charrier C, Pio J, Jean A, Moyse E, Troadec J-D (2007) Glial fibrillary acidicprotein (GFAP)-positive radial-like cells are present in the vicinity of proliferative progenitors in the nucleus tractus solitarius of Adult rat. J Comp Neurol:353–368 Available at: http://onlinelibrary.wiley.com/doi/10.1002/cne.21301/abstract?systemMessage=Due+to+scheduled+maintenance%2C+access+to+Wiley+Online+Library+will+be+disrupted+on+Saturday%2C+5th+Mar+between+10%3A00-12%3A00+GMT%5Cnhttp://onlinelibrary.wiley.com/doi/10.1002/c.

Pérez Fontán JJ, Diec CT, Velloff CR (2000) Bilateral distribution of vagal motor and sensory nerve fibers in the rat's lungs and airways. Am J Physiol - Regul Integr Comp Physiol 279:713–728.

Peruzzo B, Pastor FE, Blázquez JL, Schöbitz K, Peláez B, Amat P, Rodríguez EM (2000) A second look at the barriers of the medial basal hypothalamus. Exp Brain Res 132:10–26. [PubMed: 10836632]

Platha-Salaman C (2001) Cytokines and feeding. Int J Obes:48–52.

Poligone B, Baldwin AS (2001) Positive and negative regulation of NF-κB by COX-2. Roles of different prostaglandins. J Biol Chem 276:38658–38664. [PubMed: 11509575]

Prevot V, Cornea A, Mungenast A, Smiley G, Ojeda SR (2003) Activation of erbB-1 signaling in tanycytes of the median eminence stimulates transforming growth factor beta1 release via prostaglandin E2 production and induces cell plasticity. J Neurosci 23:10622–10632. [PubMed: 14627647]

Prevot V, Hanchate NK, Bellefontaine N, Sharif A, Parkash J, Estrella C, Allet C, de Seranno S, Campagne C, d'Anglemont de Tassigny X, Baroncini M (2010) Function-related structural plasticity of the GnRH system. A role for neuronal-glial-endothelial interactions. Front Neuroendocrinol 31:241–258 Available at: 10.1016/j.yfrne.2010.05.003. [PubMed: 20546773]

Price CJ, Hoyda TD, Ferguson AV. (2008) The area postrema: A brain monitor and integrator of systemic autonomic state. Neuroscientist 14:182–194. [PubMed: 18079557]

Quan N (2008) Immune-to-brain signaling: How important are the blood-brain barrier-independent pathways. Mol Neurobiol 37:142–152. [PubMed: 18563639]

Quan N, Whiteside M, Herkenham M (1998) Time course and localization patterns of interleukin-1β messenger RNA expression in brain and pituitary after peripheral administration of lipopolysaccharide. Neuroscience 83:281–293. [PubMed: 9466417]

Quan N, Whiteside M, Kim L, Herkenham M (1997) Induction of inhibitory factor kappaBalpha mRNA in the central nervous system after peripheral lipopolysaccharide administration: an in situ hybridization histochemistry study in the rat. Proc Natl Acad Sci U S A 94:10985–10990 Available at: http://www.ncbi.nlm.nih.gov/pmc/articles/PMC23556/pdf/pq010985.pdf. [PubMed: 9380746]

Qwarnstrom EE, Page RC, Gillis S, Dower SK (1988) Binding, internalization, and intracellular localization of interleukin-1 beta in human diploid fibroblasts. J Biol Chem 263:8261–8269 Available at: http://www.ncbi.nlm.nih.gov/pubmed/2967293. [PubMed: 2967293]

Ramirez J-M (2014) The integrative role of the sigh in psychology, physiology, pathology, and neurobiology. Prog Brain Res 209:91–129. [PubMed: 24746045]

Razavi-Azarkhiavi K, Ali-Omrani M, Solgi R, Bagheri P, Haji-Noormohammadi M, Amani N, Sepand M (2014) Silymarin alleviates bleomycin-induced pulmonary toxicity and lipid peroxidation in mice. Pharm Biol 52:1267–1271 Available at: http://www.tandfonline.com/doi/full/10.3109/13880209.2014.889176. [PubMed: 25026360]

Riazi K, Galic M a, Kuzmiski JB, Ho W, Sharkey K a, Pittman QJ (2008) Microglial activation and TNFalpha production mediate altered CNS excitability following peripheral inflammation. Proc Natl Acad Sci U S A 105:17151–17156. [PubMed: 18955701]

Rocca B, Maggiano N, Habib A, Petrucci G, Gessi M, Fattorossi A, Lauriola L, Landolfi R, Ranelletti FO (2002) Distinct expression of cyclooxygenase-1 and −2 in the human thymus. Eur J Immunol 32:1482–1492. [PubMed: 11981837]

Rogers RC, Hermann GE (2012) Tumor Necrosis Factor Activation of Vagal Afferent Terminal Calcium Is Blocked by Cannabinoids. J Neurosci 32:5237–5241 Available at: http://www.jneurosci.org/cgi/doi/10.1523/JNEUROSCI.6220-11.2012. [PubMed: 22496569]

Rogers RC, McTigue DM, Hermann GE (1995) Vagovagal reflex control of digestion: Afferent modulation by neural and “endoneurocrine” factors. Am J Physiol 268:G1–G10. [PubMed: 7840189]

Rubartelli A, Lotze MT, Latz E, Manfredi AA (2014) Mechanisms of sterile inflammation. Frontiers in Immunology.

Ruchaya PJ, Paton JFR, Murphy D, Yao ST (2012) A cardiovascular role for fractalkine and its cognate receptor, CX3CR1, in the rat nucleus of the solitary tract. Neuroscience 209:119–127. [PubMed: 22387113]

Rummel C, Hübschle T, Gerstberger R, Roth J (2004) Nuclear translocation of the transcription factor STAT3 in the guinea pig brain during systemic or localized inflammation. J Physiol 557:671–687. [PubMed: 14966301]

Rummel C, Sachot C, Poole S, Luheshi GN (2006) Circulating interleukin-6 induces fever through a STAT3-linked activation of COX-2 in the brain. AJP Regul Integr Comp Physiol 291:R1316–R1326 Available at: http://ajpregu.physiology.org/cgi/doi/10.1152/ajpregu.00301.2006.

Ryzhavskii BY, Lebed OA (2016) Formation of Hyaline Membranes in the Lungs of Albino Rat as a Result of Exposure to Bleomycin during the Neonatal Period. Bull Exp Biol Med 160:390–393. [PubMed: 26742747]

Sadowska GB, Chen X, Zhang J, Lim YP, Cummings EE, Makeyev O, Besio WG, Gaitanis J, Padbury JF, Banks WA, Stonestreet BS (2015) Interleukin-1β transfer across the blood-brain barrier in the ovine fetus. J Cereb Blood Flow Metab 35:1388–1395. [PubMed: 26082012]

Samad TA, Moore KA, Sapirstein A, Billet S, Allchorne A, Poole S, Bonventre JV., Woolf CJ (2001) Interleukin-1 β-mediated induction of Cox-2 in the CNS contributes to inflammatory pain hypersensitivity. Nature 410:471–475. [PubMed: 11260714]

Santos NC, Figueira-Coelho J, Martins-Silva J, Saldanha C (2003) Multidisciplinary utilization of dimethyl sulfoxide: Pharmacological, cellular, and molecular aspects. Biochem Pharmacol 65:1035–1041. [PubMed: 12663039]

Sastre M, Dewachter I, Landreth GE, Wilson TM, Klockgether T, Van Leuven F, Heneka MT (2003) Nonsteroidal Anti-Inflammatory Drugs and Peroxisome Proliferator-Activated Receptor-γ Agonists Modulate Immunostimulated Processing of Amyloid Precursor Protein through Regulation of β-Secretase. J Neurosci 23:9796–9804. [PubMed: 14586007]

Schelegle ES, Walby WF, Mansoor JK, Chen a T (2001) Lung vagal afferent activity in rats with bleomycin-induced lung fibrosis. Respir Physiol 126:9–27. [PubMed: 11311307]

Schiltz JC, Sawchenko PE (2002) Distinct brain vascular cell types manifest inducible cyclooxygenase expression as a function of the strength and nature of immune insults. J Neurosci 22:5606–5618 Available at: http://www.ncbi.nlm.nih.gov/pubmed/12097512. [PubMed: 12097512]

Schindelin J, Arganda-Carreras I, Frise E, Kaynig V, Longair M, Pietzsch T, Preibisch S, Rueden C, Saalfeld S, Schmid B, Tinevez J-Y, White DJ, Hartenstein V, Eliceiri K, Tomancak P, Cardona A (2012) Fiji: an open-source platform for biological-image analysis. Nat Methods 9:676–682 Available at: http://www.ncbi.nlm.nih.gov/pubmed/22743772%0Ahttp://www.pubmedcentral.nih.gov/articlerender.fcgi?artid=PMC3855844. [PubMed: 22743772]

Schmidt HB, Werdan K, Muller-Werdan U (2001) Autonomic dysfunction in the ICU patient. Curr Opin Crit Care 7:314–322. [PubMed: 11805528]

Schober A, Bottner M, Strelau J, Kinscherf R, Bonaterra GA, Barth M, Schilling L, Fairlie WD, Breit SN, Unsicker K (2001) Expression of growth differentiation factor-15/macrophage inhibitory cytokine-1 (GDF-15/MIC-1) in the perinatal, adult, and injured rat brain. J Comp Neurol 439:32–45. [PubMed: 11579380]

Seely AJ, Christou NV (2000) Multiple organ dysfunction syndrome: exploring the paradigm of complex nonlinear systems. Crit Care Med 28:2193–2200. [PubMed: 10921540]

Sekiyama N, Mizuta S, Hori A, Kobayashi S (1995) Prostaglandin E2 facilitates excitatory synaptic transmission in the nucleus tractus solitarii of rats. Neurosci Lett.

Selenica MLB, Alvarez JA, Nash KR, Lee DC, Cao C, Lin X, Reid P, Mouton PR, Morgan D, Gordon MN (2013) Diverse activation of microglia by chemokine (C-C motif) ligand 2 overexpression in brain. J Neuroinflammation 10:1–17. [PubMed: 23282009]

Senzacqua M, Severi I, Perugini J, Acciarini S, Cinti S, Giordano A (2016) Action of administered ciliary neurotrophic factor on the mouse dorsal vagal complex. Front Neurosci 10:1–17. [PubMed: 26858586]

Serrats J, Grigoleit JS, Alvarez-Salas E, Sawchenko PE (2017) Pro-inflammatory immune-to-brain signaling is involved in neuroendocrine responses to acute emotional stress. Brain Behav Immun.

Shapiro RE, Miselis RR (1985) The central neural connections of the area postrema of the rat. J Comp Neurol 234:344–364. [PubMed: 3988989]

Shen H, Kreisel D, Goldstein DR (2013) Processes of Sterile Inflammation. J Immunol:2857–2863.

Shrivastava P, Cabrera MA, Chastain LG, Boyadjieva NI, Jabbar S, Franklin T, Sarkar DK (2017) Mu-opioid receptor and delta-opioid receptor differentially regulate microglial inflammatory response to control proopiomelanocortin neuronal apoptosis in the hypothalamus: Effects of neonatal alcohol. J Neuroinflammation 14:1–19. [PubMed: 28086917]

Siljehav V, Shvarev Y, Herlenius E (2014) Il-1β and prostaglandin E2 attenuate the hypercapnic as well as the hypoxic respiratory response via prostaglandin E receptor type 3 in neonatal mice. J Appl Physiol 117:1027–1036 Available at: http://www.ncbi.nlm.nih.gov/pubmed/25213632. [PubMed: 25213632]

Singh N, Jabeen T, Somvanshi RK, Sharma S, Dey S, Singh TP (2004) Phospholipase A2 as a Target Protein for Nonsteroidal Anti-Inflammatory Drugs (NSAIDs): Crystal Structure of the Complex Formed between Phospholipase A2 and Oxyphenbutazone at 1.6 Å Resolution. Biochemistry 43:14577–14583 Available at: 10.1021/bi0483561. [PubMed: 15544328]

Skinner RA, Gibson RM, Rothwell NJ, Pinteaux E, Penny JI (2009) Transport of interleukin-1 across cerebromicrovascular endothelial cells. Br J Pharmacol 156:1115–1123. [PubMed: 19298391]

Skurikhin EG, Pershina OV, Reztsova AM, Ermakova NN, Khmelevskaya ES, Krupin VA, Stepanova IE, Artamonov AV, Bekarev AA, Madonov PG, Dygai AM (2015) Modulation of bleomycin-induced lung fibrosis by pegylated Hyaluronidase and dopamine receptor antagonist in mice. PLoS One 10:1–24.

Sofroniew M (2015) Astrocyte barriers to neurotoxic inflammation. Nat Rev Neurosci 16:249–263. [PubMed: 25891508]

Srinivasan M, Bongianni F, Fontana G, Pantaleo T (1993) Respiratory responses to electrical and chemical stimulation of the area postrema in the rabbit. J Physiol:409–420. [PubMed: 8246191]

Stock N, Munoz B, Wrigley JDJ, Shearman MS, Beher D, Peachey J, Williamson TL, Bain G, Chen W, Jiang X, St-Jacques R, Prasit P (2006) The geminal dimethyl analogue of Flurbiprofen as a novel Aβ42 inhibitor and potential Alzheimer's disease modifying agent. Bioorganic Med Chem Lett 16:2219–2223.

Strauss KI (2008) Antiinflammatory and neuroprotective actions of COX2 inhibitors in the injured brain. Brain Behav Immun 22:285–298. [PubMed: 17996418]

Streit WJ, Walter SA, Pennell NA (1999) Reactive microgliosis. Prog Neurobiol 57:563–581. [PubMed: 10221782]

Stromberg NO, Gustafsson PM (1996) Breathing pattern variability during bronchial histamine and methacholine challenges in asthmatics. Respir Med 90:287–296. [PubMed: 9499813]

Sun D, Jakobs TC (2013) Structural Remodeling of Astrocytes in the Injured CNS. Neuroscientist 18:567–588.

Sun L, Li M, Ma X, Feng H, Song J, Lv C, He Y (2017) Inhibition of HMGB1 reduces rat spinal cord astrocytic swelling and AQP4 expression after oxygen-glucose deprivation and reoxygenation via TLR4 and NF-KB signaling in an IL-6-dependent manner. J Neuroinflammation 14:1–18. [PubMed: 28086917]

Sun MK, Spyer KM (1991) GABA-mediated inhibition of medullary vasomotor neurones by area postrema stimulation in rats. J Physiol 436:669–684. [PubMed: 2061850]

Sung S, Yang H, Uryu K, Lee EB, Zhao L, Shineman D, Trojanowski JQ, Lee VM-Y, Pratico D (2004) Modulation of nuclear factor-kappa B activity by indomethacin influences A beta levels but not A beta precursor protein metabolism in a model of Alzheimer's disease. Am J Pathol 165:2197–2206. [PubMed: 15579461]

Sunkin SM, Ng L, Lau C, Dolbeare T, Gilbert TL, Thompson CL, Hawrylycz M, Dang C (2013) Allen Brain Atlas: An integrated spatio-temporal portal for exploring the central nervous system. Nucleic Acids Res.

Tachikawa M, Ozeki G, Higuchi T, Akanuma SI, Tsuji K, Hosoya KI (2012) Role of the blood-cerebrospinal fluid barrier transporter as a cerebral clearance system for prostaglandin E2 produced in the brain. J Neurochem 123:750–760. [PubMed: 22978524]

Takagi S, Furube E, Nakano Y, Morita M, Miyata S (2017) Microglia are continuously activated in the circumventricular organs of mouse brain. J Neuroimmunol:0–1 Available at: 10.1016/j.jneuroim.2017.10.008.

Takagishi M, Waki H, Bhuiyan MER, Gouraud SS, Kohsaka A, Cui H, Yamazaki T, Paton JFR, Takagishi M, Waki H, Bhuiyan MER, Gouraud SS, Kohsaka A, Cui H, Yamazaki T, Paton JFR, Maeda M (2011) IL-6 microinjected in the nucleus tractus solitarii attenuates cardiac baroreceptor reflex function in rats IL-6 microinjected in the nucleus tractus solitarii attenuates cardiac baroreceptor reflex function in rats. Am J Physiol Regul Integr Comp Physiol:183–190.

Takano T, Tian GF, Peng W, Lou N, Libionka W, Han X, Nedergaard M (2006) Astrocyte-mediated control of cerebral blood flow. Nat Neurosci 9:260–267. [PubMed: 16388306]

Tanaka H, Yanase-Fujiwara M, Kanosue K (1993) Effects of centrally and systemically administered indomethacin on body temperature in exercising rats. Am J Physiol - Regul Integr Comp Physiol.

Tian J, Kim SF, Hester L, Snyder SH (2008) S-nitrosylation/activation of COX-2 mediates NMDA neurotoxicity. Proc Natl Acad Sci U S A 105:10537–10540 Available at: http://www.pubmedcentral.nih.gov/articlerender.fcgi?artid=2492460&tool=pmcentrez&rendertype=abstract. [PubMed: 18650379]

Tohyama T, Saku K, Kawada T, Kishi T, Yoshida K, Nishikawa T, Mannoji H, Kamada K, Sunagawa K, Tsutsui H (2018) Impact of lipopolysaccharide-induced acute inflammation on baroreflex-controlled sympathetic arterial pressure regulation. PLoS One 13:1–16.

Tsai CY, Su CH, Chan JYH, Chan SHH (2017) Nitrosative stress-induced disruption of baroreflex neural circuits in a rat model of hepatic encephalopathy: A DTI study. Sci Rep 7:1–12 Available at: 10.1038/srep40111. [PubMed: 28127051]

Tsai VWW, Manandhar R, Jrøgensen SB, Lee-Ng KKM, Zhang HP, Marquis CP, Jiang L, Husaini Y, Lin S, Sainsbury A, Sawchenko PE, Brown DA, Breit SN (2014) The anorectic actions of the TGFβ cytokine MIC-1/GDF15 require an intact brainstem area postrema and nucleus of the solitary tract. PLoS One 9:1–10.

Tzouvelekis A, Pneumatikos I, Bouros D (2005) Serum biomarkers in Acute Respiratory Distress Syndrome an ailing prognosticator. Respir Res:1–19. [PubMed: 15631627]

Uhlen M et al. (2005) A human protein atlas for normal and cancer tissues based on antibody proteomics. Mol Cell Proteomics 4:1920–1932. [PubMed: 16127175]

Uhlen M et al. (2015) Proteomics. Tissue-based map of the human proteome. Science 347:1260419.

Van Den Brule S, Huaux F, Uwambayinema F, Ibouraadaten S, Yakoub Y, Palmai-Pallag M, Trottein F, Renauld JC, Lison D (2014) Lung Inflammation and Thymic atrophy after Bleomycin are controlled by the prostaglandin D2 receptor DP1. Am J Respir Cell Mol Biol 50:212–222. [PubMed: 24003988]

van der Kooy D, Koda LY (1983) Organization of the projections of a circumventricular organ: the area postrema in the rat. J Comp Neurol 219:328–338. [PubMed: 6619341]

Vance KM, Rogers RC, Hermann GE (2015) PAR1-Activated Astrocytes in the Nucleus of the Solitary Tract Stimulate Adjacent Neurons via NMDA Receptors. J Neurosci 35:776–785 Available at: http://www.jneurosci.org/cgi/doi/10.1523/JNEUROSCI.3105-14.2015. [PubMed: 25589770]

Vandendriessche B, Rogge E, Goossens V, Vandenabeele P, Stasch JP, Brouckaert P, Cauwels A (2013) The Soluble Guanylate Cyclase Activator BAY 58–2667 Protects against Morbidity and Mortality in Endotoxic Shock by Recoupling Organ Systems. PLoS One 8.

Vargas-Caraveo A, Pérez-Ishiwara DG, Martínez-Martínez A (2015) Chronic psychological distress as an inducer of microglial activation and leukocyte recruitment into the area postrema. Neuroimmunomodulation 22:311–321. [PubMed: 25765708]

Vargas-Caraveo A, Sayd A, Maus SR, Caso JR, Madrigal JLM, García-Bueno B, Leza JC (2017) Lipopolysaccharide enters the rat brain by a lipoprotein-mediated transport mechanism in physiological conditions. Sci Rep 7:1–15. [PubMed: 28127051]

Vaseghi M, Salavatian S, Rajendran PS, Yagishita D, Woodward WR, Hamon D, Yamakawa K, Irie T, Habecker BA, Shivkumar K (2017) Parasympathetic dysfunction and antiarrhythmic effect of vagal nerve stimulation following myocardial infarction. JCI Insight 2 Available at: http://www.ncbi.nlm.nih.gov/pubmed/28814663%0Ahttps://insight.jci.org/articles/view/86715.

Verhamme FM, Freeman CM, Brusselle GG, Bracke KR, Curtis JL (2019) GDF-15 in Pulmonary and Critical Care Medicine. Am J Respir Cell Mol Biol 60:621–628. [PubMed: 30633545]

Verhamme FM, Seys LJM, De Smet EG, Provoost S, Janssens W, Elewaut D, Joos GF, Brusselle GG, Bracke KR (2017) Elevated GDF-15 contributes to pulmonary inflammation upon cigarette smoke exposure. Mucosal Immunol 10:1400–1411 Available at: 10.1038/mi.2017.3. [PubMed: 28145442]

Vigier D, Portalier P (1979) Efferent projections of the area postrema demonstrated by autoradiography. Arch Ital Biol 117:308–324. [PubMed: 550737]

Villapol S (2018) Roles of Peroxisome Proliferator-Activated Receptor Gamma on Brain and Peripheral Inflammation. Cell Mol Neurobiol 38:121–132. [PubMed: 28975471]

Vitkovic L, Konsman JP, Bockaert J, Dantzer R, Homburger V, Jacque C (2000) Cytokine signals propagate through the brain. Mol Psychiatry 5:604–615. [PubMed: 11126391]

Vlemincx E, Abelson JL, Lehrer PM, Davenport PW, Van Diest I, Van den Bergh O (2013) Respiratory variability and sighing: a psychophysiological reset model. Biol Psychol 93:24–32. [PubMed: 23261937]

Vlemincx E, Van Diest I, Van den Bergh O (2012) A sigh following sustained attention and mental stress: effects on respiratory variability. Physiol Behav 107:1–6. [PubMed: 22634279]

Voss T, Barth SW, Rummel C, Gerstberger R, Hübschle T, Roth J (2007) STAT3 and COX-2 activation in the guinea-pig brain during fever induced by the Toll-like receptor-3 agonist polyinosinic:polycytidylic acid. Cell Tissue Res 328:549–561. [PubMed: 17345100]

Waki H, Gouraud SS, Maeda M, Paton JFR (2010) Evidence of specific inflammatory condition in nucleus tractus solitarii of spontaneously hypertensive rats. Exp Physiol 95:595–600. [PubMed: 19923159]

Waki H, Hendy EB, Hindmarch CCT, Gouraud S, Toward M, Kasparov S, Murphy D, Paton JFR (2013) Excessive leukotriene B4 in nucleus tractus solitarii is prohypertensive in spontaneously hypertensive rats. Hypertension 61:194–201. [PubMed: 23172924]

Wang H, Hitron IM, Iadecola C, Pickel VM (2005) Synaptic and vascular associations of neurons containing cyclooxygenase-2 and nitric oxide synthase in rat somatosensory cortex. Cereb Cortex 15:1250–1260. [PubMed: 15616132]

Wang QP, Guan JL, Pan W, Kastin AJ, Shioda S (2008) A diffusion barrier between the area postrema and nucleus tractus solitarius. Neurochem Res 33:2035–2043. [PubMed: 18373195]

Wang ZH, Xiang J, Liu X, Yu SP, Manfredsson FP, Sandoval IM, Wu S, Wang JZ, Ye K (2019) Deficiency in BDNF/TrkB Neurotrophic Activity Stimulates δ-Secretase by Upregulating C/EBPβ in Alzheimer's Disease. Cell Rep 28:655–669.e5 Available at: 10.1016/j.celrep.2019.06.054. [PubMed: 31315045]

Warren PM, Campanaro C, Jacono FJ, Alilain WJ (2018) Mid-cervical spinal cord contusion causes robust deficits in respiratory parameters and pattern variability. Exp Neurol 306:122–131. [PubMed: 29653187]

Wei F, Guo W, Zou S, Ren K, Dubner R (2008) Supraspinal glial-neuronal interactions contribute to descending pain facilitation. J Neurosci 28:10482–10495. [PubMed: 18923025]

Wei S, Yu Y, Felder XRB (2018) Blood-borne interleukin-1 beta acts on the subfornical organ to upregulate the sympathoexcitatory milieu of the hypothalamic paraventricular nucleus. Am J Physiol Regul Integr Comp Physiolhysiol Regul Integr Comp Physiol March:R447–R458.

Wei S, Zhang Z, Beltz T, Yu Y, Johnson A, Felder R (2013a) Subfornical organ mediates sympathetic and hemodynamic responses to blood-borne pro-inflammatory cytokines. Hypertension July:118–125. [PubMed: 23670302]

Wei XH, Na XD, Liao GJ, Chen QY, Cui Y, Chen FY, Li YY, Zang Y, Liu XG (2013b) The up-regulation of IL-6 in DRG and spinal dorsal horn contributes to neuropathic pain following L5 ventral root transection. Exp Neurol 241:159–168 Available at: 10.1016/j.expneurol.2012.12.007. [PubMed: 23261764]

Widdicombe JG (2003) Overview of neural pathways in allergy and asthma. Pulm Pharmacol Ther 16:23–30. [PubMed: 12657497]

Wilhelms DB, Kirilov M, Mirrasekhian E, Eskilsson A, Kugelberg UO, Klar C, Ridder DA, Herschman HR, Schwaninger M, Blomqvist A, Engblom D (2014) Deletion of Prostaglandin E2 Synthesizing Enzymes in Brain Endothelial Cells Attenuates Inflammatory Fever. J Neurosci 34:11684–11690 Available at: http://www.jneurosci.org/cgi/doi/10.1523/JNEUROSCI.1838-14.2014. [PubMed: 25164664]

Williams M (2007) The Merck Index: An Encyclopedia of Chemicals, Drugs, and Biologicals, 14th ed. Edited by Maryadele J. O'Neil(Editor), Patricia E. Heckelman (Senior Associate Editor), Cherie B. Koch (Associate Editor), and Kristin J. Roman (Assistant Editor). Merck and. J Am Chem Soc 129:2197 Available at: 10.1021/ja069838y.

Willis A, Mihalevich M, Neff RA, Mendelowitz D (1996) Three types of postsynaptic glutamatergic receptors are activated in DMNX neurons upon stimulation of NTS. Am J Physiol 271:R1614–9. [PubMed: 8997360]

Willis CL (2011) Glia-Induced Reversible Disruption of Blood–Brain Barrier Integrity and Neuropathological Response of the Neurovascular Unit. Toxicol Pathol 39:172–185. [PubMed: 21189317]

Willis CL, Garwood CJ, Ray DE (2007) A size selective vascular barrier in the rat area postrema formed by perivascular macrophages and the extracellular matrix. Neuroscience 150:498–509 Available at: http://www.ncbi.nlm.nih.gov/pubmed/17945430 [Accessed September 24, 2014]. [PubMed: 17945430]

Wu YH, Ko TP, Guo RT, Hu SM, Chuang LM, Wang AHHJ (2008) Structural Basis for Catalytic and Inhibitory Mechanisms of Human Prostaglandin Reductase PTGR2. Structure 16:1714–1723 Available at: 10.1016/j.str.2008.09.007. [PubMed: 19000823]

Wuchert F, Ott D, Murgott J, Rafalzik S, Hitzel N, Roth J, Gerstberger R (2008) Rat area postrema microglial cells act as sensors for the toll-like receptor-4 agonist lipopolysaccharide. J Neuroimmunol 204:66–74 Available at: 10.1016/j.jneuroim.2008.07.017. [PubMed: 18786731]

Wuchert F, Ott D, Rafalzik S, Roth J, Gerstberger R (2009) Tumor necrosis factor-α, interleukin-1β and nitric oxide induce calcium transients in distinct populations of cells cultured from the rat area postrema. J Neuroimmunol 206:44–51 Available at: 10.1016/j.jneuroim.2008.10.010. [PubMed: 19081643]

Xia Q, Hu Q, Wang H, Yang H, Gao F, Ren H, Chen D, Fu C, Zheng L, Zhen X, Ying Z, Wang G (2015) Induction of COX-2-PGE2 synthesis by activation of the MAPK/ERK pathway contributes to neuronal death triggered by TDP-43-depleted microglia. Cell Death Dis 6:e1702.

Xiang Y, Zhao M ming, Sun S, Guo XL, Wang Q, Li SA, Lee WH, Zhang Y (2018) A high concentration of DMSO activates caspase-1 by increasing the cell membrane permeability of potassium. Cytotechnology 70:313–320. [PubMed: 28965287]

Xing L, Remick DG (2005) Mechanisms of Dimethyl Sulfoxide Augmentation of IL-1β Production. J Immunol 174:6195–6202. [PubMed: 15879116]

Xu J, Mora AL, LaVoy J, Brigham KL, Rojas M (2006) Increased bleomycin-induced lung injury in mice deficient in the transcription factor T-bet. Am J Physiol Lung Cell Mol Physiol 291:L658–67 Available at: http://www.ncbi.nlm.nih.gov/entrez/query.fcgi?cmd=Retrieve&db=PubMed&dopt=Citation&list_uids=16648243. [PubMed: 16648243]

Yamauchi M, Ocak H, Dostal J, Jacono FJ, Loparo KA, Strohl KP (2008) Post-sigh breathing behavior and spontaneous pauses in the C57BL/6J (B6) mouse. Respir Physiol Neurobiol 162:117–125. [PubMed: 18565803]

Yang H, Chen C (2008) Cyclooxygenase-2 in synaptic signaling. Curr Pharm Des 14:1443–1451. [PubMed: 18537667]

Yang L et al. (2017) GFRAL is the receptor for GDF15 and is required for the anti-obesity effects of the ligand. Nat Med 23:1158–1166. [PubMed: 28846099]

Yoshida A, Furube E, Mannari T, Takayama Y, Kittaka H, Tominaga M, Miyata S (2016) TRPV1 is crucial for proinflammatory STAT3 signaling and thermoregulation-associated pathways in the brain during inflammation. Sci Rep 6:1–11 Available at: 10.1038/srep26088. [PubMed: 28442746]

Young BP, Loparo KA, Dick TE, Jacono FJ (2019) Ventilatory pattern variability as a biometric for severity of acute lung injury in rats. Respir Physiol Neurobiol 265:161–171 Available at: 10.1016/j.resp.2019.03.009. [PubMed: 30928542]

Zhang Y, Jiang M, Nouraie M, Roth MG, Tabib T, Winters S, Chen X, Sembrat J, Chu Y, Cardenes N, Tuder RM, Herzog EL, Ryu C, Rojas M, Lafyatis R, Gibson KF, McDyer JF, Kass DJ, Alder JK (2019) GDF15 is an epithelial-derived biomarker of idiopathic pulmonary fibrosis. Am J Physiol Lung Cell Mol Physiol 317:L510–L521. [PubMed: 31432710]

## Highlights

- Sterile lung injury (SLI) activates radial-glia that separate area postrema from CNS
- After SLI, IL-1β & COX-2 localize to radial-glia, which project basolaterally into CNS
- Inhibition of COX-1/2 in the CNS blocks the increases in GFAP and IL-1β after SLI
- Inhibition of COX-1/2 restores sighs that reset the respiratory rhythm

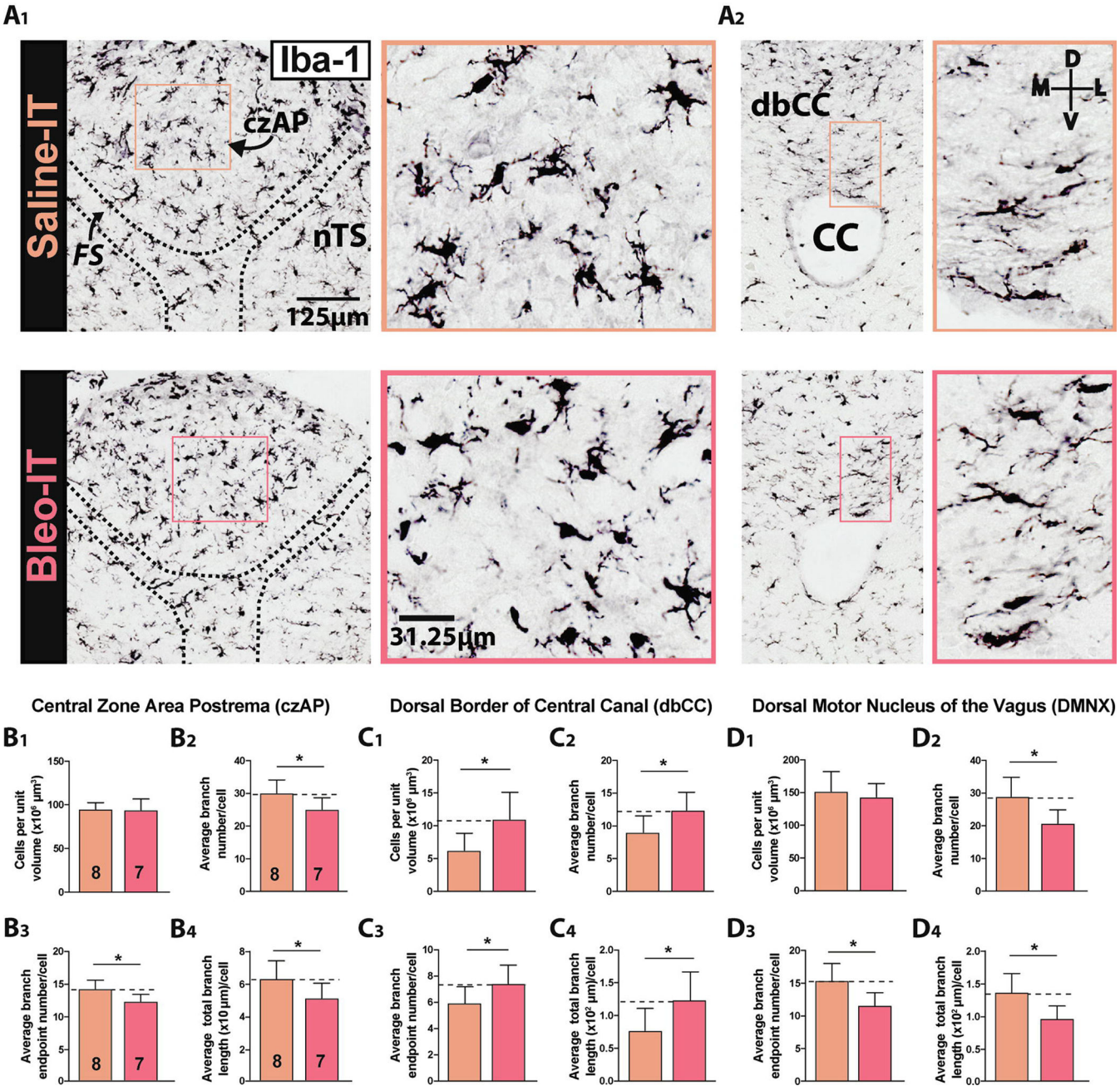


**Figure 1:**

Sterile lung injury (SLI) promotes microglia/macrophage morphologic changes throughout the dorsomedial brainstem

**A1.** Representative images of coronal brainstem sections from saline- (orange) and Bleo-treated rats (red) immunostained for Iba-1 and amplified using avidin/biotin + 3,3'-diaminobenzadine (DAB). DAB visualized Iba-1+ IR was used to count cells in the dorsal brainstem.

**A2.** Magnified representative images of Iba-1+ cells in the dorsal border of the Central Canal (dbCC, left panel) and Area Postrema (AP, right panel).

**B1.** The number of Iba-1+ cells in the czAP was not significantly different in Bleo-compared to saline-treated rats ($P = 0.87$, Two-tail t-Test).

**B2.** The branch number (Br#) in the czAP decreased in Bleo-compared to saline-treated rats ($P = 0.024$, Two-tail t-Test).

**B3.** Bleo-treated rats had fewer branch endpoints (BEPs) in the czAP compared to saline-treated rats. ($P = 0.03$, Two-tail t-Test).

**B4.** The total branch length (TBL) in the czAP was reduced in Bleo-compared to saline-treated rats ($P = 0.031$, Two-tail t-Test).

**C1.** The number of Iba-1+ cells in the dorsal border of the CC (dbCC) increased in Bleo- (n = 7) compared to saline- (n = 8) treated rats ($P = 0.018$, Two-tail t-Test).

**C2.** The BN#/Iba-1+ cell (Br#) located in the dbCC increased in Bleo-compared to saline-treated rats ($P = 0.027$, Two-tail t-Test).

**C3**. The number of BEPs/Iba-1+ cell (BEPs) in the dbCC increased in Bleo-compared to saline-treated rats ($P = 0.049$, Two-tail t-Test).

**C4.** The TBL/Iba-1+ cell in the dbCC increased in Bleo-compared to saline-treated rats ($P = 0.035$, Two-tail t-Test).

**D1.** The number of Iba-1+ cells in the Dorsal Motor Nucleus of the Vagus (DMNX) was not significantly different between Bleo- and saline-treated rats ($P = 0.53$, Two-tail t-Test).

**D2.** The Br# in the DMNX was reduced in Bleo-compared to saline-treated rats ($P = 0.01$, Two-tail t-Test).

**D3.** Bleo treated rats exhibited reduced BEPs in the DMNX in comparison to saline-treated rats ($P = 0.01$, Two-tail t-Test).

**D4.** The TBL in the in the DMNX was reduced in Bleo-compared to saline-treated rats ($P = 0.012$, Two-tail t-Test).

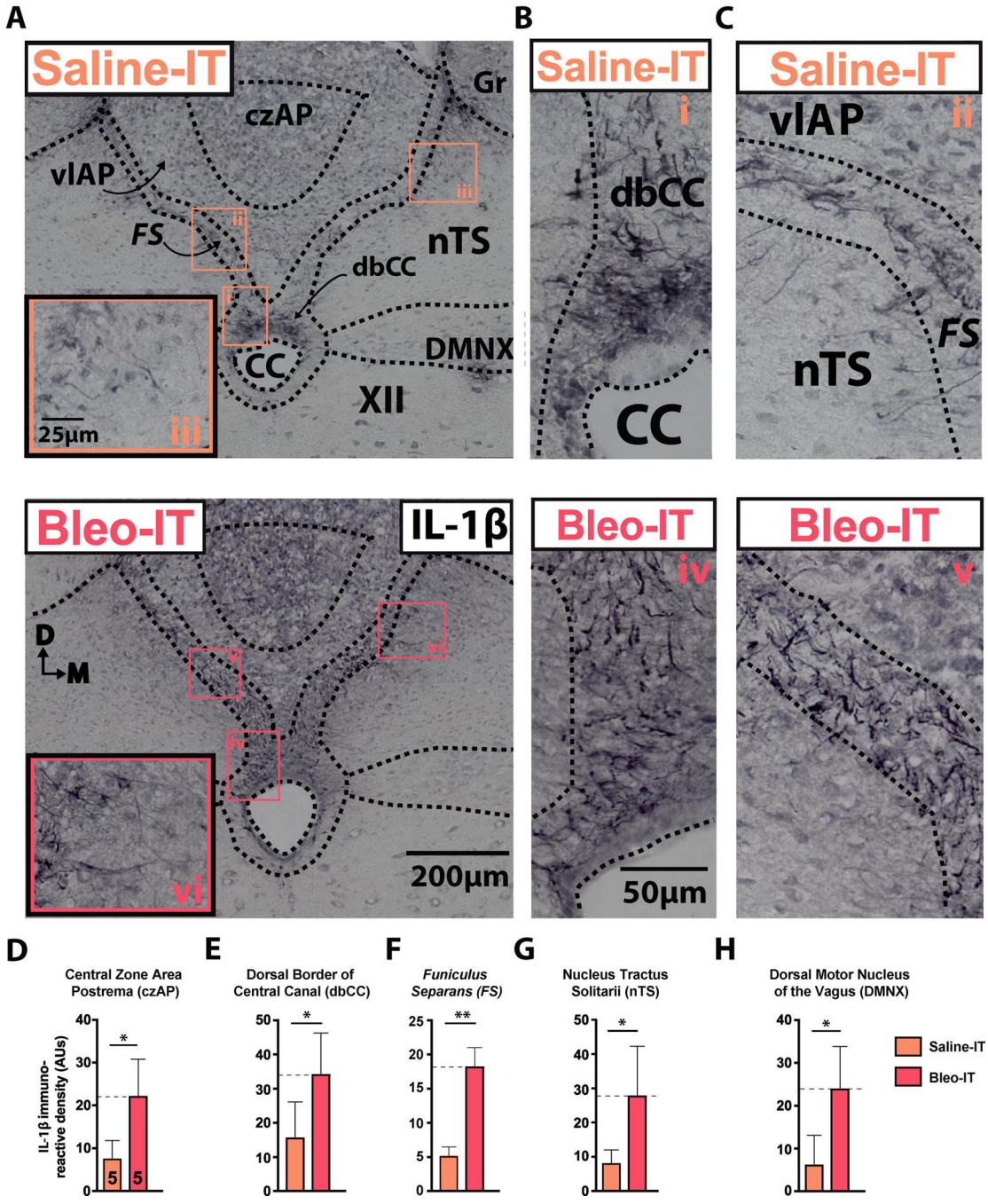


**Figure 2:**

SLI promotes IL-1β+ IR at the glial-barrier separating area postrema from adjacent dorsomedial brainstem sites.

**A.** Representative images of coronal brainstem sections from saline-treated rats (Left panel, orange text) and Bleo-treated rats (right panel, red text) immunostained for IL-1β. Small numbered boxes (orange, i - iii; red, iv - vi) indicate magnified sites in the dorsal border of the central canal (i, iv; dbCC) *funiculus separans* (ii, v; *FS*), and medial nucleus tractus solitarii (iii, vi; nTS).

**B.** Magnified representative images showing IL-1β+ immunoreactivity (IR) in the dbCC of saline (orange i) and Bleo (red iv) treated rats.
**C.** Magnified representative images showing IL-1β+ IR in the *FS* of saline- (orange ii) and Bleo-(red v) treated rats.
**D.** IL-1β+ IR in the central zone of the AP (czAP) was augmented in Bleo-treated rats (n = 5) compared to saline-treated rats (n = 5) ($P = 0.039$, Two-tail t-Test).
**E.** IL-1β+ IR in the dbCC was augmented in Bleo-treated rats compared to saline-treated rats ($P = 0.03$, Two-tail t-Test).
**F.** IL-1β+ IR in the *FS* was augmented in Bleo-treated rats compared to saline-treated rats ($P = 0.0093$, Two-tail t-Test).
**G.** IL-1β+ (IR) in the nTS was augmented in Bleo-treated rats compared to saline-treated rats ($P = 0.024$, Two-tail t-Test).
**H.** IL-1β+ IR in the Dorsal Motor Nucleus of the Vagus (DMNX) was augmented in Bleo-treated rats compared to saline-treated rats ($P = 0.01$, Two-tail t-Test).

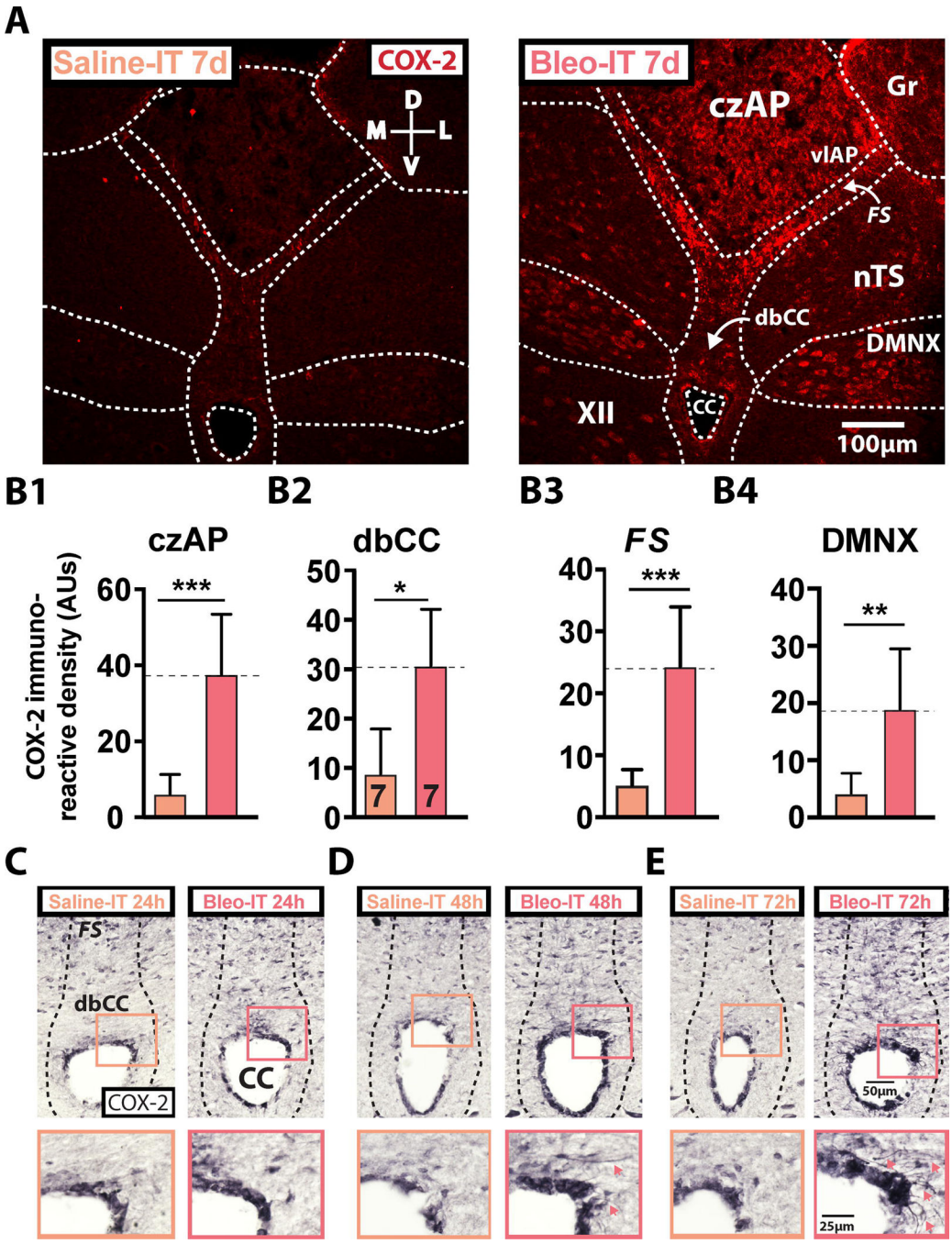


**Figure 3:**

SLI augments cyclooxygenase-2 (COX-2) at the glial-barrier separating area postrema from neighboring dorsomedial brainstem sites.

**A.** Representative images of coronal brainstem sections from saline- (left panel, orange text) and Bleo-treated rats (right panel, red text) that were fluorescently immunostained for COX-2

**B1.** COX-2+ IR was significantly augmented in the central zone of the AP (czAP) of Bleo (n = 7) treated rats compared to saline (n = 7) treated rats ($P = 0.0003$, Two-tail t-Test)

**B2.** COX-2+ IR was significantly augmented in the dorsal border of the central canal (dbCC) of Bleo-compared to saline-treated rats ($P = 0.0019$, Two-tail t-Test).
**B3.** COX-2+ IR was significantly augmented in the *funiculus separans (FS*) of Bleo-compared to saline-treated rats ($P = 0.0003$, Two-tail t-Test).
**B4.** COX-2+ IR was significantly augmented in the dorsal motor nucleus of the vagus (DMNX) of Bleo-compared to saline-treated rats ($P = 0.004$, Two-tail t-Test).
**C.** Representative images showing COX-2+ IR in coronal brainstem sections from rats that received intratracheal Bleo (n = 2, right panel) or saline (n = 2, left panel) and were euthanized 24h later. Insets show a magnified view of COX-2+ IR in the dbCC of Bleo- (red box) and saline-(orange box) treated rats.
**D.** Representative images showing COX-2+ IR in coronal brainstem sections from rats that received intratracheal Bleo (n = 4, right panel) or saline (n = 4, left panel) and were euthanized 48h later. Insets show a magnified view of the dbCC at 48h. Red arrowheads in the red box indicate COX-2 IR within basolaterally projecting radial-glia.
**E.** Representative images showing COX-2+ IR in coronal brainstem sections from rats that received intratracheal Bleo (n = 2, right panel) or saline (n = 2, left panel) and were euthanized 72h later. Insets show a magnified view of the dbCC at 72h. Red arrowheads indicate COX-2+ IR within basolaterally projecting radial-glia.

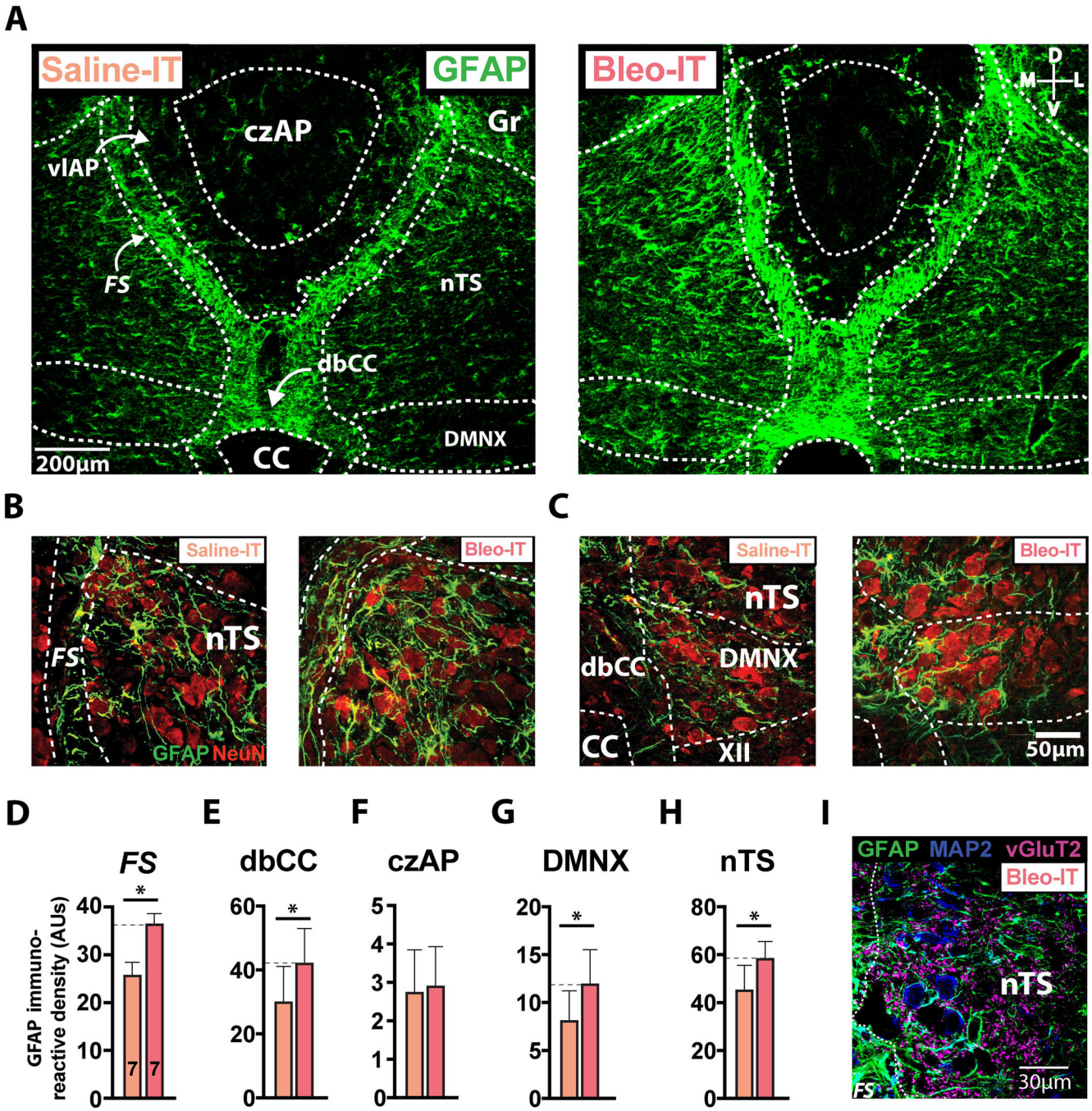


**Figure 4:**

SLI augments glial fibrillary acidic protein (GFAP) expression in the dorsal vagal complex.

**A.** Representative images of coronal brainstem sections from saline- (left panel) and Bleo-treated rats (right panel) immunostained for GFAP. Both groups exhibited strong GFAP+ IR within the *funiculus separans* (*FS*) and dorsal border of the central canal (dbCC)

**B.** Representative images showing co-labeling for GFAP (green) and the neuronal marker NeuN (red) in coronals brainstem sections containing the *FS* and medial nucleus tractus solitarii (nTS) of Bleo- (right panel, n = 3) and saline- (left panel, n = 3) treated rats.

**C.** Representative images showing co-labeling for GFAP and NeuN brainstem sections in the dbCC and adjacent dm-brainstem sites of Bleo- (right panel, n = 3) and saline- (left panel, n = 3) treated rats.

**D.** GFAP+ IR in the *FS* was increased in Bleo- (n = 7) compared to saline- (n = 7) treated rats ($P = 0.0098$, Two-tail t-Test).

**E.** GFAP+ IR in the dbCC was increased in Bleo-treated rats compared to saline-treated rats ($P = 0.044$, Two-tail t-Test).

**F.** GFAP+ IR in the central zone of the AP (czAP) was not significantly different in Bleo-compared to saline-treated rats ($P = 0.773$, Two-tail t-Test).

**G.** GFAP+ IR in the DMNX was increased in Bleo-compared to saline-treated rats ($P = 0.044$, Two-tail t-Test).

**H.** GFAP+ IR in the nTS was increased in Bleo-compared to saline-treated rats ($P = 0.034$, Two-tail t-Test).

**I.** (IHC) Co-labeling of GFAP (green), the neuronal marker MAP2 (Blue) and the glutamatergic presynaptic marker vGluT2 (magenta), showed radial-glia and astrocytes to be in close apposition to neurons and presynaptic terminals in the medial nTS.

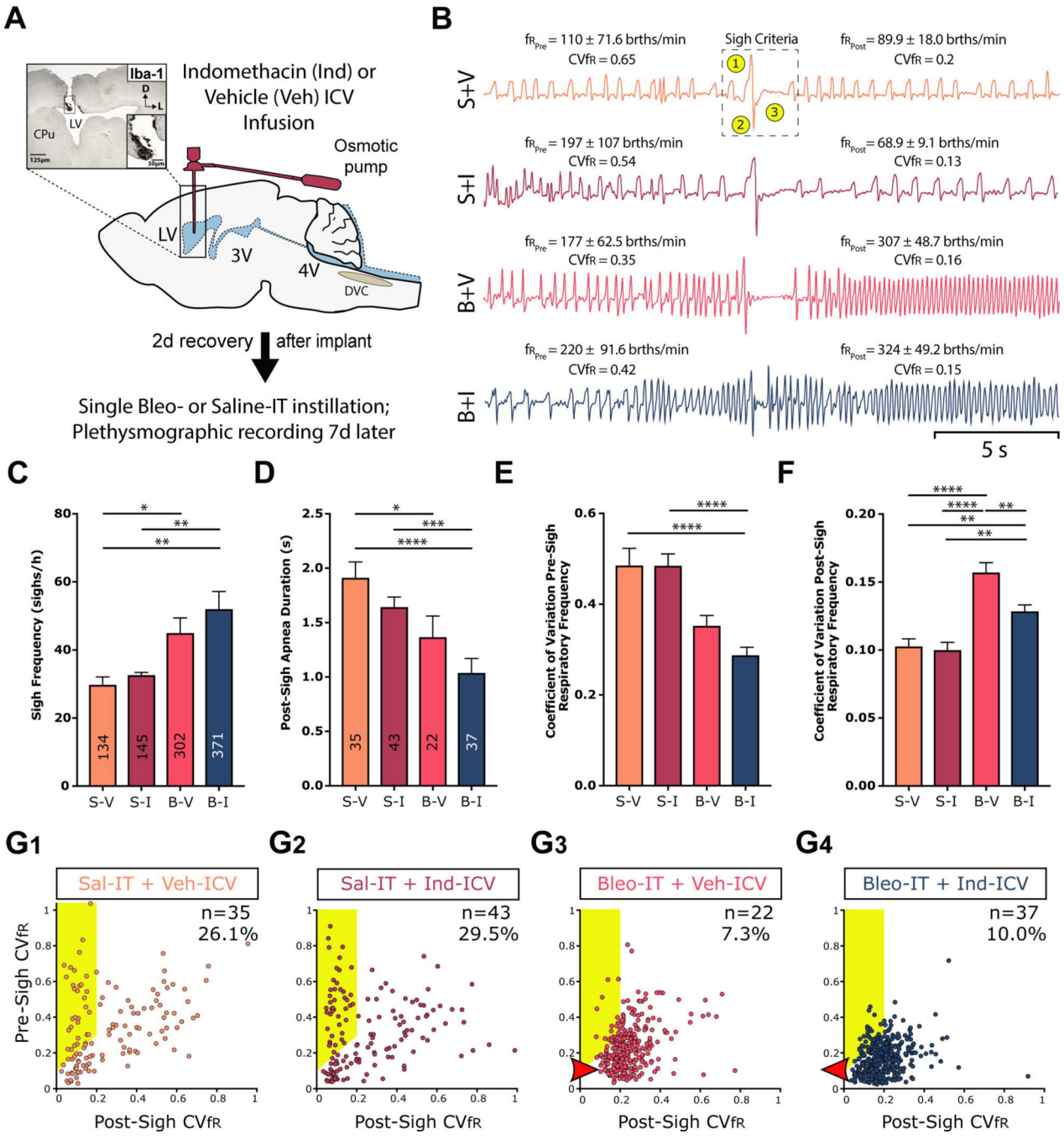


**Figure 5:**

SLI increases sigh frequency and modifies sigh dynamics, which is partially restored by ICV Indomethacin treatment.

**A.** Protocol. Rats received stereotaxic surgery to implant ICV cannulas attached to subcutaneously implanted mini-osmotic pumps (0.5 μl/h, 200 μl reservoir), which contained either vehicle (Veh, 50% DMSO) or Indomethacin (Ind, 8.3 μg/μl). 2d following cannulation, rats received Bleomycin (Bleo) or saline (Sal) intratracheally (IT); 7d later

ventilatory pattern was recorded via whole body plethysmography and rats were euthanized for IHC experiments. Group data are from 7 rats in each group.

**B.** Representative sighs for each group. The mean ± standard deviation of: i) the respiratory frequency for the 10s before and after the sigh is included for each sigh, and the coefficient of variation for the respiratory frequency (CVfR). In the top tracing, we identified sighs based on three (highlighted) criteria: 1) an augmented inspiration, 2) augmented initial expiration and 3) a prolonged expiration, which is referred to as a post-sigh apnea.

**C.** The frequency of sighs was significantly greater in Bleo-IT treated rats that received Veh-ICV (B+V) when compared to saline-IT treated that received Veh- or Ind- ICV (S+V or S+I), and was not significantly different compared to Bleo-IT treated rats that received Ind-ICV (B+I) (B+V vs. S+V: $P = 0.03$; B+V vs. S+I: $P = 0.104$; B+V vs. B+I, $P = 0.532$). The frequency of sighs was also significantly greater in B+I treated rats compared to either of the control groups (B+I vs. S+I: $P = 0.005$; B+I vs. S+V: $P = 0.0013$; Kruskal-Wallis test with Dunn's post hoc).

**D.** The duration of the apnea that followed a 'resetting' sigh was shorter in injured rats compared to sham rats, but Ind-ICV treatment did not alter apnea duration in Bleo- or saline-treated rats ((Figure 5D) B+V vs. S+V: $P = 0.04$; B+I vs. S+I: $P = 0.0008$; B+I vs. B+V: $P = 0.89$; S+V vs. S+I: $P > 0.999$; Kruskal-Wallis test with Dunn's post-hoc).

**E.** The CVfR before a resetting sigh was not significantly different in B+V treated rats compared to either of the saline-IT control groups, or Bleo-IT rats that received Ind-ICV (B+V vs. S+V: $P = 0.27$; B+V vs. S+I: $P = 0.06$; B+V vs. B+I: $P = 0.29$). However, the pre-sigh CVfR for B+I rats compared to either of the control groups (B+I vs. S+I: $P < 0.0001$; B+I vs. S+V: $P < 0.0001$; Kruskal-Wallis test with Dunn's post-hoc).

**F.** The CVfR after a resetting sigh was significantly increased in B+V treated rats compared to control groups and was significantly reduced in B+I (B+V vs. S+V: $P < 0.0001$; B+V: vs. S+I: $P < 0.0001$; B+V vs. B+I: $P = 0.007$). However, Ind-ICV treatment did not fully restore post-sigh CVfR in SLI rats; the CVfR of B+I rats was significantly greater compared to either of the control groups (B+I vs. S+I: $P = 0.002$; B+I vs. S+V: $P = 0.005$; Kruskal-Wallis test with Dunn's post-hoc).

**G.** Plots of pre-sigh CVfR vs. post-sigh CVfR for G1) S+V, G2) S+I, G3) B+V, G4) B+I treated rats. 'resetting' sigh was bounded by definition at 0.2. Both sham (S+V and S+I) groups and the injured group treated with Ind (B+I) had less variability in fR than the B+V group. Thus, the 'resetting' sighs were more effective in the B+I than the B+V group.

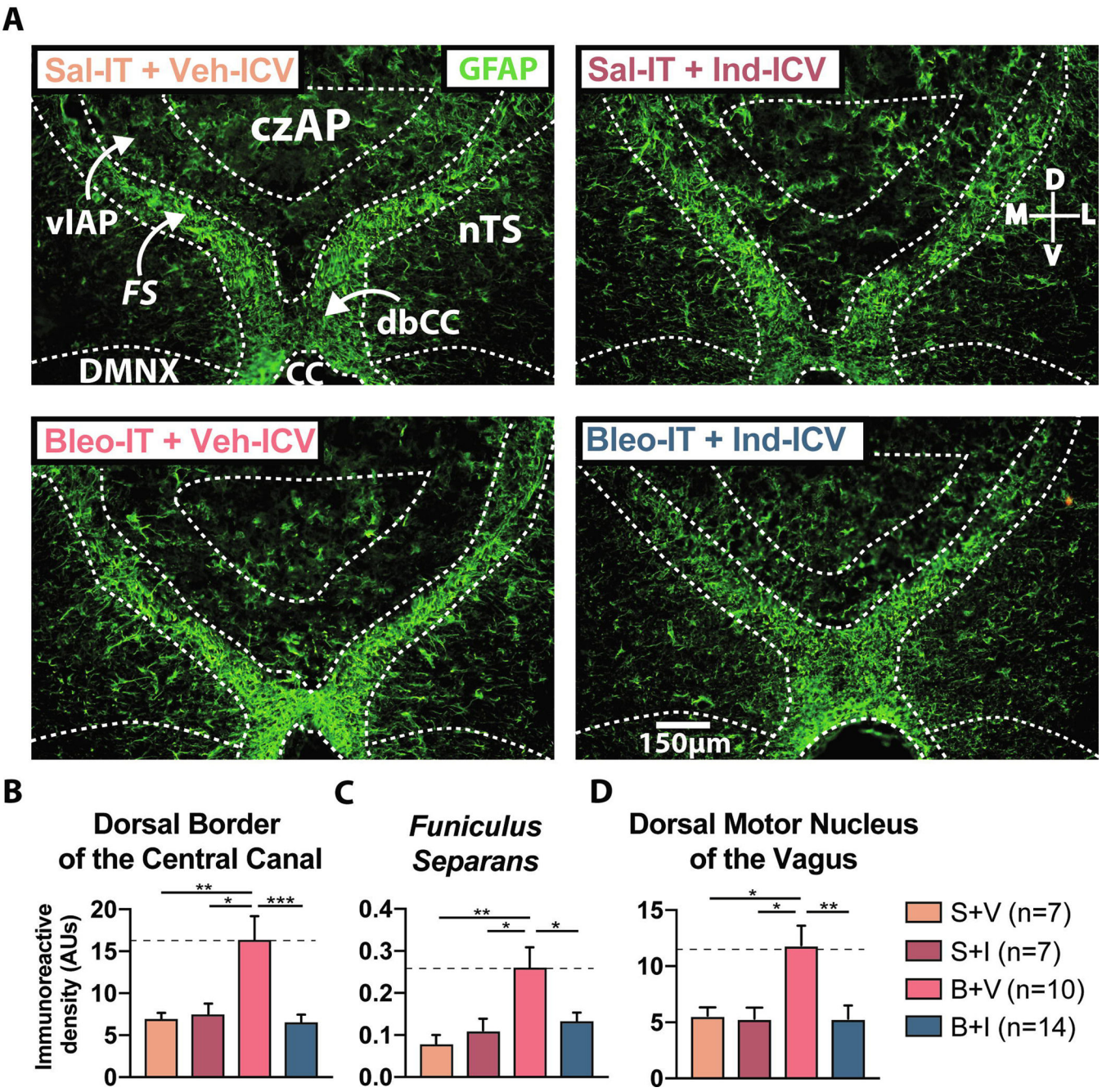


**Figure 6:**

Chronic intracerebroventricular (ICV) Indomethacin (Ind) infusion prevents the SLI-dependent increase in GFAP immunoreactivity.

**A.** Representative images of coronal brainstem sections showing GFAP+ IR throughout the dorsal brainstem for rats treated with Sal-IT + Veh-ICV (S+V, n = 7, orange), Sal-IT + Ind-ICV (S+I, n = 7, magenta), Bleo-IT + Veh-ICV (B+V, n = 11, red), Bleo-IT + Ind-ICV (B+I, n = 14, blue).

**B.** GFAP+ IR was significantly increased in the dbCC of Bleo-IT + Veh-ICV treated rats compared to Sal-IT controls and was reduced in Bleo-IT + Ind-ICV treated rats (B+V vs.

S+V: $P = 0.0079$; B+V vs. S + I: $P = 0.014$; B + V vs. B+I: $P = 0.0005$, One-way ANOVA with Tukey test).

**C.** GFAP+ IR in *funiculus separans* was augmented in Bleo-IT + Veh-ICV treated rats compared to Sal-IT controls and was significantly reduced in Bleo-IT + Ind-ICV treated rats (B+V vs. S+V: $P = 0.0042$; B+V vs. S+I: $P = 0.02$; B+V vs. B+I: $P = 0.03$, One-way ANOVA with Tukey test)

**D.** GFAP+ IR in the DMNX was augmented in Bleo-IT + Veh-ICV (B+V) treated rats compared to Sal-IT controls and was significantly reduced in Bleo-IT + Ind-ICV (B+I) treated rats (B+V vs. S+V: $P = 0.026$; B+V vs. S+I: $P = 0.019$; B+V vs. B+I: $P = 0.003$, One-way ANOVA with Tukey test).

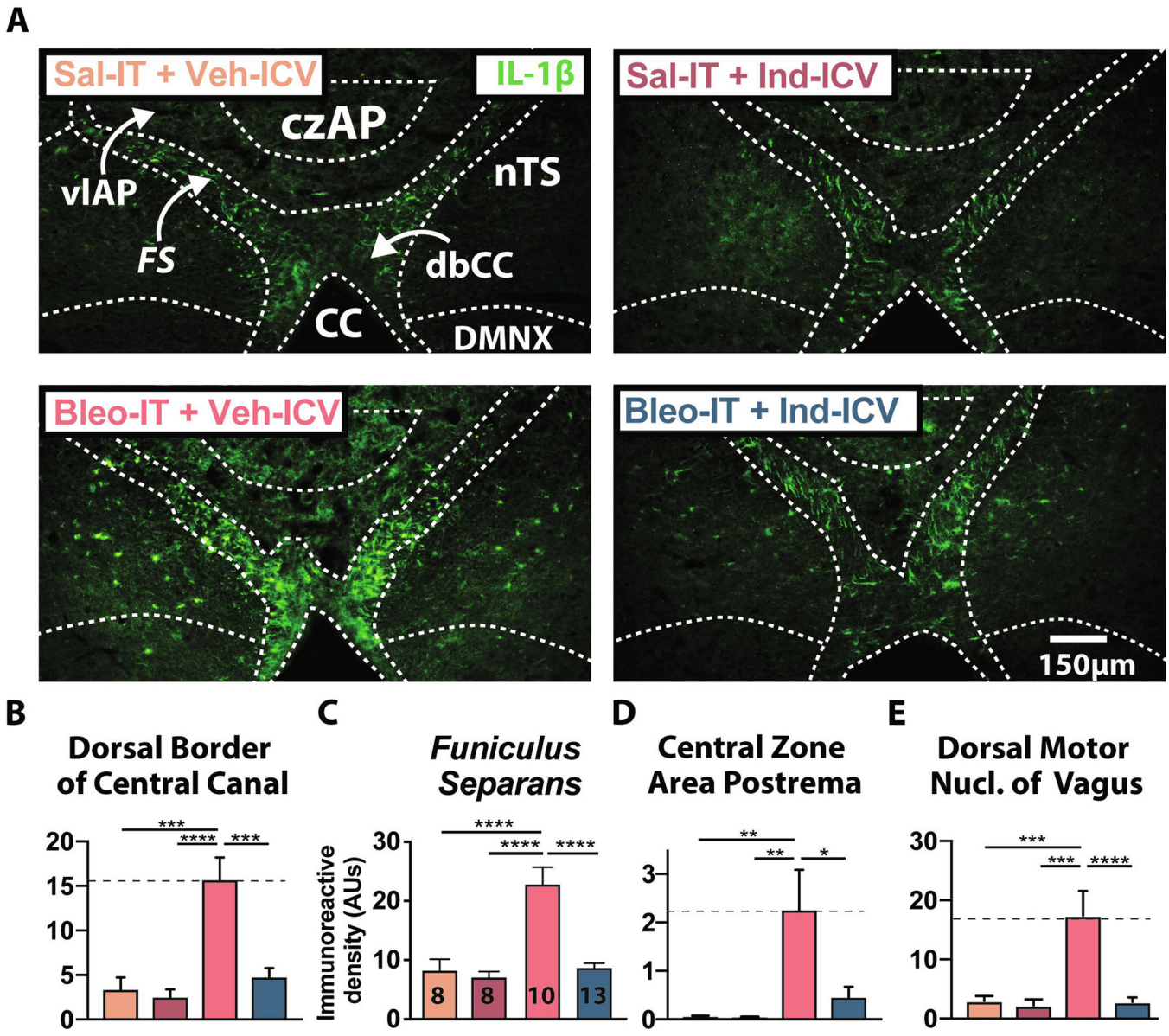


**Figure 7:**

Continuous intracerebroventricular (ICV) Indomethacin (Ind) infusion prevents the SLI-dependent increase in IL-1β immunoreactivity.

**A.** Representative images of coronal brainstem sections showing IL-1β+ IR throughout the dorsal brainstem for S+V (n = 7, orange), S+I (n = 7, magenta), B+V (n = 10, red), and B+I (n = 13, blue) rats.

**B.** IL-1β+ IR was greater in the dbCC of B+V compared to S+V and S+I rats and compared to B+I rats (B+V vs. S+V: $P = 0.0001$; B+V vs. S+I: $P < 0.0001$; B+V vs. B+I: $P < 0.0001$, One-way ANOVA with Tukey test).

**C.** IL-1β+ IR was greater in the *funiculus separans* of B+V compared to S+V and S+I rats and compared to B+I rats (B+V vs. S+V: $P < 0.0001$; B+V vs. S+I: $P < 0.0001$; B+V vs. B+I: $P < 0.000$, One-way ANOVA with Tukey test).

**D.** IL-1β+ IR was greater in the czAP of B+V compared to S+V and S+I rats and compared to B+I rats (B+V vs. S+V: $P = 0.006$; B+V vs. S+I: $P = 0.005$; B+V vs. B+I: $P = 0.011$, One-way ANOVA with Tukey test).

**E.** IL-1β+ IR was significantly increased in the DMNX of B+V compared to S+V and S+I rats and compared to B+I rats (B+V vs. S+V: $P = 0.0008$; B+V vs. S+I: $P = 0.0004$; B+V vs. B+I: $P < 0.0001$, One-way ANOVA with Tukey test).

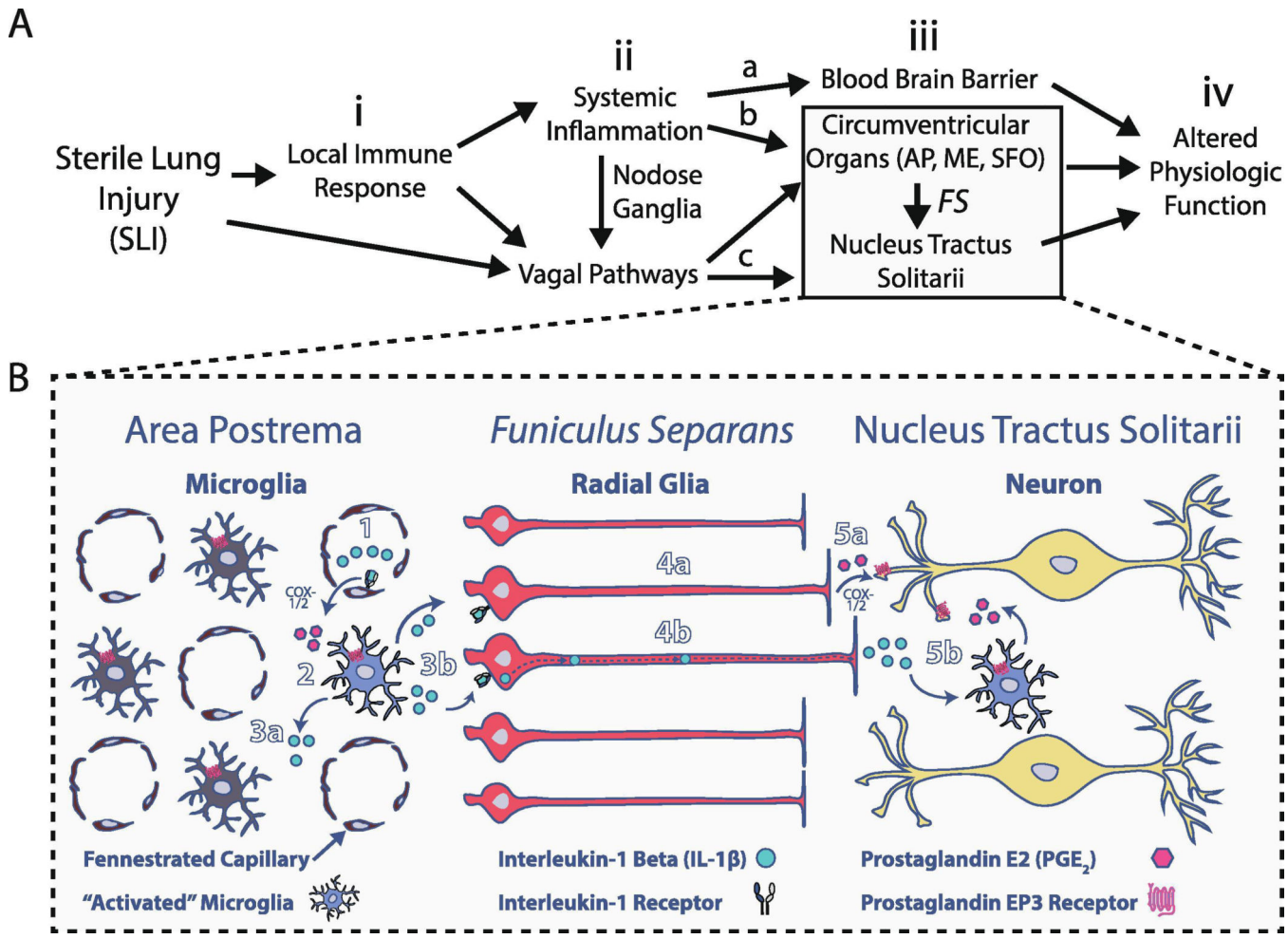


**Figure 8:**

Proposed model for peripheral to central immune transmission following SLI

A) i. Sterile lung injury can trigger local immune activation within the lung parenchyma (Cavarra et al., 2004; Matute-Bello et al., 2008; Hoshino et al., 2009; Ryzhavskii and Lebed, 2016), but may also directly activate vagal pathways that project to the nucleus tractus solitarii (nTS), and area postrema (AP) (Florez and Borison, 1967; Coleridge et al., 1976; Kubin et al., 1991; Srinivasan et al., 1993; Coleridge and Coleridge, 1994; Schelegle et al., 2001; Jung et al., 2018).

ii. If injury to the lung is severe, a systemic inflammatory response can occur (Tzouvelekis et al., 2005; Hoshino et al., 2009; Cross and Matthay, 2011; Dolinay et al., 2012; Matthay and Howard, 2012; Van Den Brule et al., 2014; Skurikhin et al., 2015). Transmission of SLI-dependent systemic inflammation to the CNS may occur through several pathways that are: a) mediated by altered permeability or immune signaling pathways at Blood Brain Barrier endothelium, b) mediated by circumventricular organs such as the AP, median eminence (ME) or subfornical organ (SFO), or c) vagally mediated through the nodose ganglia (Erickson and Banks, 2018).

iii. Data from our current study suggests part of the systemic immune response to SLI is transmitted from the periphery to the CNS via the *funiculus separans* (*FS)*, a barrier between

the AP and the dorsal brainstem composed of polarized radial glia (McKinley et al., 2003; Price et al., 2008; Maolood and Meister, 2009; Dallaporta et al., 2010; Senzacqua et al., 2016; Fernandez et al., 2017; Guillebaud et al., 2017).

iv. Transmission of SLI-dependent peripheral inflammation to dorsomedial (dm) brainstem nuclei likely mediates the respiratory and autonomic components of sickness behavior (Sekiyama et al., 1995; Rummel et al., 2006; Laaris and Weinreich, 2007; Marty et al., 2008; Ruchaya et al., 2012; Waki et al., 2013; Vance et al., 2015).

**B)** Interleukin-1 Beta (IL-1β) is systemically upregulated following SLI (Meduri et al., 1995; Tzouvelekis et al., 2005), but is likely prevented from diffusing directly into the AP parenchyma due to permeability restrictions imposed by fenestrated capillaries (Peruzzo et al., 2000; Willis et al., 2007; Quan, 2008; Willis, 2011; Morita et al., 2016). Alternatively, fenestrated capillaries can indirectly transmit IL-1β to the AP through IL-1 receptor signaling at their luminal surface; this involves cyclooxygenase (COX)-1/2 dependent synthesis of prostaglandin E2 ($PGE_2$), followed by its release into the AP parenchyma (Elmquist et al., 1997; Matsumura et al., 1998; Schiltz and Sawchenko, 2002; Rummel et al., 2004; Quan, 2008) (1). Microglia located in close proximity to AP fenestrated capillaries express $PGE_2$ receptors (EP3R), and can release IL-1β in response to $PGE_2$ binding (Elmquist et al., 1997; Eskilsson et al., 2014b) (2). This $PGE_2$-dependent IL-1β release can “activate” (dark blue) other AP-localized microglia in order to amplify the local immune response, which in turn may alter radial glial structure/function at the *FS* (3). We propose two potential mechanisms by which *FS* radial glia participate in immune transmission to dm brainstem nuclei (4a and 4b); IL-1β binding to its cognate receptor on the apical surface of *FS* radial glia promotes: 4a) COX-1/2 dependent $PGE_2$ release into the basolaterally facing dm-brainstem, or 4b) uptake, transcytosis, and basolateral release of IL-1β into the dm brainstem. Finally, $PGE_2$ released directly by radial glia (5a) or through nearby microglia (COX-1/2 mediated) (5b), can alter neuronal activity in dm-brainstem sites such as the nTS.

**Table. 1:**

Primary and secondary antibodies utilized in the current study.

| 1° Antibody | Species | Dilution | Manufacturer | Product # |
|---|---|---|---|---|
| COX-2 | Goat (Gt) | 1: 1000 | Abcam | ab23672 |
| GFAP | Chicken (Ch) | 1 : 1000 | Abcam | ab4674 |
| lba-1 | Rabbit (Rb) | 1 : 1000 | Wako | 019-19741 |
| IL-1 1β/Pro-IL-1β | Rb | 1 : 500 | Abcam | ab9722 |
| IL-6 | Gt | 1 : 500 | R&D | AF506 |
| MAP-2 | Rb | 1 : 5000 | Abcam | ab32454 |
| NeuN Alexa® Fluor 647 | Rb | 1 : 1000 | Abcam | ab190565 |
| TNF-α | Gt | 1 : 2000 | R&D | AF-510-NA |
| VGIuT2 | Guinea Pig (GP) | 1 : 2000 | Millipore | AB2251-I |
| **2° Antibody** | **Species** | **Dilution** | **Manufacturer** | **Product #** |
| Anti-Ch Alexa® Fluor 488 | Donkey (Dk) | 1 : 1000 | Jackson ImmunoResearch (JIR) | 703-545-155 |
| Anti-Gt Alexa® Fluor 647 | Dk | 1: 1000 | JIR | 705-295-003 |
| Anti-Gt Biotinylated Bt | Dk | 1 : 5000 | JIR | 705-065-003 |
| Anti-GPTRITC | Dk | 1 : 1000 | JIR | 706-545-148 |
| Anti-Rb Alexa® Fluor 488 | Dk | 1 : 1000 | JIR | 711-475-152 |
| Anti-Rb Alexa® Fluor 647 | Dk | 1 : 1000 | JIR | 711-295-152 |
| Anti-Rb Bt | Dk | 1 : 5000 | JIR | 711-065-152 |

Abbreviations are as follows: Cyclooxygenase-2 (COX-2); Glial fibrillary acidic protein (GFAP); Ionized calcium-binding adapter molecule (lba-1); lnterleukin-1 beta (IL-1β); lnterleukin-6 (IL-6); Microtubule associated protein 2 (MAP2); Neuronal Nuclei (NeuN);Tumor necrosis factor-alpha (TNF-α); vesicular glutamate transporter 2 (VGIuT2).